NOVEL NUCLEIC ACID SENSORS

FOR

THE RAPID DETECTION OF *CRYPTOSPORIDIUM PARVUM*

Dissertation zur Erlangung des
naturwissenschaftlichen Doktorgrades
der Bayerischen Julius-Maximilians-Universität Würzburg

vorgelegt von

Mandy Esch

aus Parchim

Würzburg, 2001

Eingereicht am: 17.7.2001

Mitglieder der Promotionskommission
Vorsitzender: Prof. Dr. Rainer Hedrich
Gutachter: Prof. Dr. Roland Benz
Gutachter: Prof. Dr. Richard A. Durst

Tag des Promotionskolloquiums: 17.10.2001
Doktorurkunde ausgehändigt am:……

ACKNOWLEDGMENT

This dissertation was conducted at the Food Science Department of Cornell University and at the Analytical Chemistry Division of the National Institute of Standards and Technology (NIST).

I would like to thank both of my thesis advisors, Professor Richard A. Durst (Cornell University) and Professor Roland Benz (Bayerische Julius-Maximilians-Universität Würzburg), for letting me freely arrange the projects of this thesis and work independently on them. I am very grateful to Professor Durst for funding the projects of this thesis and for enabling me to work in his laboratory as well as at the Cornell Nanofabrication Facility (CNF). CNF is a state of the art facility, and working there permitted me to fabricate microfluidic devices that I used for biological applications. Through these devices, I could combine the science of biology with that of engineering, and work on truly biotechnological projects.

Further, I would like to thank the colleagues from the laboratories I worked in, especially Michael Skvarla and the CNF staff for teaching me methods in microfabrication. Learning these methods and applying the tools and processes of microfabrication to biological projects is exciting, because it leads to new devices with which we can study biosystems in an interdisciplinary fashion. I also feel very fortunate that I had the possibility to learn from Sui Ti Siebert and Professor Antje Bäumner, who both introduced me to the biochemistry and engineering of liposomes.

The second part of this dissertation was conducted at NIST. Here I am indebted to Dr. Laurie Locascio and Dr. Michael Tarlov, in whose respective laboratories I worked. Working at NIST was a wonderful and rewarding experience for me, because I had the possibility to learn new methods such as surface plasmon resonance (SPR) spectroscopy. I am also thankful to Dr. Geoffrey Saupe, whom I worked very closely with, and who taught me how to apply SPR spectroscopy to experiments that involve nucleic acid hybridization .

Finally, I thank my family and friends for their support throughout my studies and writing of my dissertation.

CONTENTS

Synopsis……..…….5

Zusammenfassung…….……..6

1. Introduction……...8

Cryptosporidium parvum…….8

Diseases Caused by *C. parvum* and Route of Transmission……...8

Life Cycle of *C. parvum*……...8

Challenges Encountered in Attempts to Remove *C. parvum* from Water……9

Detecting *C. parvum* Using Antibodies……10

Detecting *C. parvum* Using Synthetic Nucleic Acids……11

Importance of Nucleic Acid Diagnostics for the Detection of Pathogens……12

Traditional Nucleic Acid Detection Techniques……..……13

Nucleic Acid Detection by Oligonucleotide-Tagged Liposomes……14

2. Development of a Test-Strip for the Rapid and Sensitive Detection of *Cryptosporidium parvum*……16

Abstract……16

Introduction……17

Background……17

Detection of *C. parvum* by Using a Novel Test-Strip……18

Experimental Section……19

Reagents……19

Oligomers……20

Encapsulant Preparation……20

Liposome Preparation……21

Conjugating Reporter Probes to Liposomes……21

Preparation of Test-Strips……22

Assay Protocol……24

Detection and Quantification……24

Nucleic Acid Sequence-Based Amplification (NASBA)……24

Results and Discussion……26
Characterization of Liposomes……26
Optimizing the Test-Strip……26
Determining the Limit of Detection……30
Determining the Compatibility of the Test-Strip Assay with the NASBA Methodology……33
Specificity of the Test……35
Conclusions……36

3. Development of a Microfluidic Chip for the Detection of *Cryptosporidium parvum* by Means of Fluorescent Signals Generated by Liposomes……37

Abstract……37
Introduction……38
Background……38
The Concept of the Microfluidic Chip……40
Experimental Section……41
Oligomers……41
Preparation of Acetylthioacetate (ATA)-Tagged Liposomes Containing Carboxyfluorescein……41
Conjugating Reporter Probes to ATA-Tagged Liposomes……42
Preparation of Capture Probe/Hexane Monolayers on Gold-Covered Glass Slides……44
Preparation of the Microfluidic Chip……44
Assay Protocol……45
Detection and Quantification……46
Nucleic Acid Sequence-Based Amplification (NASBA)……46
Results and Discussion……47
Design and Fabrication of the Microfluidic Chip……47
Minimizing the Background Signals Generated in the Chip……50
Determining the Limit of Detection……53
Specificity of the Assay……56
Testing of RNA Amplified by NASBA……57
Reusability of the Chip……58
Conclusions……59

4. Development of a Prototype Microfluidic Array for Multiple Analyte Detection……60

Abstract……60

Introduction……60

Background……60

Fabrication of a Prototype Microfluidic Array……63

Experimental Section……64

Oligomers……64

Preparation of Acetylthioacetate (ATA)-Tagged Liposomes Containing Carboxyfluorescein……64

Preparation of Gold-Covered Microscope-Glass Slides……64

Preparation of the Microfluidic Array……64

Assay Protocol……66

Detection and Quantification……66

Results and Discussion……67

Design and Fabrication of the Microfluidic Array……67

Minimizing the Background Binding……68

Analyzing Multiple Samples Simultaneously……71

Conclusions……72

5. Electrochemical Detection of *Cryptosporidium parvum* Using Interdigitated Microelectrode Arrays in a Microfluidic Chip……..……... 73

Abstract……73

Introduction……73

Background……73

Electrochemical detection Using Liposomes and Interdigitated Microelectrode Arrays……75

Experimental Section……76

Oligomers……76

Preparation of Reporter Probe-Tagged Liposomes Containing Ferri- and Ferrohexacyanide……76

Preparation of Interdigitated Electrode Arrays……76

Preparation of the Microfluidic Chip……78

Assay Procedure……78
Electrochemical Detection and Quantification……79
Results and Discussion……80
Design and Fabrication of the Chip……80
Characterization of Liposomes……83
Detecting Ferri- and Ferrohexacyanide Using Interdigitated Electrode Arrays……83
Influence of Assay Reagents on the Detection with Interdigitated Electrodes……86
Dose-Response Curve……90
Conclusions……91
6. Oligonucleotide Detection by Surface Plasmon Resonance Spectroscopy……92
Abstract……92
Introduction……92
Background……92
SPR and Nucleic Acid Hybridization……94
Experimental Section……95
Oligomers……95
Preparation of Reporter Probe-Tagged Liposomes……95
SPR Experimental Setup……95
Depositing Gold on the Lens……96
Preparing Organic Layers on the Gold Surface……96
Assay Protocol……97
Data Analysis……98
Results and Discussion……99
Immobilization of Capture Probes and Deposition of Blocking Layers on a Gold Surface……99
Hybridization of Targets to Mixed Layers of Capture Probes and Blocking Molecules……102
Sandwich-Hybridization with Reporter Probe-Tagged Liposomes……103
Conclusions……105
7. References of Chapters 1 to 6……107

SYNOPSIS

Recent advances in the development of immunoassays and nucleic acid assays have improved the performance and increased the sensitivity of sensors that are based on biochemical recognition. The new approaches taken by researchers include detecting pathogens by detecting their nucleic acids, using new nontoxic reporter entities for generating signals, and downscaling and miniaturizing sensors to micromigration and microfluidic formats.

This dissertation connects some of these successful approaches, thereby leading to the development of novel nucleic acid sensors for rapid and easy detection of pathogens. The author's goal was to develop diagnostic tools that enable investigators to detect pathogens rapidly and on site. While the sensors can be used to detect any pathogen, the author first customized them for detecting particularly *Cryptosporidium parvum*, a pathogen whose detection is important, yet presents many challenges.

Chapter 2 of this thesis presents a novel test-strip for the detection of *C. parvum*. The test-strip is designed to detect nucleic acids rather than proteins or other epitopes. While test strips are commonly used for sensors based on immunological recognition, this format is very new in applications in which nucleic acids are detected. Further, to indicate the presence or absence of a specific target on the test strip, dye-entrapped, oligonucleotide-tagged liposomes are employed. Using liposomes as reporter particles has advantages over using other reporter labels, because the cavity that the phospholipidic membranes of the liposomes form can be filled with up to 10^6 dye molecules. By using heterobifunctional linkers liposomes can be tagged with oligonucleotides, thereby enabling their use in nucleic acid hybridization assays. The developed test-strip provides an internal control. The limit of detection is 2.7 fmol/μL with a sample volume of 30 μL.

In chapter 3 the detection of nucleic acids by means of oligonucleotide-tagged liposomes is scaled down to a microfluidic assay format. Because the application of biosensors to microfluidic formats is very new in the field of analytical chemistry, the first part of this chapter is devoted to developing the design and the method to fabricate the microchip devices. The performance of the microchips is then optimized by

investigating the interactions of nucleic acids and liposomes with the material the chips consist of and by passivating the surface of the chips with blocking reagents. The developed microfluidic chip enabled us to reduce the sample volume needed for one assay to 12.5 μL. The limit of detection of this assay was determined to be 0.4 fmol/μL.

Chapters 4 and 5 expand on the development of the microfluidic assay. A prototype microfluidic array that is able to detect multiple analytes in a single sample simultaneously is developed. Using such an array will enable investigators to detect pathogens that occur in the same environment, for example, *C. parvum* and *Giardia duodenalis* by conducting a single test. The array's ability to perform multiple sample analysis is shown by detecting different concentrations of target nucleic acids. Further, the author developed a microfluidic chip in which interdigitated microelectrode arrays (IDAs) that consist of closely spaced microelectrodes are integrated. The IDAs facilitate electrochemical detection of cryptosporidial RNA. Electrochemical detection schemes offer benefits of technical simplicity, speed, and sensitivity. In this project liposomes are filled with electrochemically active molecules and are then utilized to generate electrochemical signals.

Chapter 6 explores the feasibility of liposomes for enhancing signals derived from nucleic acid hybridization in surface plasmon resonance (SPR) spectroscopy. SPR spectroscopy offers advantages because nucleic acid hybridization can be monitored in real time and under homogeneous conditions because no washing steps are required. SPR spectroscopy is very sensitive and it can be expected that, in the future, SPR will be integrated into microfluidic nucleic acid sensors.

ZUSAMMENFASSUNG

Jüngste Fortschritte in der Entwicklung von Immuno- und Nucleinsäure- Assays haben die Arbeitsleistung und die Spezifität von Sensoren, die auf biochemischer Erkennung basieren (Biosensoren), verbessert. Neu entwickelte Methoden umfassen die Detektion von Pathogenen durch die Detektion ihrer RNA oder DNA, das Benutzen von neuen nicht-toxischen Reporter Molekülen, um Signale in Sensoren zu erzeugen,

und die Verkleinerung und Miniaturisierung von Sensoren zu Mikromigrations- und Mikrofluid Formaten.

Die in dieser Dissertation entwickelten Sensoren, die der Detektion von Pathogenen dienen, verbinden einige der neu entwickelten Methoden. Das Ziel der Autorin war es, Sensoren zu entwickeln, die es ermöglichen, Pathogene an Ort und Stelle zu detektieren. Die entwickelten Sensoren können zur Detektion von einer Reihe von Pathogenen benutzt werden. In dieser Dissertation sind sie für die spezifische Detektion von *Cryptosporidium parvum* entwickelte worden.

Kapitel 2 der Dissertation präsentiert einen neuen Teststreifen für die Detektion von *C. parvum*. Der Teststreifen detektiert die RNA von *C. parvum*, die als Reaktion auf einen Hitzeschock produziert wird. Das Teststreifen-Format ist üblich für Sensoren, die auf immunologischer Erkennung basieren. Es ist jedoch neu für Anwendungen in denen RNA oder DNA detektiert werden sollen. Die An- oder Abwesenheit eines bestimmten Ziel Moleküls wird durch Liposomen, die Oligonukleotide auf der Aussenseite ihrer Membranen enthalten und mit Farbstoff gefüllt sind, angedeutet. Die Experimente zeigten, dass die mit dem entwickelten Test-Streifen kleinste detektierbare Konzentration von RNA in einem 30 μL Probenvolumen 2.7 fmol/μL ist.

In Kapitel 3 ist die Signalerzeugung durch Liposomen in ein Mikrofliess-System integriert. Da die Entwicklung von Mikrofliess-Systemen ein sehr neues Forschungsgebiet ist, befasst sich ein Teil dieses Kapitels mit dem Design und der Herstellung des Microchips. Die Untersuchung von Interaktionen von Nukleinsäuren und Liposomen mit dem Material aus dem der Chip hergestellt ist und die Passivierung dieses Materials ist dabei ein Schwerpunkt. Das Probenvolumen, dass zur Detektion mit dem entwickelten Mikrofliess-Sensor nötig ist, konnte auf 12.5 μL reduziert werden. Die kleinste detektierbare Konzentration von Nucleinsäuren ist 5 fmol/μL.

In Kapitel 4 und 5 erweitert die Autorin die Entwicklung des Mikrofliess-Sensors aus Kapitel 3. Das Detektionsformat ist auf ein Array, das für die gleichzeitige Detektion von mehreren Pathogenen benutzt werden kann, angewandt. Eine Methode zum Herstellen eines Arrays-Prototypen ist entwickelt. Ferner, stellte die Autorin verzahnte Mikroelektroden her und benutzte diese um die elektrochemische Detektion der RNA von *C. parvum* zu ermöglichen.

In Kapitel 6 ist die Anwendbarkeit von Liposomen zur Erhöhung von Signalen von Nukleinsäure-Hybridisierungen in Surface Plasmon Resonance Spectroscopy (SPR) untersucht.

1

INTRODUCTION

CRYPTOSPORIDIUM PARVUM

DISEASES CAUSED BY *C. PARVUM* AND ROUTE OF TRANSMISSION

The microorganisms of the species of *Cryptosporidium* are protozoan parasites that infect birds, fish, reptiles, mammals,[50] and also human beings.[51] Among the recorded species of *Cryptosporidium*, *Cryptosporidium parvum* has the most significant impact on the health of human beings.[51-53] Infections by this parasite cause acute gastrointestinal symptoms in normally healthy people, and can lead to life-threatening conditions in individuals with impaired immune systems, such as patients with acquired immune deficiency syndrome (AIDS).[54]

The principal mode of transmission of *C. parvum* is by ingestion of oocysts from animal feces that entered water reservoirs. Researchers have found that *C. parvum* can occur in all types of surface waters such as lakes, reservoirs, streams, and rivers.[55] The main sources of contamination of surface waters are products from agricultural pollution (i.e., animal feces used as manure) and products from sewage-treatment processes in communities in which infection exists.[55] Between 1984 and 1996, waterborne transmission of *C. parvum* provoked massive outbreaks in the United States, Great Britain, and Japan.[56-58]

LIFE CYCLE OF *C. PARVUM*

The life cycle of *C. parvum* takes place within a single host and may be completed within one to eight days. Infected individuals excrete oocysts of the parasite in their feces. These oocysts are 4 to 6 μm in size and carry the infective, banana-shaped sporozoites within them. When ingested by another host, these sporozoites attach themselves to the epithelial cells lining the small intestine. The sporozoites then

enter the cell and grow into trophozoites without being connected to the cytoplasm of the cell. The trophozoites undergo asexual reproduction and form up to eight merozoites. These either reinfect the host and become trophozoites, or develop into type 2 meronts that also undergo asexual reproduction. The resulting merozoites enter other cells of the small intestine and develop either into a male microgamont or a female macrogamont. The microgamont produces microgametes, which on release fertilize the mature macrogamont (macrogamete). The formed zygotes develop into the oocysts that contain the sporozoites. About 80% of these oocysts are excreted with the feces. The remaining 20% will reinfect the host without leaving it.

Descriptions of the complicated life cycle of *C. parvum* have been published by "The Group of the Experts",[59] and Smith and co-workers.[60]

CHALLENGES ENCOUNTERED IN ATTEMPTS TO REMOVE *C. PARVUM* FROM WATER

Before surface water is safe for consumption, contaminants such as pathogenic bacteria, algae, zooplankton, precipitates, particles that cause turbidity or color, and natural and synthetic organic molecules must be removed from it. The processes normally used to remove these contaminants include flocculation with subsequent clarification, adsorption, filtration (including microstraining), disinfection, and sludge treatment.

Some of these treatment processes are also effective to a certain degree for removing *C. parvum* oocysts. For example, because oocysts are negatively charged (most of the particles that occur naturally in water carry a small negative potential on their surface), they are enmeshed in precipitates generated by the addition of certain metallic salts such as aluminum sulphate and ferric sulphate. The generated flocs are usually removed in sedimentation tanks or by filtration. If oocysts are enmeshed in residual flocs, it can be expected that they will be filtered out along with those flocs.[61]

However, because of their small size, low density, and spherical shape, single oocysts or even small clumps are not easily retained by commonly used filters.[61] Recycling the filter backwash water gives oocysts a further opportunity to penetrate the water treatment process.[62]

Storage of water, a procedure that reduces its turbidity and the number of coliform bacteria, does not effectively reduce the number of oocysts in the water since, due to their small size, their settling rate is very small. For example, it takes several hundred days for oocysts to settle in a tank that is 20 m deep.[62] Additionally, oocysts survive in water for several months.[62]

Some treatment processes use ion-exchange procedures to remove nitrates and other ions. These processes will not kill or remove oocysts.[62] The most effective method for killing most other microorganisms is by disinfection using chlorine. However, the dosages of chlorine that are usually used and are acceptable for human consumption do not inactivate *C. parvum's* oocysts.[63, 64]

Several authors who have reviewed the effectiveness of water treatment processes conclude that commonly used water treatment processes cannot be relied upon to remove all cryptosporidial oocysts. [58, 62, 65]

DETECTING *C. PARVUM* USING ANTIBODIES

A successful scheme for the detection of *C. parvum* requires collecting and concentrating the oocysts from environmental water samples, separating the oocysts from contaminating debris, and finally detecting them.

The standard procedure for detecting *C. parvum* uses fluorescently labeled antibodies that stain the oocysts, which can thereupon be identified microscopically.[65] However, a study by Moore et al. demonstrated that some carbohydrate epitopes at the oocyst wall are labile after chlorine treatment and under oxidizing conditions similar to those used to eliminate bacteria found in drinking water.[66] Therefore, although the oocysts would still be infectious, they would not be detected by the use of antibodies toward these epitopes. A further drawback of detection using epifluorescence microscopy is that commercially available antibodies cross-react with organisms other than *C. parvum*.[67] Finally, the standard procedure does not permit researchers to determine the viability of oocysts. A procedure for rapidly and accurately detecting oocyst viability would enable researchers to assess (1) the risk posed by the detected oocysts, and (2) the effectiveness of newly developed disinfection procedures.

Various detection methods that overcome the difficulties encountered with epifluorescence microscopy have been reported.[68-74] Slifko et al.[68, 69] developed a detection scheme that focuses on determining oocyst viability by specifically identifying the reproductive stages of *C. parvum*. Host cells are first infected with *C. parvum*; after 24 to 48 hours, infective foci in the cell culture are identified intracellularly by labeling them with antibodies specific to the reproductive stages of the parasite. The method is very sensitive, however, culturing the cells is time-consuming.

DETECTING *C. PARVUM* USING SYNTHETIC NUCLEIC ACIDS

More recently developed detection schemes rely on detecting DNA or RNA specific to *C. parvum*.[70-74] The methods that detect RNA instead of DNA offer two advantages. First, due to the rapid turnover and postmortem decay of cellular RNA, the presence of certain RNA molecules has been correlated with the viability of oocysts.[73] Second, in viable organisms, there are many more copies of RNA than of DNA, and therefore the sensitivity of detection is increased. Vesey et al. developed a technique for detecting rRNA by in situ hybridization, using fluorescently labeled oligonucleotide probes.[74] In combination with immunofluorescence staining, the method enabled species-specific detection and assessment of oocyst viability that correlated with in vitro excystation. However, the method encounters problems when detection is attempted in environmental water concentrates that contain autofluorescent algae and mineral particles.

Other researchers demonstrated the successful use of polymerase chain reaction (PCR) protocols for amplifying species-specific gene fragments, thus enabling traditional methods to detect cryptosporidial nucleic acids subsequently.[70, 75] The method using reverse-transcription PCR (RT-PCR) in combination with gel electrophoresis was shown to detect a single viable oocyst that had been spiked into sample concentrates from creek and river water.[72]

Previously, the nucleic acid sequence-based amplification (NASBA) technique was utilized to amplify mRNA coding for the heat-shock protein (hsp70) produced by *C. parvum*.[76] The mRNA serving as template for NASBA is produced by *C. parvum* as

a response to heat shock. This response is expected to take place in viable organisms only. Therefore, testing for the RNA product of NASBA will allow researchers to distinguish viable from nonviable *cryptosporidial oocysts*.

NASBA is a continuous, isothermal process that others have employed to amplify single-stranded RNA.[77-80] This amplification technique has an advantage over other RNA-amplification techniques (e.g. RT-PCR), because it does not require thermal cycling and, therefore, no special equipment is needed.

IMPORTANCE OF NUCLEIC ACID DIAGNOSTICS FOR THE DETECTION OF PATHOGENS

Nucleic acid diagnostics provide capabilities for detecting pathogens that cannot be reached by immunological methods. The detection of nucleic acids is based on the non-covalent biological recognition of complementary strands of DNA or RNA.[1] The recognition is highly specific and, under certain conditions, it is extremely sensitive to even a single mismatched basepair within the nucleic acid molecule.[2, 3] Therefore, microorganisms whose DNA is analyzed can be detected and distinguished from one another with high accuracy.

Utilizing amplification methods in schemes for detecting nucleic acids enhances the sensitivity of the detection. The development of techniques such as the polymerase chain reaction (PCR, first introduced by Mullis et al.[4, 5]) enable specific nucleic acid sequences to be amplified. That means that, if the amplified sequence is the sequence to be detected, the analyte itself is amplified. Producing many copies of the analyte from only a few copies dramatically increases the chances of detecting it. Several reviews of detection schemes for diagnosis of infectious pathogens based on PCR can be found in the literature.[6-8]

Nucleic acid diagnostics are applied to detections relevant in medicine as well as in environmental monitoring. Used in preventive medicine, these diagnostic methods can identify inherited predispositions to develop diseases such as leukemia, breast cancer, and autoimmune disease before they are manifested clinically by detecting specific sequences within the genome of a person.[9, 10, 11]

Since the base sequences vary from gene to gene and from organism to organism, environmental pathogens have also been accurately detected by nucleic acid diagnostics.[12, 13] When detecting pathogens, the detection of RNA has advantages over the detection of DNA. Since RNA is subject to a rapid turnover within the organism, only organisms with an active transcription will contain RNA. Because the gradual decrease in levels of certain RNA molecules in microorganisms has been correlated with the loss of their infectivity,[14] the detection of these molecules enables researchers to distinguish between viable and nonviable organisms. However, to take fully advantage of the decay of RNA, researchers have to investigate the fate of the RNA in the organism of interest carefully, since not every RNA is suitable as an indicator of viability.[14]

TRADITIONAL NUCLEIC ACID DETECTION TECHNIQUES

In standard laboratories the most commonly used method for detecting nucleic acids and gaining information about fragment length is gel electrophoresis. The nucleic acids are separated from each other in terms of their size. They can then be stained with intercalating dyes and be detected by fluorescence methods. Gel-electrophoresis does not provide information on the sequence of the nucleic acids. Furthermore, ethidium bromide, an intercalating dye that is considered to cause cancer, is widely used even though new dyes that pose smaller health risks have been developed.

To identify nucleic acids with a specific sequence in a mixture of molecules, the investigator first separates the molecules by gel-electrophoresis, and then transfers them to solid supports such as nylon or nitrocellulose membranes.[15, 16] The membranes are incubated in a solution containing oligonucleotides that are complementary to the sequence of interest. These complementary oligonucleotides are tagged with radioactive,[15,16] color-producing,[17] or chemiluminescent[18] labels and hybridize to the sequence of interest on the membrane. Unhybridized oligonucleotides are washed away, and the oligonucleotides that hybridized are identified by the label. This method is commonly referred to as "Southern blot" if DNA is identified, and "Northern blot" if RNA is identified. Originally, probes were often labeled with the radioactive isotope ^{32}P. Today, however, many researchers use nonisotopic labels.[19] Isaac and colleagues

have summarized easy-to-follow protocols for working with oligonucleotides that are tagged with nonisotopic labels.[19]

Two other commonly used methods are the dot-blot and reverse dot-blot assays.[20, 21] Here the nucleic acids are not separated by gel-electrophoresis. Instead, they themselves are directly immobilized on a membrane and then hybridized to labeled complementary probes (dot-blot), or else complementary oligonucleotides are immobilized on membranes and then the nucleic acids in the sample solution hybridize to these immobilized probes (reverse dot-blot).

Matthews et al.[22] and Manak et al.[23] have written detailed reviews of nucleic acid methodologies. The traditional methods have several disadvantages. Besides utilizing chemicals that pose health risks, they are time-consuming, they cannot be transported to the field, and they require a large amount of sample solution.

NUCLEIC ACID DETECTION BY OLIGONUCELOTIDE-TAGGED LIPOSOMES

In immunoassays and in nucleic acid assays, so-called reporter particles (or reporter labels) generate signals that indicate the presence or absence of target molecules. Radioactive isotopes, the labels originally used for detecting nucleic acids,[15, 16] are now being replaced by other indicators. Among signal-generating labels are enzymes such as horseradish peroxidase,[24] fluorescing labels,[25, 26] chemiluminescing labels,[18] electroactive molecules,[27-32] and sol-particles such as colloidal carbon,[33] colloidal dyes,[34] gold and silver, [35, 36] latex particles[37], and liposomes.[38-40]

In the projects of this dissertation liposomes are used as reporter particles. The unique structure of liposomes offers advantages over other reporter particles. Liposomes are artificially prepared vesicles that consist of a phospholipidic membrane and an aqueous cavity. Typically, they are 200 nm to 400 nm in diameter. The cavity can be filled with molecules diluted in aqueous solutions. Bangham et al. initially discovered and characterized liposomes in 1965.[41] Since then, liposomes have been used in a variety of applications, for example, to the study biological membranes, for targeted drug delivery for the treatment of cancer, and for gene delivery.[42] Because the liposome membrane consists of various phospholipids with functional “head groups”, they can be tagged with biomolecules (for example, antibodies) that participate in the

binding events of the assay. Hence, liposomes have already been employed in immunoassays.[43]

Liposomes contribute to the improvement of immunoassays in two ways. First, because each liposome can contain up to 10^6 signal-generating molecules (for example, fluorescent dye molecules),[44] and these molecules can be released under controlled conditions, the signal yielded from one binding event is amplified in comparison with signals yielded by other reporter particles. The second advantage derives from the fluidic nature of the phospholipid membrane. Depending on the temperature and the lipid composition of the membrane, the tags can move and change their location in the membrane.[45, 46] Therefore, the tags may move into places where several binding events can occur, thereby reinforcing an initial binding event.

Several reports have demonstrated the improvement of immunoassays when liposomes were used instead of single tags such as single fluorophores.[47-49] In a flow-injection immunoassay in which liposomes were used to detect the analyte, the sensitivity of that assay was increased a thousandfold in comparison with the same assay conducted using a single fluorophore as the reporter entity.[49]

In this dissertation the author uses heterobifunctional linkers to prepare liposomes tagged with oligonucelotides and filled with fluorescent dye, or alternatively, with electrochemically detectable solutions. The oligonucleotide tag on the membranes of the liposomes enables their use for detecting nucleic acids on migration test-strips (chapter 2), in microfluidic chips (chapters 3-5), and in surface plasmon resonance (SPR) spectroscopy (chapter 6).

2

Development of a Test-Strip for the Rapid and Sensitive Detection of *Cryptosporidium parvum*

ABSTRACT

To meet the technical challenge of accurately and rapidly detecting *Cryptosporidium parvum* oocysts in environmental water, the author developed a single-use visual-strip assay. The first step in the overall assay procedure involves extracting *C. parvum's* mRNA coding for heat-shock protein hsp70, followed by amplification using nucleic acid sequence-based amplification (NASBA) methodology as described previously.[1] Subsequently, generated amplicons are hybridized with dye-entrapping liposomes bearing DNA oligonucleotides (reporter probes) and biotin on their surface. The liposome–amplicon complex is then allowed to migrate upward on a nitrocellulose membrane strip. On the nitrocellulose strip, antisense reporter probes are immobilized in a capture zone and antibiotin-antibodies are immobilized in a second zone above the capture zone. Depending on the presence or absence of amplicon in the sample, the liposomes will bind to the capture zone, or they will be caught my means of their biotin tag in the second zone. Visual detection or gray-scale densitometry allows the quantification of liposomes that are present in either zone. The detection limit of the assay was determined to be 80 fmol amplicon/test. High accuracy is achieved and an internal assay control is established using this competitive format, because the presence (or absence) of liposomes can be quantified in the two capture zones.

Modified from: Esch, M. B.; Baeumner, A.; Durst, R. A. "Rapid Visual Detection of Viable *Cryptosporidium parvum* on Test Strips using Oligonucleotide-tagged Liposomes" *Analytical Chemistry*, **2001**, 73(13); 3162-3167.

INTRODUCTION

BACKGROUND

In order to detect *Cryptosporidium parvum* in water samples, investigators typically collect the samples on site and then transport them back to a laboratory in which the actual analysis takes place. The analysis requires extensive bench-top equipment and skilled personnel who are thoroughly familiar with the applied detection scheme. This procedure is not suited for routinely monitoring the occurrence of *C. parvum* in water treatment facilities. Rather, it is used to respond to a suspected threat indicated by the occurrence of cases of *Cryptosporidiosis* among the inhabitants of a community.

Environmental monitoring used as preventive measures can be performed only with tools that enable investigators to conduct rapid, on site detection. Such tools would ideally be field-portable and would provide the same or superior sensitivity as full-scale laboratories. The need for detection equipment that is easy to transport for use on site has led to the downscaling of conventional bench-top instruments on one hand, and the development of completely new, miniaturized detection formats on the other hand. However, most of the research and development done in this field focuses on the detection of medical conditions rather than the detection of environmental pathogens and pollutants. For detecting DNA, many companies started to develop easy-to-use test kits that use PCR (or another amplification method), but that employ novel detection formats chosen to provide sensitivity, speed, and convenience as well as patent protection.

Efforts to downscale nucleic acid detection schemes include the integration of target amplification methods that do not require temperature cycling. Current techniques can be grouped into two categories: those that operate through a temperature-cycling mechanism, and those that operate at a constant temperature. Isothermal techniques have the advantage of not requiring expensive instrumentation for regulating temperature; however, they tend to use larger volumes of reagents.[2-4]

Nucleic acid sequence-based amplification (NASBA) is one example of a continuous, isothermal amplification process. This technique was first developed to

amplify nucleic acids that enabled the detection of HIV viruses.[5] Since then it has been employed for amplifying single-stranded RNA by several other groups.[6-8] Previously, NASBA was utilized to amplify mRNA coding for the heat-shock protein (hsp70) produced by *C. parvum*.[1]

DETECTION OF *C. PARVUM* BY USING A NOVEL TEST-STRIP

In the first part of this dissertation, the author presents a novel test-strip assay for the convenient and rapid detection of amplicons produced by NASBA from *C. parvum* mRNA. So far, test-strips have been used for sensors based on immunological recognition. Here, we developed a test-strip for the detection of nucleic acids.

The detection is based on a competitive binding assay and on signal generation by liposomes. Dye-containing liposomes are tagged with biotin and oligonucleotides (reporter probes). These probes are complementary to a specific region in the amplicon sequence and to a synthetic oligonucleotide sequence (antisense-reporter probe) immobilized on a nitrocellulose membrane strip. In the first step, *C. parvum* amplicon is mixed with the probe-tagged liposomes. Thus, if the target sequence (amplicon) is present, the reporter probes on the liposomes will bind to the target. Subsequently, the mixture is allowed to migrate along the membrane strip. If no target sequence is present, liposomes will bind (via the reporter probe) to the antisense-reporter probe immobilized in the first capture zone on the strip (see fig. 2.1). However, if amplicon is present in the sample, the reporter probes on the liposomes will have bound to the amplicon prior to entering the strip and therefore will not bind in the capture zone. The biotin that the liposomes also contain on their surface enables the binding of these liposomes to the second zone in which antibiotin antibodies are immobilized. Gray-scale densitometry is employed to quantify the amount of liposomes present in either zone.

The described assay format allows quantifying the presence (or absence) of liposomes in two zones (capture zone and antibiotin-antibody zone). Therefore, the results obtained from this assay are very accurate. Additionally, the format establishes an internal assay control.

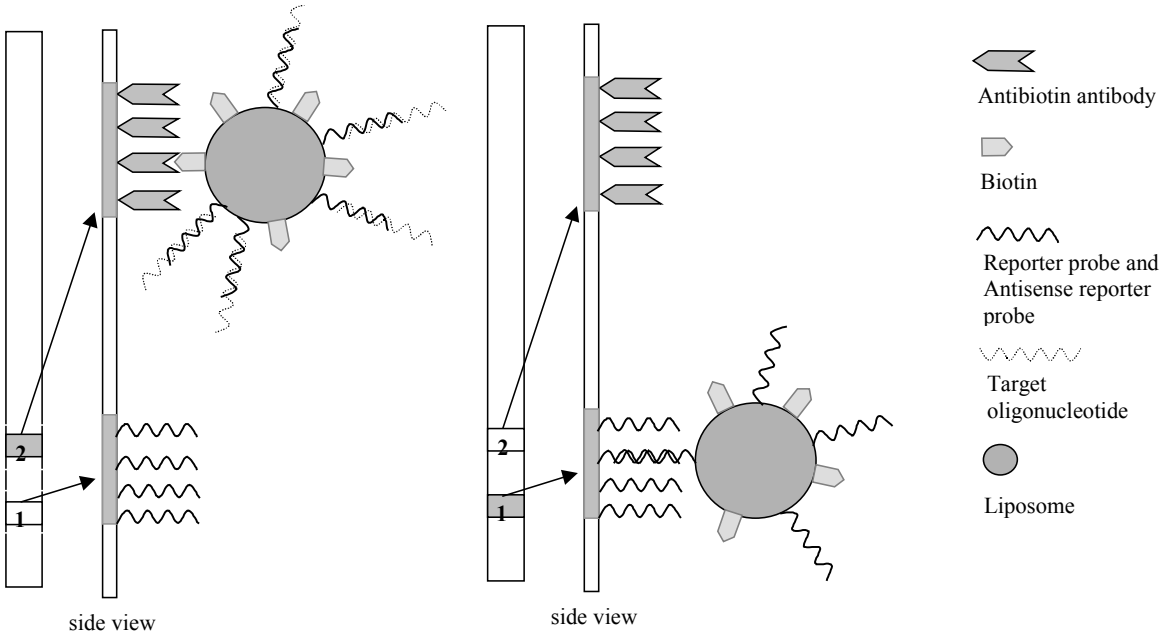

Fig. 2.1 Competitive assay format on a test-strip. The test-strip has two zones: 1) an oligonucleotide zone consisting of immobilized probe that is complementary to the reporter probe, and 2) an antibiotin-antibody zone. If the target RNA is present at the hybridization step, the liposomes bind to the antibiotin-antibody zone. Otherwise the liposomes bind to the oligonucleotide zone.

EXPERIMENTAL SECTION

REAGENTS

Common laboratory reagents were purchased from Sigma Chemical Co. (St. Louis, MO), Aldrich Chemical Co. (Milwaukee, WI), Boehringer Mannheim (Indianapolis, IN), or Fisher Scientific (Pittsburgh, PA). Ficoll Type 400, polyvinylpyrrolidone (PVP, 10,000 Da), and cholesterol were obtained from Sigma Chemical Co. Plastic-backed nitrocellulose sheets, 32 x 32 cm with 8 μm pore size came from Sartorius Co. (Goettingen, Germany). Sulforhodamine B dye and N-(4-(p-maleimidylmethyl) cyclohexane-1-carbonyl)-dipalmitoyl phosphatidyl ethanolamine (MMCC-DPPE) and dipalmitoyl phosphatidyl ethanolamine conjugated with biotin (DPPE-biotin) were obtained from Molecular Probes (Eugene, OR). The lipids

dipalmitoyl phosphatidyl choline (DPPC) and dipalmitoyl phosphatidyl glycerol (DPPG) were obtained from Avanti Polar Lipids Inc. (Alabaster, AL). Succinimidylacetylthioacetate (SATA) was purchased from Pierce (Rockford, IL). Nonfat dry milk (NFDM) was acquired locally (Geneva, NY). Polycarbonate syringe filters of 0.2, 0.4 and 3.0 μm pore size were purchased from Poretics (Livermore, CA). Antibiotin and streptavidin came from Rockland (Gilbertsville, PA). Test kits for Nucleic Acid Sequence-Based Amplification (NASBA™) were provided by Organon Teknika (Boxtel, The Netherlands).

OLIGOMERS

Since DNA is more stable than the NASBA-generated amplicon RNA, experiments for optimizing the test-strip were conducted with synthetic target DNA that has the same sequence as the amplicon. The 103-mer synthetic target DNA sequence (5'- aga agg acc agc atc ctt gag tac ttt ctc aac tgg agc taa agt tgc acg gaa gta atc agc gca gag ttc ttc gaa tct agc tct act gat ggc aac tga a - 3') and all other oligonucleotides used for this study were synthesized by the BioResource Center, Cornell University (Ithaca, NY). The reporter probe, a DNA 20-mer (5'- gtg caa ctt tag ctc cag tt - 3'), complementary to a part of the amplicon, was modified with a C3-amino-linker at the 3' end. An antisense sequence to the reporter probe was biotinylated at the 5' end and used as the capture probe.

ENCAPSULANT PREPARATION

A 150 mM sulforhodamine B solution was prepared in 0.02 M tris(hydroxymethyl)aminomethane (TRIS) buffer (pH 7.4) containing a volume fraction of 0.01% sodium azide. The final osmolality of this solution was 376 mOsmol/kg. To keep the liposomes intact, all other buffers used for liposome preparation were prepared with an osmolality of up to 50 to 100 mOsmol/kg higher than the encapsulant osmolality. Sucrose was used to adjust osmolalities.

LIPOSOME PREPARATION

Liposomes were prepared using a modified version of the reverse phase evaporation method described by Siebert and co-authors.[9] DPPC, DPPG, and cholesterol were dissolved in 8 mL of a solvent mixture consisting of chloroform, isopropyl ether, and methanol in a volume ratio of 6:6:1. DPPE-MMCC and DPPE-biotin were initially dissolved in a chloroform/methanol solution (volume ratio: 4:1) and an aliquot was added to the first lipid solution so that the final solution contained mole fractions of 3% and 0.2% of DPPE-MMCC and DPPE-biotin, respectively. While sonicating the suspension under a low stream of nitrogen at 45 ^{o}C, 2 mL of encapsulant were added. Using a vacuum rotary evaporator, the organic solvent was removed. The last two steps were repeated once. After the liposomes were formed, they were left for 10 min at 45 ^{o}C and finally forced twice through each of the 3.0 µm, 0.4 µm, and 0.2 µm pore-size polycarbonate syringe filters. Unencapsulated dye was separated from the liposomes by size-exclusion chromatography using Sephadex G-50-150.

When encapsulated in high concentrations, the fluorescence of sulforhodamine B undergoes self-quenching. Therefore, the encapsulation efficiency was determined by measuring the fluorescence intensity of liposome solutions before and after lysis at a wavelength of 596 nm (the excitation wavelength was 543 nm). Lysis was caused by adding 170 µL of 930 mM n-octyl-D-glucopyranoside to 3 mL of the liposome solution.

CONJUGATING REPORTER PROBES TO LIPOSOMES

The C3-amino-linker-modified reporter probe (105 mmol reporter probe dissolved in 0.05 M phosphate buffer, pH 7.8, containing 1 mM ethylenediaminetetraacetate (EDTA)) was derivatized with an acetylthioacetate group by incubation with 315 mmol of freshly prepared succinimidylacetylthioacetate (SATA) dissolved in DMSO (see fig. 2.2). After 90 min, the reaction was stopped with 41 µmol Tris-HCl (0.5 M stock solution). Hydroxylamine hydrochloride was used to deacetylate the acetylthioacetate-reporter probe to yield the reactive sulfhydryl group.

The reaction was allowed to proceed for 90 min and the pH was brought down to 7.0 by adding 0.5 M KH_2PO_4. For conjugation, the maleimide-tagged liposomes were reacted with SH-reporter probe for 4 hours at room temperature and then overnight at 4 ^oC. All unconjugated maleimide groups were capped with cysteine solution isotonic to the encapsulant. The liposomes were then purified on a Sepharose CL-4B column. The liposomes were kept in the dark at 4 ºC in Tris-HCl buffer with an osmolality 100 mOsmol/kg higher than the osmolality of the encapsulant. These storage conditions prevent leakage of dye from liposomes.

PREPARATION OF TEST-STRIPS

Nitrocellulose membranes were wetted for 20 min in 0.01 M K_2HPO_4/KH_2PO_4 buffer, pH 7.0, containing 0.15 M NaCl and a volume fraction of 10% methanol. They were then dried for 45 min under vacuum (15 psi) at 40 ^oC. The biotinylated antisense-reporter probe was incubated with streptavidin in a 4:1 molar ratio for 15 min. Using a thin-layer-chromatography plate applicator (Camag Scientific Inc., Wrightsville Beach, NC), we applied the mixture to the membrane 15 mm above the bottom edge. At 5 mm above the first band, a band of antibiotin was applied. The oligonucleotide was immobilized by baking at 55 ^oC for 60 min under vacuum (15 psi).

The coated nitrocellulose sheet was then immersed in the blocking agent (0.02 M Tris-HCl buffer, 0.15 M NaCl, pH 7.00 containing volume fractions of 5% PVP and 0.07% nonfat dry milk) for 30 min and dried for two hours at room temperature under vacuum. The membranes were stored in vacuum-sealed plastic bags at 4 ^oC and were cut into strips immediately prior to use. Each membrane was cut into 4.5 mm x 8 cm strips, so that, because of the way the upper and lower bands were applied, each strip contained 10 pmol of streptavidin and 40 pmol of antisense reporter probe in the first (oligonucleotide) zone, and 80 pmol of antibiotin antibody in the second (antibiotin) zone. The prepared test-strips are stored in vacuum-sealed bags at 4 °C. Under these conditions of storage, the authors were able to use them for up to 6 months after preparation.

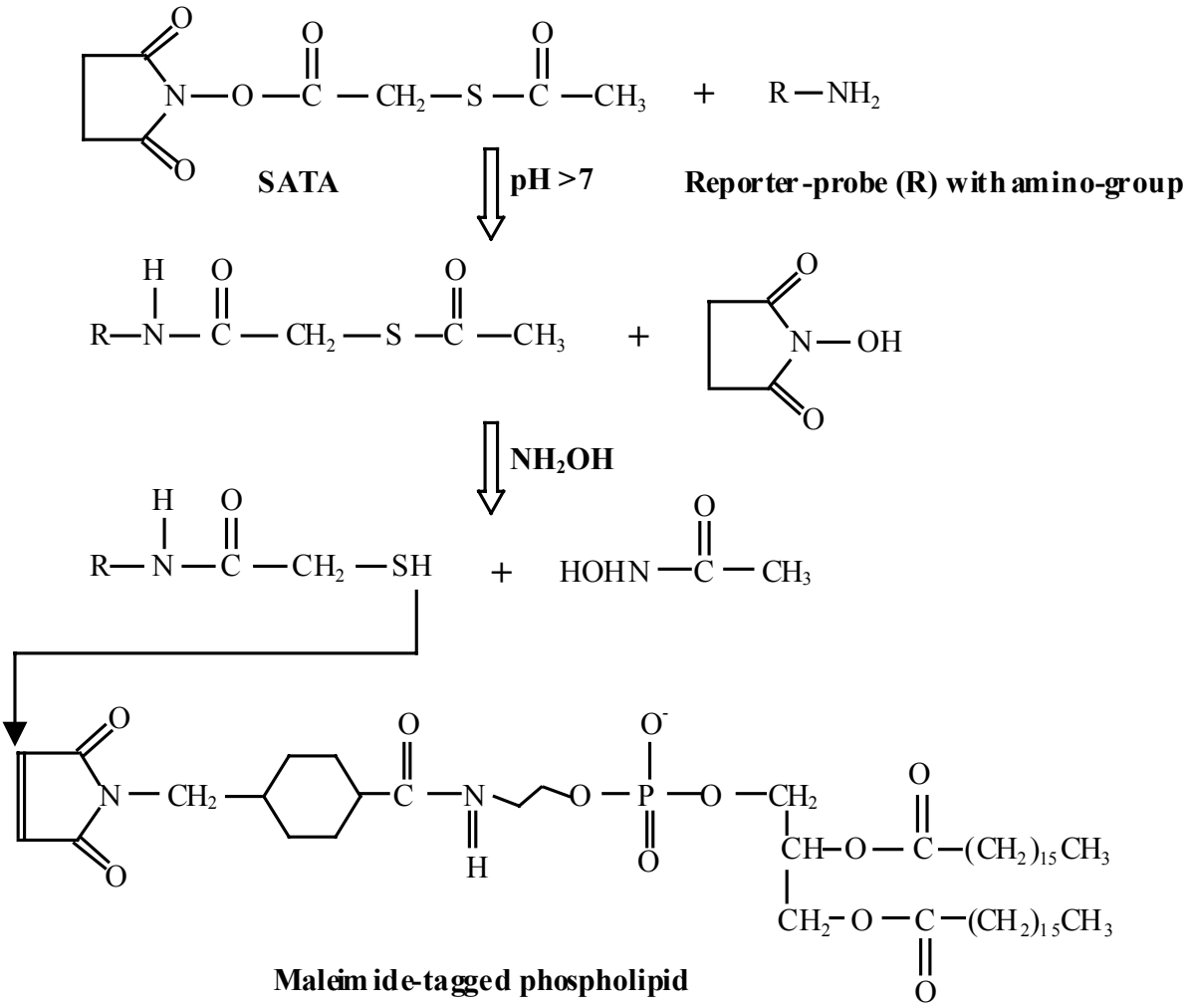

Fig. 2.2 Conjugation of reporter probe oligonucleotides to maleimide-activated phospholipids that are components of the liposomes. The reporter probes are modified so that they contain amino-groups at their 3′ ends. N-Succinimidyl S-Acetylthioacetate (SATA) reacts with the amino-groups, thereby forming acetylthioacetate (ATA)-tags on the reporter probes. Hydroxylamine (NH_2OH) then deprotects the ATA-tags and generates reactive sulfhydryl groups that bind to the maleimide-tags on the phospholipids.

ASSAY PROTOCOL

The hybridization was carried out in a 60 μL reaction mixture containing either synthetic target DNA or NASBA-generated amplicons and varying concentrations of formamide, Standard Sodium Citrate (SSC) solution (a 20x SSC standard solution contains 3 M sodium chloride and 0.3 M sodium citrate, pH 7.0), Ficoll Type 400, and sucrose. After 20 min incubation at 40 ^{o}C, the test-strip was placed into the test tube. It should be noted that the liposomes bind in either of the two zones under nonequilibrium, but steady-state, conditions. Therefore the test-strips were removed from the test solutions as soon as the liquid front reached the top edge of the strip.

DETECTION AND QUANTIFICATION

Gray-scale densitometry was performed with a scanner (Epson) and Scan Analysis™ software (Biosoft, Cambridge, UK). The red coloration is converted to gray-scale density, which can be quantified.

NUCLEIC ACID SEQUENCE-BASED AMPLIFICATION (NASBA)

The extraction of nucleic acids from *C. parvum* and the amplification of the mRNA coding for the heat shock protein (hsp70) by NASBA was conducted as described previously.[1] Briefly, the mRNA production in oocysts was stimulated by heating the oocysts for 20 min at 42 °C. The oocysts' membranes were disrupted by incubation in lysis buffer (provided in Qiagen RNeasy kit and Organon Teknika Boom extraction kit). NASBA reactions were performed on either hsp70 mRNA isolated from *C. parvum* oocysts, H_20 (negative control), or mRNA from other microorganisms (for specificity testing) using the Organon Teknika NASBA kit. The principles of NASBA are shown in fig. 2.3.

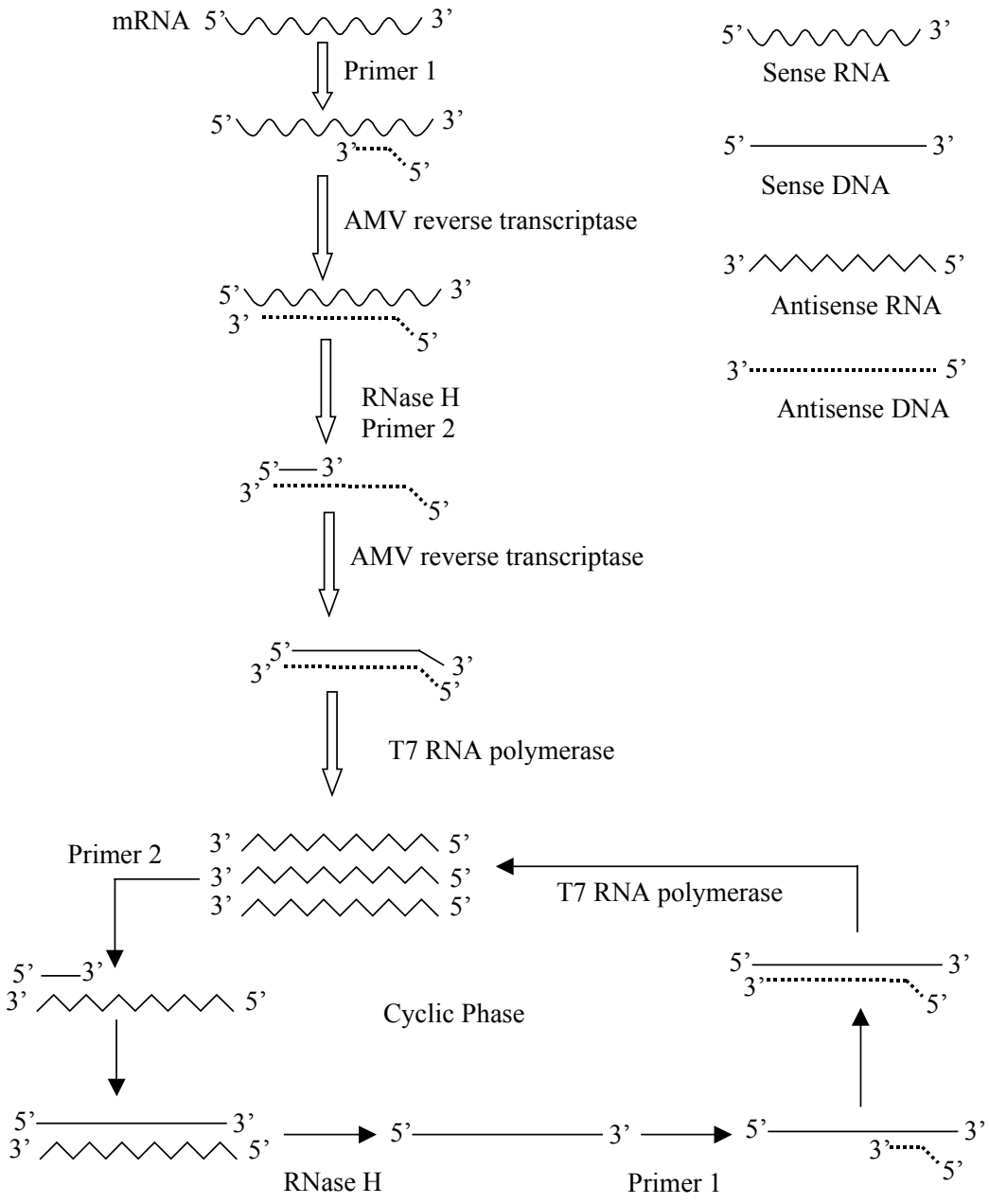

Fig. 2.3 NASBA amplification principle. The standard reaction NASBA mixture contains T7 RNA polymerase, RNase H, AMV (avian myeloblastosis virus) reverse transcriptase, nucleoside triphosphates, two specific primers and appropriate buffer components.

RESULTS AND DISCUSSION

CHARACTERIZATION OF LIPOSOMES

For this study, sulforhodamine B (SRB) was incorporated into liposomes. Since the fluorescence of the dye is quenched when encapsulated in high concentrations, the amount of dye that is not entrapped can be determined in a spectrofluorometer. Hence, intact liposome solutions show little fluorescence in contrast to lysed liposomes (free SRB in solution). An encapsulation efficiency of 3.3% was calculated after liposome preparation, assuming that the concentration of encapsulated SRB equaled the initial concentration of 150 mM.

OPTIMIZING THE TEST-STRIP

Detecting the sequence specific to *C. parvum* begins by hybridizing it to the reporter probes on the liposomes. The second hybridization takes place in the capture zone on the test-strip. To avoid false positive results, the hybridization should be as specific as possible. Therefore the components of the hybridization mixture need to be optimized with respect to hybridization stringency and also to liposome stability.

Stringency can be defined as the severity of the hybridization conditions used. Under conditions of high stringency, only duplexes of higher melting temperature remain annealed (hybrids in which the DNA sequences are perfectly complementary exhibit higher melting temperatures than those with mismatching bases). The melting temperature (T_m) is the temperature at which half of all hybridized duplexes are dissociated. For long oligonucleotides, it has been determined as:

$$T_m = \frac{81.5^{\circ}C + 16.6 \log [Na^+] + 0.41 (\%G+C) - 500}{n - 0.61 (\% \text{ formamide})}$$

with $[Na^+]$ being the concentration of Na^+ in mol/L, % formamide the volume percent of formamide in the hybridization medium, and n the length of the shortest chain in the

duplex.[10] Usually, hybridization occurs most readily at 25 ºC below the T_m of a hybrid. In practice, however, the optimum hybridization conditions must be determined empirically.[10]

To determine the optimum stringency conditions, varying concentrations of Standard Sodium Citrate (SSC) buffer and formamide were investigated. On the basis of these data, temperature and incubation time were optimized. Results were generated by testing duplicate strips with concentrations of synthetic target DNA of 0, 100, and 400 fmol per test. The gray-scale density in the oligonucleotide zone was plotted against the target concentration, and the data were fitted linearly. Table 2.1 summarizes the slopes of the generated curves. The slopes of the curves provide adequate information for comparing the sensitivity of the test under varying test conditions. In this context, a more negatively sloped curve indicates a higher sensitivity.

SSC concentration						
	2x	3x	4x	5x		
slope	-133	-173	-221	-174		
Formamide/volume fraction in %						
	15	20	25	30		
slope	-173	-183	-88	-11		
Incubation time/min						
	0	5	10	15	20	
slope	-89	-149	-175	-232	-315	
Temperature/°C						
	25	30	35	40	45	50
slope	-42	-95	-98	-252	-180	-208

Table 2.1 Optimizing the experimental conditions. Dose-response curves were generated from duplicate strips at target concentrations of 0, 100 and 400 fmol per test. The gray-scale density was measured in the oligonucleotide zone and plotted against the target concentration. By fitting the plots linearly we obtained slopes that indicate which assay conditions increase the sensitivity of the assay. (Since the gray-scale density in the oligonucleotide zone is highest for control samples that do not contain analyte and decreases with increasing analyte concentration, more negative slopes indicate a higher sensitivity).

The SSC concentration was optimized first. To provide an acceptable level of stringency, the experiment was initially conducted with a hybridization medium containing a volume fraction of 15% formamide and 15 min incubation at 40 °C. Although salt concentrations of 2x SSC in the hybridization solution are sufficient to provide osmotic conditions in which liposomes do not lose their integrity (at lower salt concentrations the liposomes lose part of the entrapped dye), the optimum SSC concentration was found to be 4x SSC. SSC concentrations higher than 4x SSC led to increasing (less negative) slopes, indicating a lower sensitivity.

The formamide concentration was optimized next. It is the second most important component since it provides stringency, but it produces lysis of liposomes at higher concentrations (fig. 2.4). When used in hybridization mixtures containing 4x SSC, with 15 min incubation time at 40 °C, increasing formamide concentrations up to a volume fraction of 20% in the test solution resulted in increased sensitivity. In the absence of formamide, hybridization at all target concentrations was very low. At volume fractions higher than 20%, the signal decreased. This was due to either liposome lysis (and thus fewer liposomes available for signal generation) or too stringent conditions (and thus fewer liposomes binding in the first capture zone).

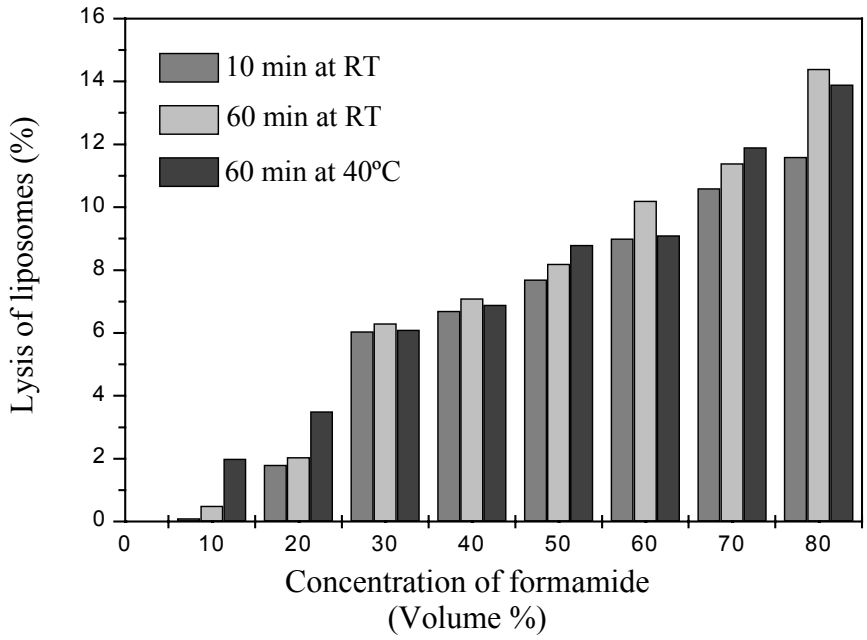

Fig. 2.4 Stability of liposomes in media containing 2x SSC and varying concentrations of formamide after 10 and 60 min of incubation. The percentage of lysed liposomes is plotted against the concentration of formamide in the solution.

For determining of the optimum assay temperature, the liposome–target mixtures were incubated at temperatures ranging from 25 to 50 °C. A temperature of 40 °C was found to be optimum (using 4x SSC and 20% formamide). Also, it was observed that longer incubation times resulted in higher sensitivity. The longest incubation time investigated was 20 min. Since it was desired to keep testing times as short as possible, longer incubation times were not investigated. Additionally, using a volume fraction of 0.2% Ficoll type 400 and 0.125 M sucrose in the incubation mixture improved the sensitivity of the test further.

The hybridization steps are influenced by the underlying hybridization kinetics. Wolf et al. found that hybridization rates for DNA attached to latex particles approach those of DNA in solution.[11] Because we use reporter probes that are end-linked to liposomes that are similar in size to the particles used by Wolf et al., solution hybridization kinetics should apply to the first hybridization step. Secondly, according to Reinhartz et al., who developed a paper chromatography hybridization assay (PACHA), the hybridization on the nitrocellulose strip is controlled by the flow velocity and by the volume of sample migrating across the oligonucleotide zone.[12] In our experiments, sample volume and flow velocity were held constant.

The assay format resembles a conventional competitive assay. Therefore, the tag density on the liposome surface and the amount of immobilized probes on the membrane were optimized in order to achieve maximum sensitivity. Initially, different amounts of reporter probe tags on the liposomes were investigated using liposomes with 0.1%, 0.2%, and 0.4% (mole fractions) tag. Tests with 0.4% tagged liposomes showed the highest resolution for analyte amounts between 0.1 pmol/test and 1 pmol/test. However, the highest sensitivity in the range between 0 pmol/test and 0.1 pmol/test and better reproducibility were achieved with 0.1% (mole fraction) tagged liposomes.

In initial experiments, we directly immobilized the antisense-reporter probes on the nitrocellulose strip. We obtained unreproducible results, possibly because the probes redissolved during membrane preparation and assay incubation steps (fig. 2.5). Thus, we used the principle of probe immobilization via biotin-streptavidin. The combination of 10 pmol of streptavidin and 40 pmol of biotinylated capture probe per strip gave the highest sensitivity. It was important to avoid biotinylated liposomes

binding to streptavidin in this capture zone. Thus, a high ratio of streptavidin and biotinylated probe (1:4, molar ratio) was used. Smaller and larger amounts of immobilized probe lowered the signal intensity in the oligonucleotide zone as well as the sensitivity of the test. Finally, the optimum amount of antibiotin-antibody immobilized in the antibiotin zone was determined to be 80 pmol per strip.

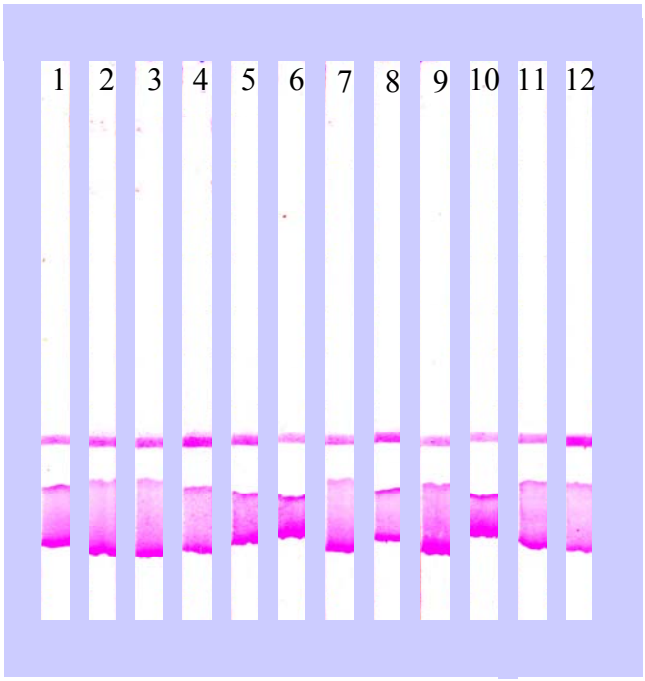

Fig. 2.5 Direct immobilization of capture probes on test strips caused irreproducible results: Assays were performed with target concentrations of 0 fmol/test (test strip # 1, 5, 9), 50 fmol/test (# 2, 6, 10), 100 fmol/test (# 3, 7, 11), and 400 fmol/test (# 4, 8, 12).

Determining the Limit of Detection

The detection limit was determined using the optimized assay described above. Amounts of synthetic target DNA ranging from 0 pmol to 2.9 pmol per assay were tested. Dose-response curves at the oligonucleotide and antibiotin zones were obtained by gray-scale densitometry (fig. 2.6 and 2.7). Fig. 2.8 shows one set of the test-strips from which the gray-scale values plotted in figures 2.6 and 2.7 were obtained. Both zones provide a region in which the exact amount of target can be determined (80 fmol/test to 2.9 pmol/test).

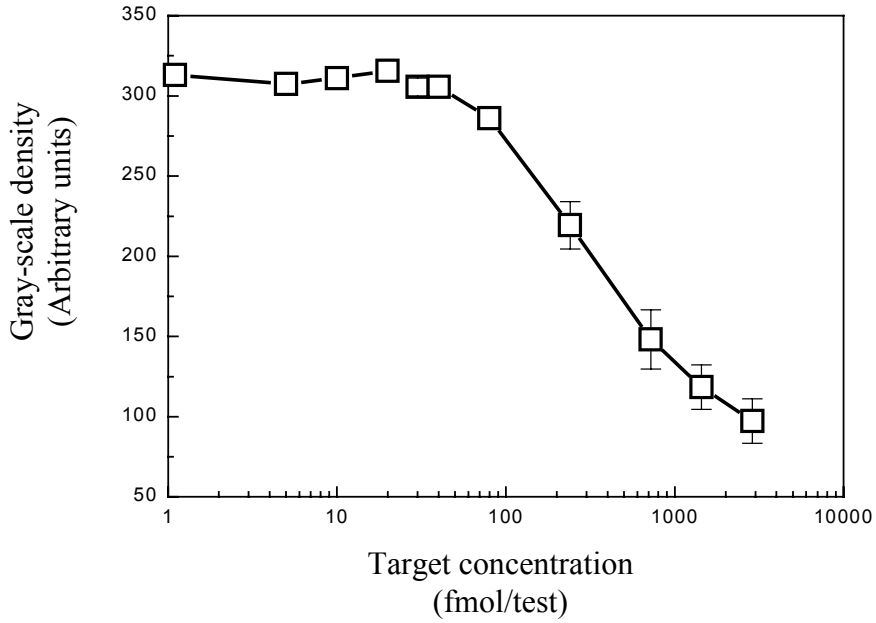

Fig. 2.6 Dose-response curve for the synthetic target, measured at the oligonucleotide zone. Each point represents the mean of three measurements. Error bars represent ±1 standard deviation.

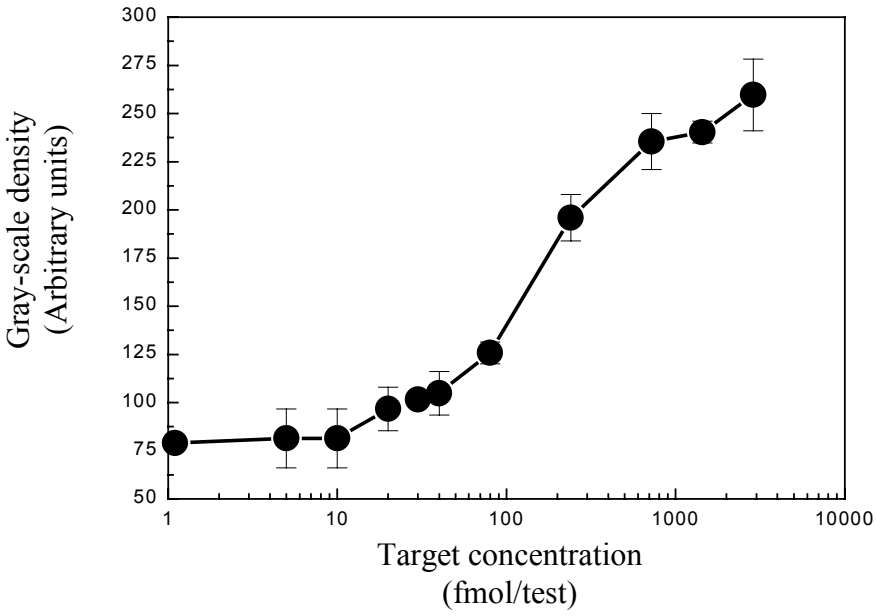

Fig. 2.7 Dose-response curve for the synthetic target, measured at the antibiotin-antibody zone. Each point represents the mean of three measurements. Error bars represent ±1 standard deviation.

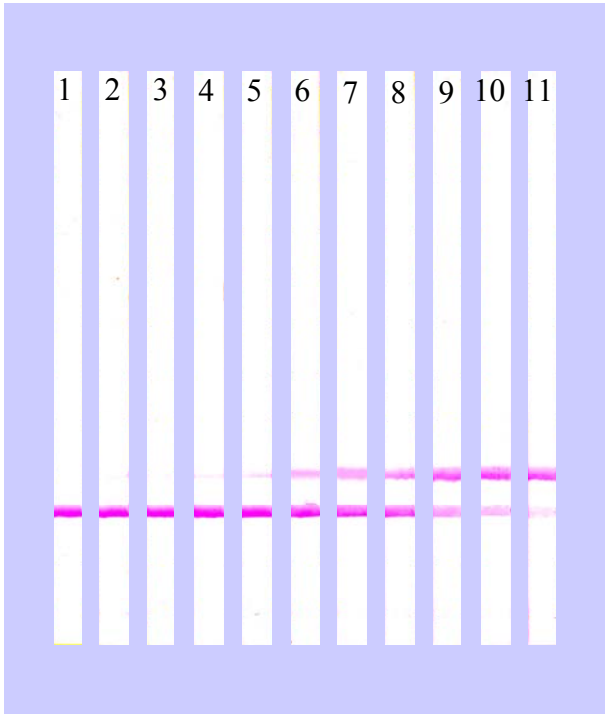

Fig. 2.8 Dose-response on test strips on which samples with varying target concentrations were detected: #1 = control; #2 = 5 fmol/test; #3 = 10 fmol/test; #4 = 20 fmol/test; #5 = 30 fmol/test; #6 = 40 fmol/test; #7 = 80 fmol/test; #8 = 240 fmol/test; #9 = 720 fmol/test; #10 = 1440 fmol/test; #11 = 2880 fmol/test.

The detection limit (defined as the smallest concentration of analyte that can be statistically distinguished with 99% confidence from the measurement value of the blank control) is, under optimum conditions, 80 fmol/test at both zones. Control experiments with liposomes that lack the reporter probe tag showed no observable binding at the oligonucleotide zone but strong binding at the antibiotin zone. The same result was obtained if the test-strip was not coated with probe in the oligonucleotide zone.

In contrast, the detection limit is 240 fmol/test when nonoptimized test strips that were coated with less or more capture probe than the optimum amount were used (combinations of streptavidin to capture probe used for these experiments were: 6.5 pmol to 26 pmol, 8 pmol to 32 pmol, 12 pmol to 48 pmol, and 13 pmol to 52 pmol; dose-response curves not shown).

The dose-response curves demonstrate that the test-strip assay is very sensitive. Two reasons account for this high sensitivity. First, the migration format brings the probes into close proximity with each other, thereby limiting the diffusional distances, i.e., minimal bulk diffusion of the reacting species. Second, the use of liposomes as

signal reporter-particles has advantages over the use of conventional reporter-particles such as latex, gold, or a single fluorophore. Large numbers of dye molecules can be incorporated into the liposomes, thereby increasing the measured intensity of the signal. By using liposome-tagged analytes in a competitive flow-injection immunoassay, Lee et al. demonstrated a thousandfold increase in sensitivity when compared with a single fluorophore-tagged analyte.[13] Furthermore, the two-dimensional fluidic nature of the liposome membrane allows the probes on the liposome surface to diffuse within the membrane.[14] After one event of binding to an immobilized probe occurs, additional probes on the same liposome move into positions where additional binding can take place, thereby reinforcing the initial binding event. Liposomes may also become deformed to bind to the immobilized oligonucleotide.

Although test-strips using a sandwich assay provide higher sensitivities (ca. 1 fmol per test, reported by Rule et al.[15]), the competitive assay format has advantages. It covers a wider range of detectable analyte concentrations, and it precludes the false-negative results at high analyte concentration that can occur in sandwich assays due to overloading the capture- and reporter probes, i.e., the so-called "hook effect." In the test that Rule et al. reported, false-negative results occurred at concentrations above 100 fmol/test. In addition, the second binding reaction of biotin to antibiotin antibodies can be used as an internal control. If no signal is obtained in either zone, it is clear that the assay was invalid, and thus no interpretation of data is possible.

Determining the Compatibility of the Test-Strip Assay with the NASBA Methodology

The test strip is designed to detect amplicons generated by NASBA from extracts of *C. parvum*. To prove that NASBA-generated amplicons can be detected with the developed test-strip, we conducted the following experiment. Water samples were spiked with ten oocysts of *C. parvum*. The samples then underwent an extraction procedure so that the DNA and RNA were released from the oocysts. The mRNA coding for the heat-shock protein hsp70 was amplified by using primers developed by Baeumner et al..[1] After the NASBA reaction was completed, we conducted assays in

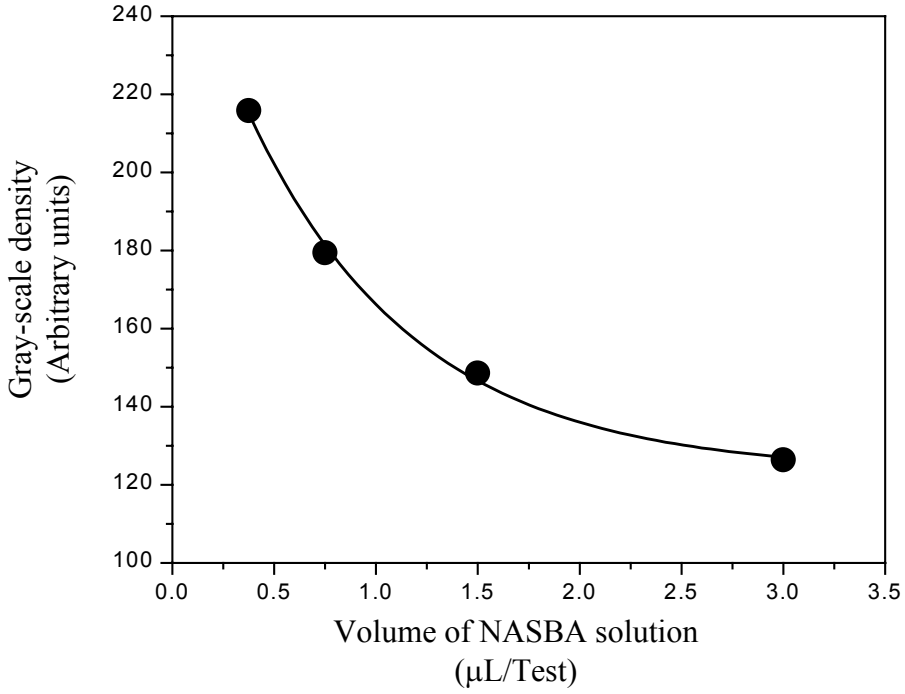

Fig. 2.9 Testing different volumes of RNA amplified by NASBA. Water samples were spiked with ten *C. parvum* oocysts. The RNA is extracted from the oocysts, and the amplicons are subsequently generated by amplification with NASBA methodology. The compatibility of the test-strip assay and NASBA is tested by conducting the assay with different volumes of the NASBA solution containing the generated amplicon. The gray-scale density was measured in the oligonucleotide zone and plotted against the volume of NASBA solution.

which we tested volumes of this solution ranging from 0.375 μL to 3.0 μL per test. The measured gray-scale density of the oligonucleotide zone was plotted against the solution volume (fig. 2.9) and, by using the dose-response curve, we correlated the gray-scale density to the amount of mRNA present in the sample. The measured gray-scale densities correlated to target concentrations that were in the dynamic range of the dose-response curve. For example, in the specific case of 0.375 μL NASBA solution per test, the gray-scale density correlated to 204 fmol of synthetic target sequence. As measured in the antibiotin-antibody zone, the estimated value of target was slightly higher. Any volumes of the NASBA mixture conducted with a negative control that did not contain oocysts gave signals that were always lower than the detection limit (in the oligonucleotide zone as well as in the antibiotin antibody zone).

SPECIFICITY OF THE TEST

Signals lower than the detection limit (and therefore identified as negative samples) were obtained when tests were conducted with solutions of NASBA extracts of organisms other than *Cryptosporidium parvum* (*Giardia lamblia*, *Cyclospora*, *Listeria iranovii*, *Listeria monocytogenes*, *Salmonella typhimurium*, *E. coli* culture no. a33, *E. coli* culture no. 43895; fig. 2.10), similar to results obtained earlier.[1] However, researchers should be aware of two recently published studies that report on *Cryptosporidium wrairi* and *Cryptosporidium meleagridis* having gene sequences that are identical (or matching to 98%) to the mRNA sequence utilized in this study.[16]

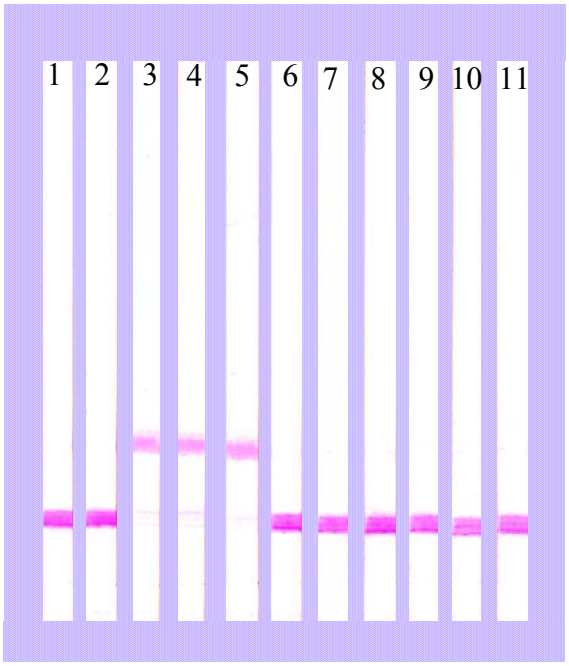

Fig. 2.10 Testing samples with organisms other than *C. parvum*. Assays were conducted with spiked samples that underwent extraction and amplification by NASBA: #1 = negative control (NASBA not conducted); #2 = negative control (NASBA conducted); #3 = 10 oocysts of *C. parvum*; #4 = 25 oocysts of *C. parvum*; #5 = 50 oocysts of *C. parvum*; #6 = 500 organisms of *Giardia lamblia*; #7 = 100 organisms of *Cyclospora*; #8 = 100 organisms of *Listeria iranovii*; #9 = 100 organisms of *Listeria monocytogenes*; #10 = 100 organisms of *Salmonella typhimunium*; #11 = 100 organisms of *Escherichia coli* culture # a33.

CONCLUSIONS

The author has developed a test-strip to be used for the rapid visual detection of amplified oligonucleotides. The assay was very sensitive and specifically detected RNA amplicons generated by NASBA from *C. parvum* hsp70 mRNA. The test-strip assay was shown to be compatible with the NASBA amplification methodology. The assay could be conducted in 30 minutes and is therefore much faster than oligonucleotide detection by Southern blotting or by agarose gel staining. Oligonucleotides that are separated using agarose gels are commonly stained by chemicals such as ethidium bromide, which poses a potential health threat. Our method avoids using such chemicals. The method is suitable for large-scale screening and for batch-processing analyses. Since the analyte concentration is directly related to the color intensity in the antibiotin zone, the unequivocal test result can easily be read. Because of the relative simplicity of the method, nontechnical personnel can easily perform the procedure.

One of the goals of this research was to demonstrate the applicability of the competitive assay format to a test strip on which liposomes indicate the presence of the target nucleic acid. Although the test was developed for *C. parvum*, the principles are transferable to any other organism by changing the oligonucleotides used as the reporter probe and as the antisense to the reporter probe.

3

Development of a Microfluidic Chip for the Detection of *Cryptosporidium Parvum* by Means of Fluorescent Signals Generated by Liposomes

ABSTRACT

This chapter describes a microfluidic chip that enables the detection of viable *Cryptosporidium parvum* by detecting RNA amplified by nucleic acid sequence-based amplification (NASBA). The mRNA serving as the template for NASBA is produced by viable *Cryptosporidium parvum* as a response to heat shock. The chip utilizes sandwich-hybridization by hybridizing the NASBA-generated amplicon between capture probes and reporter probes in a microfluidic channel. The reporter probes are tagged with carboxyfluorescein-filled liposomes. These liposomes, which generate fluorescence intensities not obtainable from single fluorophores, allow the detection of very low concentrations of targets. The limit of detection of the chip is 5 fmol of amplicon in 12.5μL of sample solution. Samples of *C. parvum* that underwent heat shock, extraction, and amplification by NASBA were successfully detected and clearly distinguishable from controls. This was accomplished without having to separate the amplified RNA from the NASBA mixture.

The microfluidic chip can easily be modified to detect other pathogens. We envision its use in μ-Total Analysis Systems (μ-TAS) and in DNA-array chips utilized for environmental monitoring of pathogens.

Modified from: Esch, M. B.; Locascio, L.; Tarlov, M. J.; Durst, R. A. "Detection of Viable *Cryptosporidium parvum* in a Microchip" *Analytical Chemistry*, **2001**, 73(13); 2952-2958

INTRODUCTION

BACKGROUND

The evaluation of environmental samples and the immediate and reliable assessment of possible risks caused by toxic or pathogenic contamination of the environment could be improved through the availability of inexpensive, field-portable testing equipment. For example, the analysis of toxic industrial wastes could be conducted without transporting samples back to a laboratory, thereby eliminating the variables associated with delays in testing. The same applies to the detection of agricultural contamination such as overdoses of herbicides and pesticides, and the detection of pathogens in water treatment facilities.

The efforts to develop field-portable testing devices include the downscaling of existing laboratory equipment to hand-held devices that contain chips (up to 4 cm long) with micrometer-scale features. Additionally, completely new detection schemes that can fit onto small platforms such as microchips are developed. Besides the ease of transporting such devices to the testing site, downscaling a detection scheme has significant other advantages.[1] The devices consume less reagent and less solution from the sample. Usually, multiple samples can be analyzed in parallel, thereby speeding up the analysis. The greatest advantage, however, is the low cost at which these devices can be produced.[1] This makes the development of analytical devices based on microchip formats very attractive to industrial companies. Starting in the early 1990s with only a few research groups working in this area, the field of biomicrochips and microfluidics is today one of the fastest growing fields in analytical chemistry.

Early research in the field of microfluidics resulted in the development of flow injection analysis (FIA) systems.[2] Several FIA systems were developed for the immunological detection of toxic agents.[3-6] However, while the amounts of sample and reagents needed were reduced because of the small capillaries used, the overall size of the FIA instruments was still quite large because appropriate pumps and valves were needed to control fluid flow.

These issues have recently been addressed by developing miniaturized pumps, mixers, and valves that are fabricated primarily in silicon as integrated parts of microfluidic systems.[7-10] Microfluidic systems that contain such valves and mixers are commonly referred to as microelectromechanical systems (MEMS).[11] Kovacs summarizes the special considerations that have to be taken into account when dealing with microfluidics as well as the most recent efforts that are being made in the area of MEMS.[11]

The most popular approaches to controlling fluid flow in microchannels utilize electroosmotic and electrophoretic effects caused by electric fields. These methods alleviate the need for micromechanical pumps and any moving parts within the microchips; however, electrodes have to be integrated into the microfluidic devices. Pumping schemes that use electrical effects include electroosmotic pumping and traveling-wave-induced electrohydrodynamic pumping (summarized by Fuhr and co-workers).[12]

Microfluidic systems are often developed for use in DNA analysis. One example in which the downscaling of the original laboratory version of equipment to a microchip format was successful is electrophoresis. Electrophoresis has been scaled down from slab-gel assays to capillary electrophoresis and, more recently, to microchannel electrophoresis,[13-15] so that the assay time is radically reduced from several hours to a few seconds.[16]

For medical applications, detection schemes have been developed in which the DNA of interest is first amplified in a microchip by polymerase chain reaction (PCR),[17-19] and then detected by microchannel electrophoresis.[20, 21] PCR products can also be detected by hybridizing them to probes that are immobilized in the chip by methods similar to those used for preparing DNA microarrays.[22, 23] Such techniques, together with a step for preparing the sample (for example filtration of cells from blood samples as developed by Wilding et al.[24]) can be combined into a continuous microfluidic system that will enable researchers to conduct analysis without manual intervention. In fact, the development of a device that allows the sample to be prepared, separated, amplified, and detected without intervention of the operator is the goal of many researchers. This kind of microdevice has often been referred to as a microanalytical laboratory or “lab-on-a-chip.”

THE CONCEPT OF THE MICROFLUIDIC CHIP

In this chapter of the dissertation the author describes the development of a microchip that enables the detection of viable *C. parvum* via the detection of the organism's mRNA amplified by NASBA.[25] The detection is based on sandwich hybridization of capture probes, amplicon, and reporter probes. The capture probes are immobilized on the bottom of a microfluidic channel by sulfur-gold linkages. Reporter probe-tagged liposomes (filled with carboxyfluoresceine) are employed to generate signals indicating the presence or absence of the mRNA by fluorescence (see fig. 3.1).

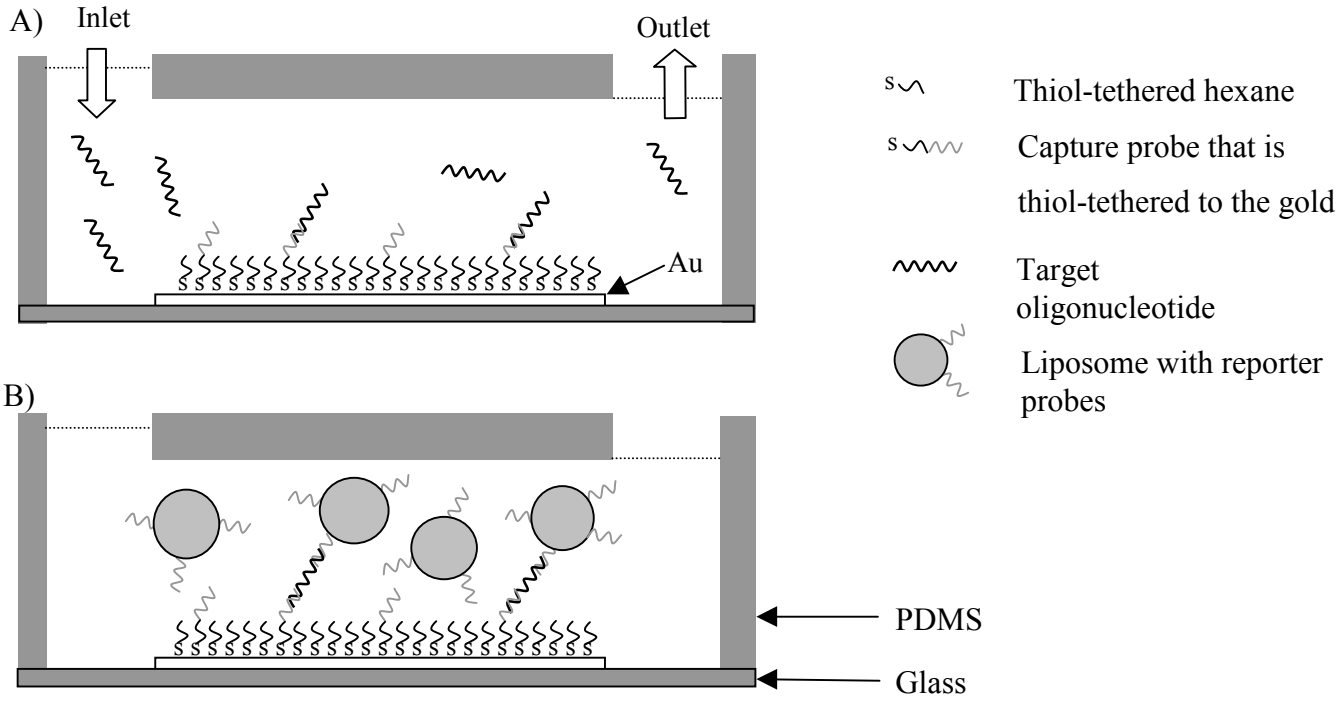

Fig. 3.1 Detection of target oligonucleotide in a microchannel (cross-section through the channel, not to scale). (A) The target hybridizes to DNA-probes (capture probes) that are bound to the surface by sulfur–gold linkages. (B) After washing excess target away, DNA (reporter probe)-tagged liposomes are introduced into the channel and bind to the already hybridized targets. The amount of bound liposomes is directly related to the amount of target present in the sample. The liposomes can be detected by fluorescence microscopy.

The microchannels are fabricated in poly(dimethyl siloxane) (PDMS), a soft plastic that can be molded using a technique called soft lithography. The small dimensions of the microchannel allow us to use very small amounts of the liposome reagents in our assay. A constant flow of liposomes through the channel reduces the limitation on the rate of hybridization imposed by diffusion processes. The speeded-up reaction enabled us to detect the target far more rapidly. By exchanging the oligonucleotides used as capture- and reporter probes, researchers can easily modify the chip to detect other pathogens. Therefore, the sensor can be applied in DNA-array chips used for multianalyte detection.

EXPERIMENTAL SECTION

OLIGOMERS

The sequences of the target, the capture probe, and the reporter probe are described in chapter 2. The reporter probe was modified with a C3-amino-linker at the 3' end. The capture probe was modified with a $-CH_2)_6$-S-S-$(CH_2)_6$OH at its 5' end. All modifications were carried out by the BioResource Center, Cornell University (Ithaca, NY).

PREPARATION OF ACETYLTHIOACETATE (ATA)-TAGGED LIPOSOMES CONTAINING CARBOXYFLUORESCEIN

The liposome encapsulant, a 100 mM carboxyfluorescein solution, was prepared in 0.02 M HEPES (N-2-Hydroxyethyl-piperazine-N'-2-ethanesulfonic acid) buffer (pH 7.5, 421 mOsmol/kg). Although carboxyfluorescein is not particularly photo-stable we used it as encapsulant because in previous applications we observed good encapsulation efficiencies when this dye was incorporated into liposomes. The liposomes were prepared based on a method published by Siebert et al.[27] This method differs from the one described in chapter 2. We have developed it further, and we therefore describe it here in detail.

We obtained the phospholipids dipalmitoyl phosphatidyl choline (DPPC), dipalmitoyl phosphatidyl glycerol (DPPG), and dipalmitoyl phosphatidyl ethanolamine (DPPE) from Avanti Polar Lipids Inc. (Alabaster, AL). We prepared a solution containing 7.2 μmol of DPPE and a volume fraction of 0.7% triethylamine in chloroform. We reacted this solution with 14.3 μmol of N-succinimidyl-S-acetylthioacetate (SATA, purchased from Pierce, Rockford, IL) to form DPPE-acetylthioacetate (DPPE-ATA). We then prepared a lipid solution containing 40.3 μmol DPPC, 4.2 μmol DPPG, and 40.9 μmol cholesterol dissolved in 8 mL of a solvent mixture consisting of chloroform, isopropyl ether, and methanol in a volume fraction ratio of 6:6:1. To this lipid solution, we added an aliquot of DPPE-ATA so that the final solution contained a mole fraction of 4% DPPE-ATA. While sonicating the lipid suspension under a low stream of nitrogen at 45 ^{o}C, we added 2 mL of encapsulant. We then removed the organic solvent, using a vacuum rotary evaporator. Each of the last two steps was repeated once. After the liposomes were formed, we let them remain under nitrogen for 10 min at 45 ^{o}C, then forced them through a final series of polycarbonate syringe filters with pore sizes of 3.0 μm, 0.4 μm, and 0.2 μm. We separated unencapsulated dye from liposomes by size-exclusion chromatography using Sephadex G-50-150 (Sigma Chemical Co., St. Louis, MO). To prevent liposomes from lysing during the separation, we used sucrose to adjust the osmolality of the buffer (0.01 M HEPES, 0.2 M NaCl, pH 7.5) to 520 mOsmol/kg. The liposomes were then dialyzed for 12 h at 4 ^{o}C against the same buffer and recovered approximately 13 mL of solution. We used dynamic light scattering to measure the diameter of the prepared liposomes, finding it to be 349 nm with a 95% confidence interval of 318 nm to 379 nm.

CONJUGATING REPORTER PROBES TO ATA-TAGGED LIPOSOMES

Two simultaneous preparations were required. First, we derivatized the C3-amino-linker-modified reporter probes (dissolved in 0.05 M phosphate buffer, pH 7.8, with 1 mM EDTA) with maleimide groups by incubating them with three times the molar quantity of N-(κ-maleimidoundecanoyloxy)sulfosuccinimide ester (sulfo-KMUS) dissolved in dimethyl sulfoxide (DMSO) (see fig. 3.2). The reagents were

allowed to react for 3 h at room temperature. Second, and at the same time, we deacetylated the ATA-groups on the liposome surface to yield unprotected thiol groups. For this reaction, we prepared a 0.5 M hydroxylamine hydrochloride solution with 25 mM EDTA in 0.1 M HEPES buffer. We then gently mixed a 1.4 mL aliquot of the liposome solution recovered from dialysis with 140 μL of the hydroxylamine

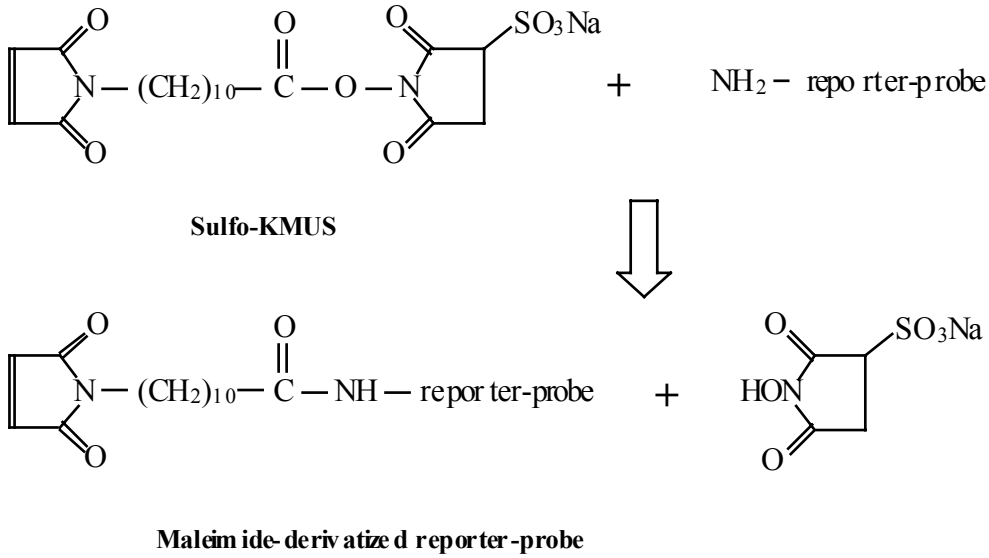

Fig. 3.2 Reaction of C3-amino-linker-modified reporter probes with N-(κ-maleimidoundecanoyloxy)sulfosuccinimide ester (sulfo-KMUS). The products of the reaction are reporter probes tagged with maleimide groups. These are then used to react with thiol groups on the surface of the liposomes.

hydrochloride solution. The reaction was allowed to proceed at room temperature in the dark for 2 h. For conjugation, we reacted the thiol groups on the liposome surface with the reporter probes we had derivatized using the maleimide groups for 4 h at room temperature and then overnight at 4 ^{o}C, at a pH of 7.0 throughout. All unconjugated thiol groups were quenched with ethylmaleimide solution isotonic to the encapsulant. The liposomes were then purified on a Sepharose CL-4B column (Sigma Chemical Co., St. Louis, MO) equilibrated with 0.02 M Tris-HCl buffer pH 7.0 (containing 0.15 M NaCl and sucrose) with an osmolality of 520 mOsmol/kg. The recovered liposomes were stored at 4 ^{o}C. When stored under these conditions, we were able to use the

liposomes for up to 9 months without observing high losses of dye (due to possible leaking) or of capture probes.

Preparation of Capture Probe/Hexane Monolayers on Gold-Covered Glass Slides

Microscope glass slides (Corning Inc., Corning, NY) were cleaned for 30 min in 70% (volume fraction) concentrated sulfuric acid and 30% (volume fraction) hydrogen peroxide (30% (volume fraction) H_2O_2 in H_2O). *Warning! This cleaning solution is extremely oxidizing, reacts violently with organics, and should be stored only in containers that are loosely hand-tightened so that no pressure builds up.* The glass slides were then rinsed with 18 MΩ deionized water and dried under a nitrogen stream.

Using a thermal evaporator and a metal mask, we deposited a 15 Å chromium layer and a 450 Å gold layer on a 15 x 15 mm area of the slides. After the deposition, we cleaned the slides thoroughly with the cleaning solution described above. We then immersed the slides for 60 min in a 1 mM solution of the disulfide-modified capture probe (diluted in 1 mM potassium phosphate buffer, pH 7.0). We washed the slides with 18 MΩ water and immediately immersed them into a 1 mM mercaptohexane solution diluted in ethanol. After 60 min, we washed the slides with ethanol and carefully dried them with nitrogen.

Preparation of the Microfluidic Chip

The microfluidic channels were fabricated using the technique shown in fig. 3.3. First, we used contact-photolithographic and wet-chemical etching methods to produce a silicon template containing negative three-dimensional images of the channels, each 300 μm wide and 50 μm high (see chapter 4, page 65 for a detailed description of the fabrication). We then used the finished silicon template to mold microchannels. To prepare the microchannels, we covered the silicon template with liquid poly(dimethyl siloxane) (PDMS; Sylgard, 184 Silicone Elastomer, Dow Corning Co., Midland, MI). After curing the PDMS for 60 min at 60 ^{o}C, we peeled off the channels from the

template. We then sealed the PDMS channels to the glass slides that we had modified with capture probes and hexane, as described above.

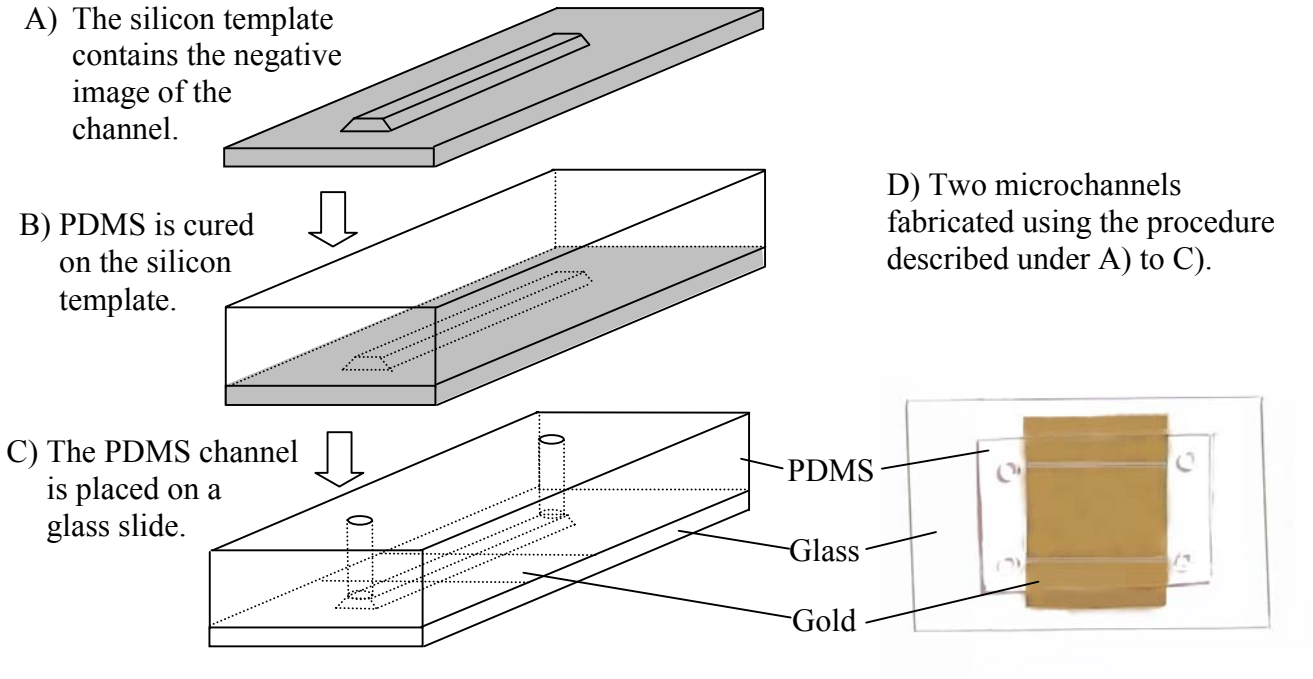

Fig. 3.3 Fabrication of a microchannel that consists of PDMS side and top walls and a glass bottom. The negative image of the channel is fabricated in silicon (A) by standard photolithography and KOH etch. The silicon wafer is then used as a template on which PDMS can be cured (B). After curing, the PDMS channel is taken off the template and placed on a glass slide that contains a region on which gold had been deposited (C). The inlet and outlet are cut into the PDMS. Photograph (D) of two microchannels fabricated using the described procedure.

ASSAY PROTOCOL

To induce the flow of aqueous solutions by gravity, we first primed the microfluidic channels with ethanol and subsequently slowly replaced the ethanol solution with aqueous buffer. After the substitution, we filled the inlet well with 12.5 μL buffer, and the outlet well with 5 μL buffer. We tilted the channels to an angle of 30^{o} so that the resulting flow would be driven by gravity. The flow velocity was 92.4 μm/s with a standard deviation of 5.4 μm/s. This corresponds to a flow rate of 1.5 ± 0.09 nL/s. A solution of blocking liposomes was then introduced into the channel for 30 min. The blocking liposomes were filled with buffer instead of carboxyfluorescein and did not have the reporter probe tag on the surface. After rinsing with buffer, we conducted the assay as shown in fig. 3.1.

We filled the inlet well with 12.5 μL of sample solution containing either synthetic DNA or RNA amplified by NASBA in hybridization buffer. The final concentrations of the components in this solution were 0.6 M NaCl, 0.06 M NaH_2PO_4, 2 mM EDTA (2 times concentrated Standard Saline Phosphate buffer with EDTA (2 x SSPE)) and a volume fraction of 40% formamide. The hybridization was allowed to proceed for 30 min. We then washed the channels with 2 x SSPE buffer. Next, we introduced the reporter probe-tagged liposomes into the channel. The final concentrations of the components in this solution were a volume fraction of 5% of liposome solution (as recovered from the Sepharose column), SSPE concentrated four times (4 x), a volume fraction of 20% formamide, a volume fraction of 0.2% Ficoll (type 400), and 0.125 M sucrose. This buffer had been previously optimized for use with liposomes in hybridization studies (see chapter 2 and Esch et al.).[28] After 30 min of hybridization, we washed the channel with a buffer containing 2x SSPE and a volume fraction of 50% formamide for 5 min.

DETECTION AND QUANTIFICATION

Using a standard fluorescence microscope equipped with a 20x long-distance working objective and a digital camera (C4742-95, Hamamatsu, NJ, U.S.A.), we acquired images of the liposomes bound in the channel. The fluorescence was quantified using software acquired from Carl Zeiss Incorporation (Thornwood, NY). To obtain accurate measurements of fluorescence, we acquired all images using the same acquisition time and we avoided bleaching of the samples by not exposing them to the light source beforehand.

NUCLEIC ACID SEQUENCE-BASED AMPLIFICATION (NASBA)

Samples were produced by extracting the mRNA from *C. parvum* and conducting NASBA using the procedure as described in chapter 2. It should be noted that the product of this amplification method is a complementary RNA to the mRNA that *C. parvum* produces as a response to heat shock.

RESULTS AND DISCUSSION

DESIGN AND FABRICATION OF THE MICROFLUIDIC CHIP

In order for a microfluidic chip to detect RNA or DNA, the chip must be designed with special attention to the detection method as well as to methods for immobilizing capture probes in the chip. The goal in this study was to design a chip that could be used for fluorescent detection by means of microscope and CCD camera and that could be easily modified to utilize interdigitated microelectrode arrays for electrochemical detection. Other requirements were that the chip should be easy to fabricate and, if possible, should also be reusable.

When choosing the materials from which the chip could be fabricated, it is important to consider the suitability of that material for immobilizing oligonucleotides on its surface. Researchers have deployed various materials to immobilize oligonucleotide probes. In this project we use a gold surface for this purpose. We first

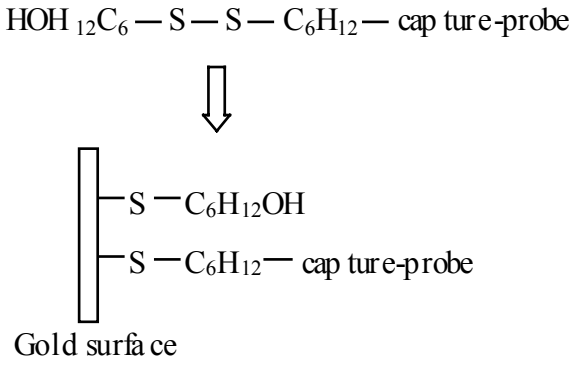

Fig. 3.4 Immobilizing capture probes on a gold surface. The capture probe is first modified with a dithiol at the appropriate end. When diluted in 1 mM phosphate buffer the capture probes self-assemble on the gold surface by means of thiol–gold linkages.

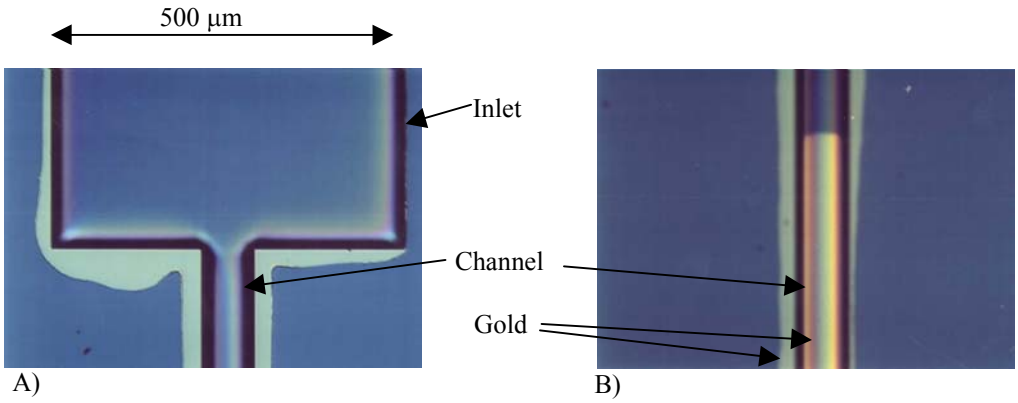

Fig. 3.5 Silicon wafer containing a 50 μm deep microfluidic channel. Gold was deposited onto the bottom of the channel. The top edge of the channel is covered with gold: (A) Inlet and beginning of the channel; (B) Middle section of the channel.

modified the oligonucleotide with a dithiol group at the appropriate end, and then we placed the oligonucleotide, diluted in a phosphate buffer, on a cleaned gold surface. A monolayer of olignucleotides will then self-assemble on the gold (fig. 3.4).[29] This method is easy to utilize and to reproduce.

During the course of this project the developed chip underwent several iterations in which its functionality improved. The first concept for the chip's design was to fabricate a microchannel in a silicon substrate. We deposited gold on the bottom of the channel and then anodically bonded a glass chip that has the same thermal expansion coefficient as the silicon chip to the top opening of the channel. Although this design was useful for detecting fluorescence, we were not successful with integrating interdigitated microelectrodes for electrochemical detection into this chip. Integrating such electrodes requires that their contacts be accessible outside of the channel while the channel remains completely sealed. The first design concept did not meet this requirement, since the channel must be sealed by bonding it anodically to a glass chip. This procedure requires completely flat and clean surfaces without depositions (such as the electrode contacts). Another disadvantage of the silicon–glass chip is that silicon is conductive. It therefore needs to be covered with insulating layers of silicon dioxide and silicon nitride to provide insulation for electrochemical measurements. This requires an additional step during the fabrication.

Finally, the deposition of gold on the bottom of the channel was not always successful since it also deposited on the top edges of the channel as fig. 3.5 shows. The reason that the gold is deposited on the outside edges is that the already etched channel is unevenly covered with photoresist (fig. 3.6).

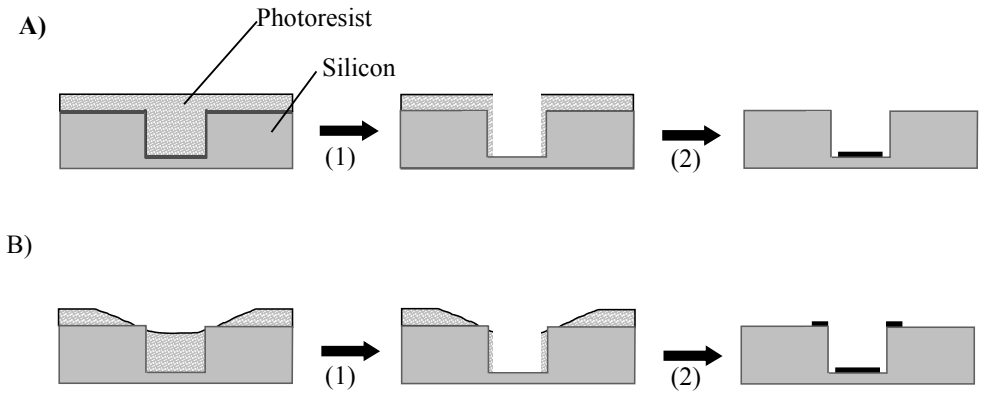

Fig. 3.6 Ideal and actual deposition of gold onto the bottom of a 50 μm deep channel in silicon: (A) In the ideal case the photoresist covers the channel and the surface of the wafer evenly. The area in the channel on which the gold will be deposited is exposed to UV light and the photoresist in this area will dissolve in a developing solvent (step 1). Subsequently, gold is deposited on the entire wafer and the photoresist is developed, thereby lifting off the gold covering it (step 2). Only the initially developed area remains covered with gold. (B) A possible reason for gold being deposited on the top edges of the channel is an uneven coverage of the wafer with photoresist caused by the entrapment of most of the photoresist in the channel and an outward movement of the remaining resist during the spinning process.

On the other hand, the use of a glass–PDMS chip enabled the microelectrodes to be integrated. The electrodes and the gold field for immobilizing the capture probes were deposited on the glass. We then fabricated microchannels in PDMS by soft lithography methods as introduced by Whitesides and colleagues. The glass chips sealed to the open bottom of the PDMS channel (see fig. 3.3). Since PDMS seals to glass even when gold depositions are present, the integration of electrodes could be accomplished with this design.

The glass–PDMS chip features several other advantages in comparison with the silicon chip. While the silicon needs to be wet-etched from the backside to yield holes serving as inlet and outlet, holes can easily be cut into the cured PDMS using a scalpel. This eliminates aligning the mask for the holes and depositing photoresist as well as the

additional wet-etch. Since the sealing of glass and PDMS is not permanent, the PDMS channels can be removed from the glass and reused with new glass chips. This shortens the time needed to prepare each chip. Fabricating glass–PDMS chips is generally easier and less time-consuming than fabricating silicon chips.

For these reasons, we used the glass–PDMS chip for all experiments in which microchips are employed. The author describes the fabrication protocol in detail in the experimental section. The results obtained when using the chip with fluorescent detection are described in the following paragraphs. The results obtained when using the chip with electrochemical detection are summarized in chapter 5.

MINIMIZING THE BACKGROUND SIGNALS GENERATED IN THE CHIP

Initial experiments showed that the sensitivity of our chip is limited by the background signal it generates when no target is present if the gold surface has been modified with capture probes only. Fig. 3.7A and fig. 3.7B show fluorescent images of channels in which the assay was conducted with a positive sample (containing synthetic target at a concentration of 400 fmol/μL) and a control. The fluorescence obtained from these two images does not differ because target and liposomes adsorb nonspecifically to the gold surface.

A study by Levicky et al. suggests that, in mixed monolayers consisting of capture probes and mercaptohexanol (both bound to gold by means of a sulfur–gold linkage), the mercaptohexanol can act as a passivating reagent that prevents nonspecific adsorption of the target oligonucleotide.[30] Besides passivating the gold surface, the mercaptohexanol also forces the sulfur-bound capture probes to be oriented upward from the surface, making them more accessible for hybridization.[30]

To test the effectiveness of such a mixed monolayer for preventing nonspecific adsorption of targets and liposomes in our chip, we conducted assays in channels modified with capture probes and mercaptohexanol. Fig. 3.7C and fig. 3.7D show that the fluorescence obtained from a positive sample and a control remained the same, suggesting that the mixed layer did not prevent the liposomes from absorbing nonspecifically. We therefore prepared mixed layers of capture probes and various other passivating reagents and conducted assays in which we measured the fluorescence

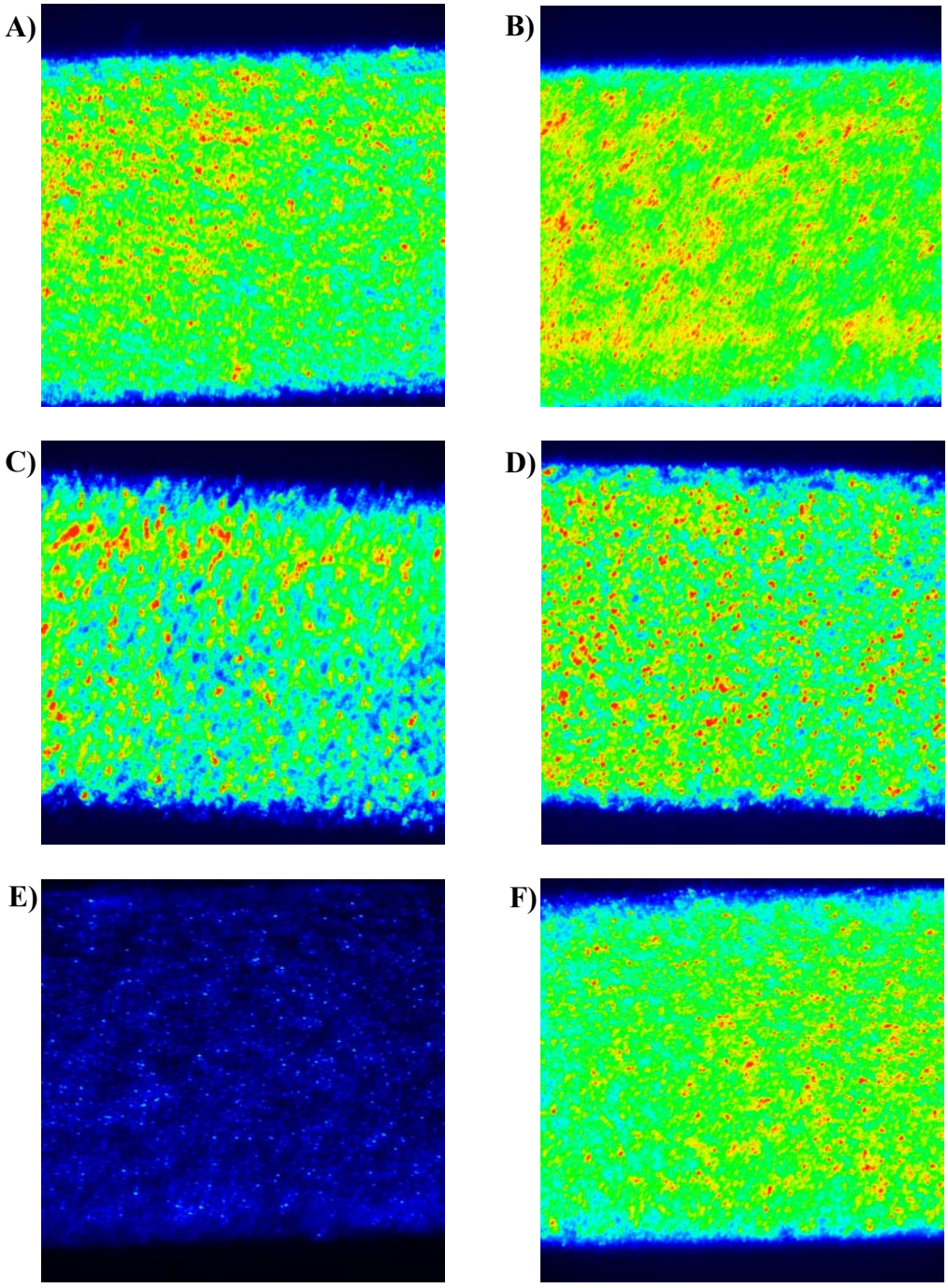

Fig. 3.7 Fluorescent images of channels that were not treated with any blocking reagent: (A) no analyte present; (B) analyte concentration is 400 fmol/μL. Images of channels treated with mercaptohexanol: (C) no analyte present; (D) analyte concentration is 400 fmol/μL. Images of channels that were treated with mercaptohexane and blocking liposomes: (E) no analyte present; (F) analyte concentration is 400 fmol/μL. Low fluorescence is indicated by blue coloration, medium fluorescence by green, high fluorescence by yellow, and very high fluorescence by red.

Blocking Reagent	Difference in the fluorescence obtained for solutions with target concentrations of 0 and 400 fmol/μL (arbitrary units)
No Blocking	65 ± 540
Mercaptohexane and Blocking Liposomes	1610 ± 181
Blocking Liposomes	1556 ± 207
Mercaptohexane $HS(CH_2)_5CH_3$	1307 ± 567
Bovine Serum Albumin (BSA)	1305 ± 337
Alkylated 1-Thiahexa(ethylene oxide) $HS(CH_2CH_2O)_6C_{10}H_{21}$	916 ± 1047
Oligo(ethylene glycol)-terminated Thiol $HS(CH_2)_{11}(OCH_2CH_2)_6OH$	484 ± 372
Mercaptohexanol $HS(CH_2)_6OH$	110 ± 254
Mercaptopropionic Acid $HS(CH_2)_2COOH$	-138 ± 247

Table 3.1 Differences in fluorescence obtained for sample solutions containing synthetic target in concentrations of 0 and 400 fmol/μL solution in sensors modified with different blocking reagents. Each number represents the mean of three experiments ± one standard deviation.

generated by triplicates of positive samples (solutions containing synthetic target at a concentration of 400 fmol/μL) and negative controls. The differences between the fluorescence intensities of the controls and the positive samples that are obtained using different blocking reagents are listed in table 3.1. The greatest difference in fluorescence was generated using a blocking layer that combined mercaptohexane and untagged liposomes that contain buffer instead of dye ("blocking liposomes"). Fig. 3.7E and fig. 3.7F show fluorescent images of channels that are treated with mercaptohexane and blocking liposomes. There are two ways in which this blocking

layer passivates the gold. The capture probes and mercaptohexane yield a mixed monolayer that appears to resist the nonspecific adsorption of the negatively charged liposomes. Nonspecific binding is further decreased by presaturating the surface with blocking liposomes. We found that mercaptohexane and blocking liposomes worked very well as passivating reagents when each was used independently of the other. However, the degree of passivation was increased when these two blocking reagents were combined. A possible explanation is that the mixed monolayer of capture probes and mercaptohexane still contains small areas in which the formation of the layer is not complete. The blocking liposomes adsorb to these areas. Because blocking liposomes don't contain carboxyfluoresceine and are not tagged with reporter probes, they do not interfere with the assay. They decrease the background signal because they adsorb to the areas to which otherwise carboxyfluoresceine-filled liposomes would have nonspecifically adsorbed during the assay.

We also tested bovine serum albumin (BSA) as a passivating reagent. BSA has been successfully employed for blocking nonspecific binding in immunoassays[31] and on test strips.[25] Our experiments showed that treating the gold surface with BSA reduces nonspecific liposome adsorption to approximately the same degree as a mixed monolayer of mercaptohexane and capture probes.

Although monolayers consisting of alkylated 1-thiahexa(ethylene oxide) compounds, and oligo(ethylene glycol)-terminated layers are known to resist the adsorption of certain proteins on gold,[32, 33] these reagents did not generate great differences in fluorescence intensity between the controls and the positive samples. A similar result was found for mixed monolayers with capture probe and 3-mercaptopropionic acid.

DETERMINING THE LIMIT OF DETECTION

The limit of detection was determined by exposing the chip (modified with a mixed layer of capture probe, mercaptohexane, and blocking liposomes) to 12.5 μL of sample solutions that contained synthetic target oligonucleotide in concentrations ranging from 0 to 800 fmol/μL. Plotting the measured fluorescence against the analyte concentration yielded the dose-response curve shown in fig. 3.8. The lowest detectable target concentration was 0.4 fmol/μL. We define the limit of detection as the analyte

concentration at which the confidence interval yielded by doubling the calculated standard deviation of the fluorescence obtained for this concentration does not overlap with the same interval from controls.[34, 35] At a target concentration of 0.4 fmol/μL this interval ranges from 897 to 1833 (arbitrary units for fluorescence) and does not overlap with the interval for the control sample [462-846 (arbitrary units)]. The calculated detection limit of 0.4 fmol/μL compares very well with the RNA-sensing test-strip we

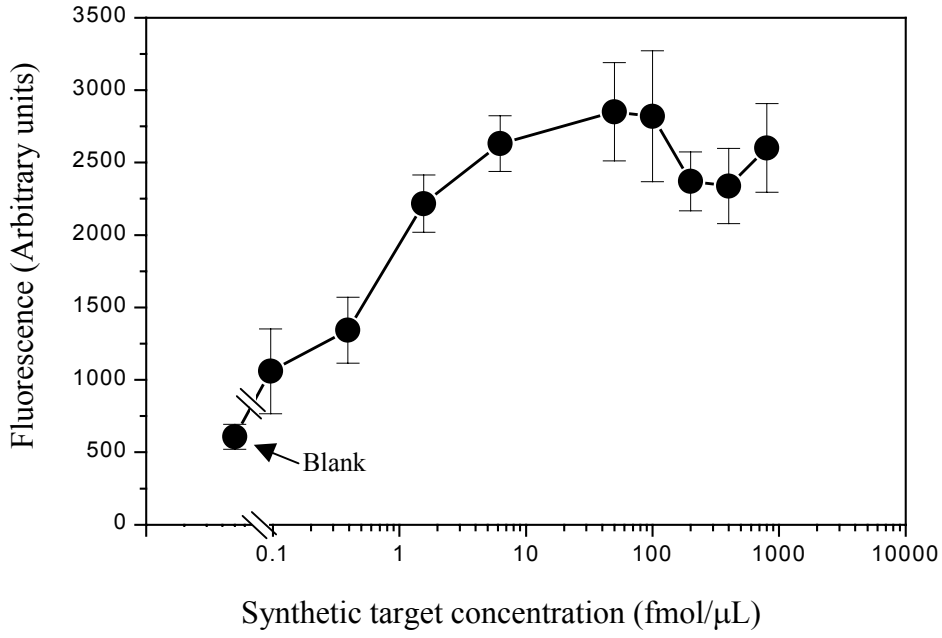

Fig. 3.8 Dose-response curve for the synthetic target. Each point represents the mean of three measurements. Error bars represent ±1 standard deviation.

recently developed for *C. parvum*.[25] This test-strip has a detection limit for measuring RNA concentration of 3 fmol/μL with a sample volume of 30 μL. The high sensitivities achieved with the microfluidic chip and the test-strip are in part attributable to the advantages offered by dye-filled liposomes. Because one liposome contains more than one fluorescein molecule in its aqueous cavity,[36] the signal generated from one binding event is larger than the signal generated with a single fluorescein tag as reporter molecule. However, because of their size, each liposome occupies multiple target sites.

At high analyte concentrations, this limits the number of liposomes that bind to the surface. On the other hand, due to the two-dimensional fluidic character of the liposome membrane, reporter probes are mobile and may migrate. Several reporter probes on a single liposome can therefore hybridize simultaneously with immobilized target (each liposome theoretically contains reporter probes at a mole fraction of 2% on the outer surface of their membrane). This results in strong binding of liposomes in the presence of high concentrations of target.[36]

Because we do not need to lyse the liposomes to detect the fluorescence, the fluorescence is restricted to exactly the sites where the sandwhich–complex of capture probe, target, and reporter probe is formed. This makes the developed assay applicable to arrays of capture probes in which each site in the array contains a capture probe toward a target from a different pathogen. The pattern of fluorescence in the array gives then information which organisms were present in the sample.

On the other hand, the fluorescence molecules inside the liposomes undergo selfquenching to a certain degree. We therefore expect that in a microfluidic chip in which we utilize reporter molecules other than fluorescence-generating dyes, such as electrochemically detectable molecules, the generated signals will be greater and the sensitivity of the assay will be further improved. The development of such a chip includes the integration of electrodes into the chip and the search for a reagent with which the liposomes can be lysed without generating high background signals.

An advantage of the microfluidic format is that the steady flow of liposomes moving through the microchannel constantly places liposomes with free reporter probes within close proximity to the immobilized target. This close juxtaposition speeds up the reaction by minimizing the limitation on the rate at which hybridization can occur under normal diffusion processes.

The dose-response curve shows that the fluorescence intensity initially increases dramatically as target concentrations increase, but then the intensity reaches a maximum value at 25 fmol/µL when the capture probes become saturated. Introducing the sample solution and the liposomes sequentially into the channel of the microfluidic chip prevents the reporter- and capture probes from being simultaneously saturated with target (even at high target concentrations), because the reporter probes are not exposed to the bound targets until all unbound target is washed out of the channel. Therefore false-negative results, as observed in other assay formats in which sandwich-

hybridization is utilized,[37] do not occur. However, we see a slight decrease in fluorescence intensity when the sample contains high concentrations of analyte (more than 200 fmol/μL) and a slight increase after that. Most likely, this is the result of variations of the fluorescence at these concentrations (these may appear higher because we used a logarithmic axis to show the concentration).

SPECIFICITY OF THE ASSAY

It is particularly important that positive signals are measured only in response to the target of interest. We conducted experiments to prove that the developed microfluidic chip does not give false-positive results with targets from organisms other than *C. parvum*. We tested targets that were modified so that they contained mismatched basepairs ranging from a single-base mismatch up to a 20-base mismatch (100%) within each of the 20-mer regions that under ideal conditions are complementary to the capture probe and the reporter probe. The mismatches were evenly distributed throughout these regions.

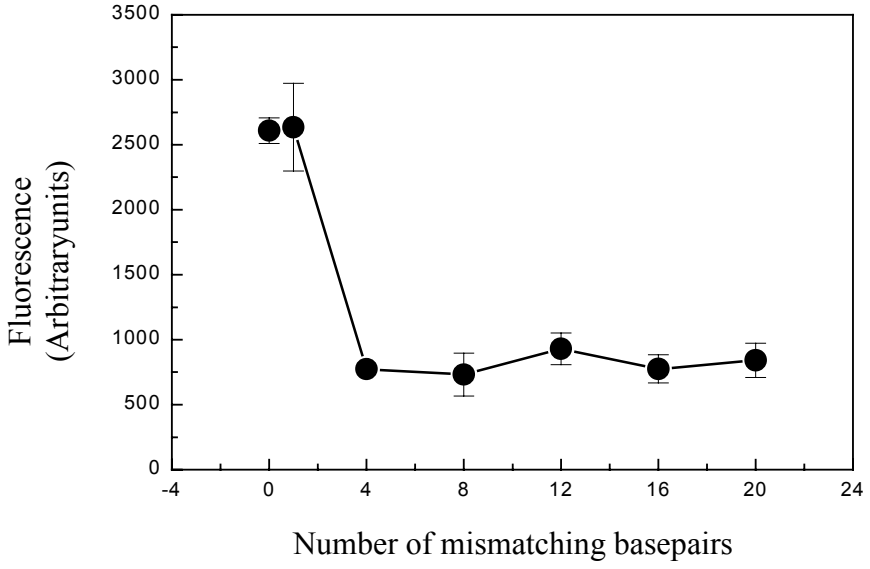

Fig. 3.9 Fluorescence obtained in experiments conducted with targets that contained mismatching basepairs ranging from 1 to 20 within each of the 20-mer sequences that hybridize with the capture and reporter probes. Each point represents the mean of three measurements. Error bars represent ±1 standard deviation.

The fluorescence values yielded by testing these modified targets in samples with a concentration of 52 fmol/μL are shown in fig. 3.9. We compared the fluorescence obtained for the mismatched targets with the fluorescence obtained for the perfect match. The targets in which mismatches ranged between 4 (20%) and 20 (100%) generated fluorescence intensities slightly higher than that obtained by the target concentration that was earlier defined as the limit of detection for perfectly complementary targets. The single-base mismatched target could not be readily distinguished from the perfect complement. However, we consider this result sufficient, because we chose a target sequence that occurs only in *C. parvum*. The author nevertheless points out that a recently published study has identified this particular sequence or a very similar sequence in two other strains of *Cryptosporidium*.[38]

TESTING OF RNA AMPLIFIED BY NASBA

The detection of *C. parvum* in water treatment plants requires that organisms be collected from several liters of sample water and then separated from contaminating debris.[39] Such procedures sometimes recover only a few organisms, and the amount of RNA extracted from them cannot readily be detected without amplification. Since even very low numbers of *C. parvum* can cause life-threatening conditions in immunocompromised people, it is necessary to develop test schemes that can detect this small amount of RNA.[40] Many researchers have developed protocols to facilitate the amplification of the recovered DNA or RNA.[41,42] It has been shown that the target RNA for which our sensor is developed can be specifically and reliably amplified from as few as ten organisms by NASBA when proper primers are used.[26] To test the compatibility of our chip with NASBA, we conducted experiments with different amounts of RNA generated by NASBA from *C. parvum* extracts. We found that the fluorescent signals obtained for all positive samples were higher than those obtained for the limit of detection, and they were readily distinguishable from those obtained for control samples that did not contain *C. parvum* extracts (see fig. 3.10). To accomplish this, it was not necessary to separate the amplified RNA from the components of the NASBA.

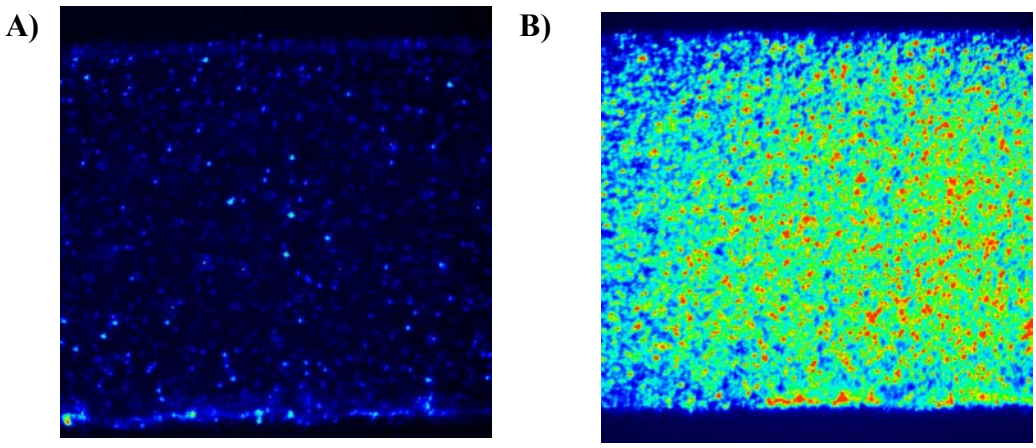

Fig. 3.10 Fluorescent images of channels in which samples from the NASBA reaction were tested: (A) negative NASBA sample; (B) positive NASBA sample. Low fluorescence is indicated by blue coloration, medium fluorescence by green, high fluorescence by yellow, and very high fluorescence by red.

REUSABILITY OF THE CHIP

We examined whether the result of a measurement was reproducible if we reused the same chip for multiple consecutive detections of target. After conducting simultaneous tests with control solutions and positive samples (containing synthetic target at a concentration of 8 fmol/μL) on six different chips (three loaded with controls, three loaded with positive samples), we dehybridized the probes in each chip by treatment with deionized water, then repeated the tests using the same chips two more times. The average of the three fluorescence values obtained as averages of the three simultaneously conducted experiments for the control was 880±230 (an arbitrary unit), while for the sample containing the target we obtained an average fluorescence of 1900±130 (an arbitrary unit). These results indicate that the chip is not altered after the first set of experiments, and therefore it is reusable.

CONCLUSIONS

We have developed a sensitive microfluidic RNA sensor that uses oligonucleotide-tagged liposomes as hybridization markers in a sandwich-hybridization assay. Assays conducted with the described chip are specific, and the chip is capable of measuring target concentrations as low as 0.4 fmol/μL with a 12.5 μL aliquot of sample solution. RNA that was extracted from viable *C. parvum* oocysts was amplified by NASBA and successfully detected. NASBA-generated amplicons can be detected without separating them from the NASBA–enzyme mixture.

We successfully demonstrated the feasibility of dye-entrapped liposomes as reporter particles in a microfluidic system. Because the liposomes do not need to be lysed to measure the fluorescent signal, the developed format can be used in microfluidic array chips in which a number of spatially separated binding sites may be used to indicate the presence or absence of multiple targets in one sample.

4

Development of a Prototype Microfluidic Array for Multiple Analyte Detection

ABSTRACT

A microfluidic patterning approach is used to fabricate a prototype microfluidic array for simultaneous analysis of multiple samples containing nucleic acids. The detection of nucleic acids in the array is based on the sensing scheme developed earlier (see chapter 3). To optimize the sensing in the array, we made a few modifications. The ability of the microfluidic array to analyze multiple samples simultaneously is demonstrated by detecting samples with different target concentrations. The practical application of the array extends to multiple analyte detection. The use of the array is envisioned in "lab-on-a-chip" devices for the simultaneous detection of *C. parvum* and *Giardia duodenalis* in a single sample.

INTRODUCTION

BACKGROUND

DNA microarrays —also known as "DNA-chips"— are microchips on which many different oligonucleotides are immobilized on spatially separated sites. The sizes of the individual sites can range from several μm to only a few nm in scale and therefore the assembly of such oligonucleotide spots on one chip leads to the formation of high-density two-dimensional patterns.

Originally, one of the goals of researchers who fabricated microarray chips was to utilize these DNA-chips to obtain sequence information from DNA molecules. This

sequencing technique, called "sequencing by hybridization (SBH)," uses an array that contains a slightly different oligonucleotide on each spot.[1, 2] A sample of unknown DNA is applied to the array and the pattern of hybridization reveals the information about the sequence. However, as Lemieux et al. report, it is difficult to obtain uniform hybridization signals for a large number of different oligonucleotides in parallel.[4, 5] This is due to the slightly different hybridization optima of molecules with different sequences.

Alternative applications for DNA microarrays are diagnostic devices. Here the DNA arrays are used to detect mutations in the genome and to assess genetically inherited predispositions.[5-8] In the future, the use of DNA arrays will enable medical personnel to test a patient's blood sample for many possible predispositions at the same time, thereby improving and accelerating diagnosis and preventive care.

Microarrays can also be utilized to identify multiple pathogens in a single sample rapidly without additional effort to conduct the analysis. For this application, the appropriate capture probes have to be immobilized on the different spots in the array. After a hybridization assay is conducted, the signals yielded from each site indicate which pathogens are present in the sample.

The DNA microarrays themselves can also be assembled as a collection of spatially separated arrays on one platform. If each array on such a platform is individually addressable, this device will enable researchers to process several samples simultaneously. The analysis of samples is thereby reduced to a fraction of the time usually needed. Another advantage of microarray sensors is that because of their small size they can be integrated into platforms that contain other microchips. In a true "lab-on-a-chip", these other microchip components would facilitate all of the steps that are needed before a sample can be analyzed with the array. For example, the sample could be treated so that DNA and RNA are released from cells in one chip of the platform. Subsequently, the released DNA and RNA could be amplified. On such a device, a microfluidic network connects the individual chips with each other. Such a fully integrated sensor, or μ-Total Analysis System (μ-TAS) will reduce the time and effort needed to prepare the samples and to conduct the analysis since no manual transfer and no manipulations of the samples in between steps will be needed. Currently, efforts are being made to develop such a device for medical applications.

Two strategies are commonly used to prepare microarrays. Either the oligonucleotides are synthesized directly on the chip, or the oligonucleotides are deposited on individually addressed spots. When very-high-density microarrays are required, preparing the oligonucleotides by synthesis has advantages because it provides higher spatial resolution of small features. An example of the synthesis strategy is the method developed by Fodor and co-workers.[10] This method uses nucleotide phosphoramidites modified with photo-labile protection groups. The photo-labile protection groups allow light to be used as an activating agent. A round of synthesis involves light-directed deprotection and coupling of the new nucleotide. Photolithographic masks define the regions on the chip that will be exposed to the light and in which the nucleotides are activated. The surface is then incubated with one of the four bases and coupling takes place. After washing away all uncoupled bases, the investigator can begin a new cycle. This method allows the preparation of very-high-density arrays with up to 250, 000 features per cm^2.

Another example of the synthesis strategy is the ink-jet printing technology.[11] Here the oligonucleotides that are being synthesized are covered with a light-sensitive hydrophobic material by an ink-jet printer. To address the spots for the next round of synthesis, this material is exposed to light, which makes it susceptible to dissolving in a specific solvent, thereby freeing the oligonucleotides for coupling. After the coupling took place the covering material is washed away and a new layer of light-sensitive material is applied.

Although the synthesizing strategy allows the manufacturing of very high-density arrays, it requires much effort to design the masks and produce the arrays. Therefore, it is useful for mass production rather than prototyping in a laboratory. The synthesizing technique is also not useful when oligonucleotides longer than 25 bases are to be prepared. This is because incomplete synthesis products will accumulate after about 100 cycles of synthesis, and the correct sequence is no longer guaranteed.

For the preparation of arrays containing oligonucleotides longer than 25 bases, it is advantageous to use deposition techniques. For example, microspotting techniques utilize pins or capillaries that are directed by mechanical motion control systems. The capillaries deposit small amounts of DNA onto the chip.[12-15]

FABRICATION OF A PROTOTYPE MICROFLUIDIC ARRAY

In this project we fabricated a prototype microarray that can be used for multiple analyte detection and for simultaneous analysis of multiple samples. The detection in this array is based on the detection mechanisms and sensor design introduced in chapter 3. The array utilizes capture probes that are immobilized on gold-coated glass slides by sulfur–gold linkages. It consists of closely spaced channels that are individually addressable. In each channel a separate sample can be analyzed. Each channel has the potential for containing capture probes that bind the targets of different pathogens, thereby enabling the detection of multiple analytes within each channel.

We used a microchannel patterning technique (similar to a technique used for patterning antibodies[16]) to immobilize the capture probes in the array. A microfluidic

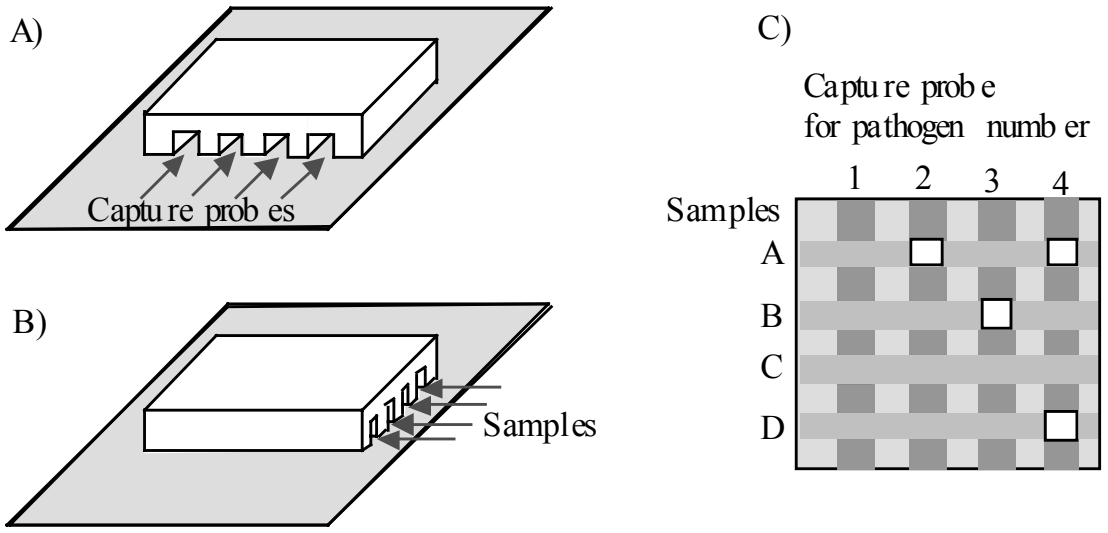

Fig. 4.1 (A) Preparation of the microfluidic array. (B) The use of the array for multiple sample analysis, and (C) multiple analyte detection. The highlighted spots would indicate the presence of a pathogen.

network of five channels is molded in PDMS. To each channel a different capture probe can be applied (fig. 4.1A). We then applied the same PDMS channels in such a fashion that they lie perpendicular to the rows of immobilized capture probes. The channels are then used to conduct assays with several samples simultaneously (fig. 4.1B). Fig. 4.1C shows how the array can be utilized for multiple analyte detection.

EXPERIMENTAL SECTION

OLIGOMERS

For information on the oligonucleotides used and their modifications, see chapter 3.

PREPARATION OF ACETYLTHIOACETATE (ATA)-TAGGED LIPOSOMES CONTAINING CARBOXYFLUORESCEIN

Liposomes containing a 100 mM carboxyfluorescein solution were prepared and subsequently tagged with acetylthioacetate on the outer surface of their membranes. These groups were deprotected and coupled to reporter probes. The detailed protocol used for this preparation is described in chapter 3.

PREPARATION OF GOLD-COVERED MICROSCOPE-GLASS SLIDES

Microscope-glass slides were thoroughly cleaned by immersing them in a solution containing a volume fraction of 70% concentrated sulfuric acid and a volume fraction of 30% hydrogen peroxide (30% H_2O_2 in H_2O). *Please follow the safety advice given in chapter 3 when working with this solution.* Using a thermal evaporator and a metal mask, we deposited a 15 Å chromium layer and a 450 Å gold layer on a 15 x 15 mm area of the slides. The exact procedure is described in chapter 3.

PREPARATION OF THE MICROFLUIDIC ARRAY

The microfluidic channels were prepared in PDMS [poly(dimethyl siloxane); Sylgard, 184 Silicone Elastomer, Dow Corning Co., Midland, MI] using silicon

templates that contained negative three-dimensional images of the channels. The silicon templates were fabricated using a chromium mask with features of the channels generated by a GCA pattern generator PG3600 (Ultratech Stepper, Wilmington, MA, USA), a Hybrid Technology Group (AB-M, San Jose, CA) contact-aligner and subsequent KOH wet-etch as shown in fig. 4.2. On the template each channel was 50 μm wide and 10 μm high. The channels were 50 μm apart from each other. The initially liquid PDMS was cured on the finished silicon template. After the curing was allowed to proceed for 60 min at 60 ^{o}C, we removed the PDMS from the template and prepared individual inlets for each channel. The channels were then placed on the thoroughly cleaned gold-coated glass slides (for cleaning solution, see cleaning of the glass slides before gold deposition).

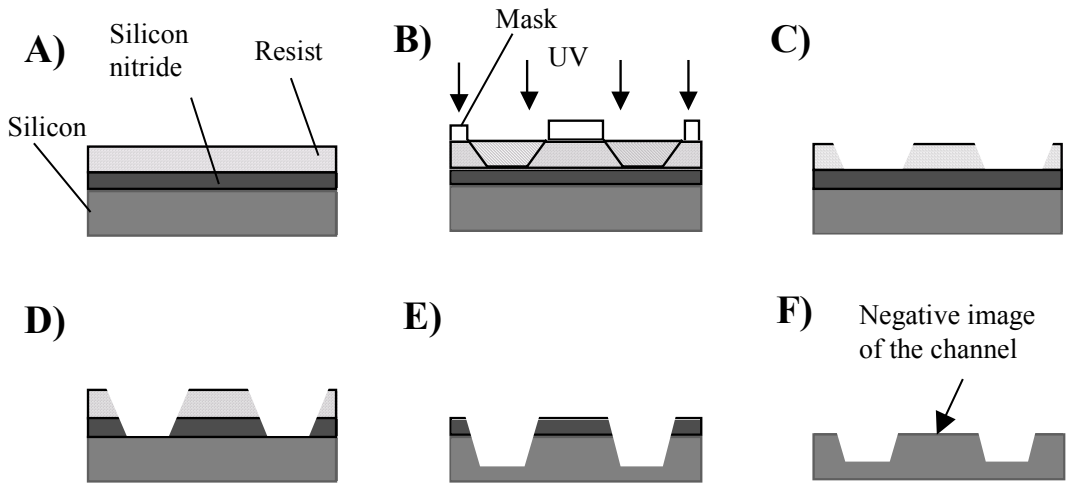

Fig. 4.2 Fabrication of silicon templates containing negative images of microchannels for use in preparing microchannels in PDMS: A) The silicon wafer is covered with 1000 Å of silicon nitride and 1.3 μm of photoresist (Shipley 1813, Microchem, Newton, MA). B) Using a metal mask, the images of the channels are exposed to UV light (405 nm) for 4.4 s. C) The exposed photoresist is washed away by a solvent (AZ 300, Clariant, Somerville, NJ). D) At the exposed areas the silicon nitride is etched by using a reactive ion etch process via a Plasmatherm 72 etcher (UNAXIS, Zurich, Switzerland). During this process the photoresist acts as a mask. After finishing the etch process the photoresist is removed by plasma ashing using Plasmatherm 72 (UNAXIS). E) The exposed silicon is etched by a potassium hydroxide solution (KOH) at 70 ºC. Here the silicon nitride acts as a mask. F) The remaining silicon nitride is stripped off with concentrated HF solution.

The immobilization of the capture probes in defined areas was accomplished by using the microfluidic channels as guiding templates. For this preparation, the flow of solution through the microfluidic channels must first be induced by priming the channels with ethanol (100%). Subsequently, we slowly replaced the ethanol solution with aqueous phosphate buffer (1 mM). By keeping the solution level higher at the inlet than at the outlet, we could use the hydrostatic pressure to force the liquid through the channels. Contrary to the other projects described, the channels in this project were not tilted but were kept on a flat surface. The inlets were filled with 20 μL of capture probes (1 mM capture probes in 1 mM phosphate buffer), while the outlets were filled with 3 μL of phosphate buffer. While flowing through the channels (for 60 min), the capture probes bound covalently to the exposed gold. After washing away noncovalently bound capture probes with water, we dried the inside of the PDMS channels carefully and then removed them from the slides. We then applied the same PDMS channels in such a fashion that they lay perpendicular to the rows of immobilized capture probes. The channels were filled with the appropriate blocking reagents (either BSA diluted in 50 mM phosphate buffer so that a volume fraction of 2% BSA was obtained, or hexanethiol at a concentration of 1 mM diluted in ethanol). The incubation proceeded for 60 min at room temperature. The channels were then washed with 1 mM phosphate buffer.

Assay Protocol

To start the assay, we filled the inlet well with 12.5 μL of sample solution containing the synthetic target oligonucleotide in a hybridization buffer. The hybridization buffers and incubation times are described in chapter 3.

Detection and Quantification

Using a standard fluorescence microscope equipped with a 10x long distance working objective and a digital camera (C4742-95, Hamamatsu, Somerville, NJ, U.S.A.), we obtained images of the liposomes bound in the channel. The fluorescence was quantified using software acquired from Carl Zeiss Inc. (Thornwood, NY).

RESULTS AND DISCUSSION

DESIGN AND FABRICATION OF THE MICROFLUIDIC ARRAY

An assembly of five microfluidic channels cast in poly-dimethyl siloxane (PDMS) is utilized for two purposes. The channels (each 50 μm wide and 10 μm deep, spaced 50 μm apart) serve first as a flow-guiding template to immobilize the capture probes. The same channels are then used to conduct the actual assay.

To take full advantage of the array's capability for detecting multiple analytes and simultaneously analyzing multiple samples, each microfluidic channel should have its inlets individually accessible. On the other hand, the flow rate in each of the five channels should be the same, because it influences the rate of deposition of capture probe as well as the hybridization.

Two forces influence the fluid flow in microfluidic channels. The surface tension force is given by

$$F_S = 2\pi r \gamma \cos(\theta)$$

where θ is the contact angle between liquid and surface, γ is the interfacial surface-tension in N/m (7.27×10^{-2} N/m for air/water at 20 °C, 1 ATM), and r is the radius of the capillary.[17] (This equation assumes a round shape of the channel.) The surface-tension force tends to draw liquid into the channel. The gravitational force acting on the liquid is given by

$$F_G = \rho g \pi r^2 h$$

where ρ is the liquid density, h is the height of the column, r is the radius of the column, and g is the gravitational constant.[17]

The fluid flow in the channels designed for this study was driven by gravity. This method was used because it does not require any additional instrumentation but provides acceptable flow rates. The actual channel lies horizontally on the chip and the fluid level in the inlet and the outlet provide the necessary difference in height. Because

the surface tension force is negative when aqueous solutions are applied to freshly prepared PDMS channels the flow of these solution through the channels is difficult to start. Therefore, we first used an organic solvent (ethanol) to start the flow and then slowly replaced it by aqueous buffer.

We designed the assembly of the channels as shown in fig. 4.3. To test the flow velocity in each channel, we filled them with fluorescent dye and measured the time the dye needed to travel over a distance of 20 mm in the channel. The flow velocities were 54.0 μm/s ±6.1 μm/s in channels #1 and #5; 51.0 μm/s ±7.0 μm/s in channels #2 and #4; and 55.0 μm/s ±5.4 μm/s in channel #3. Although each channel is slightly different in design (the curve is placed differently), all measured flow rates were comparable. This proved the design applicable for the intended purpose.

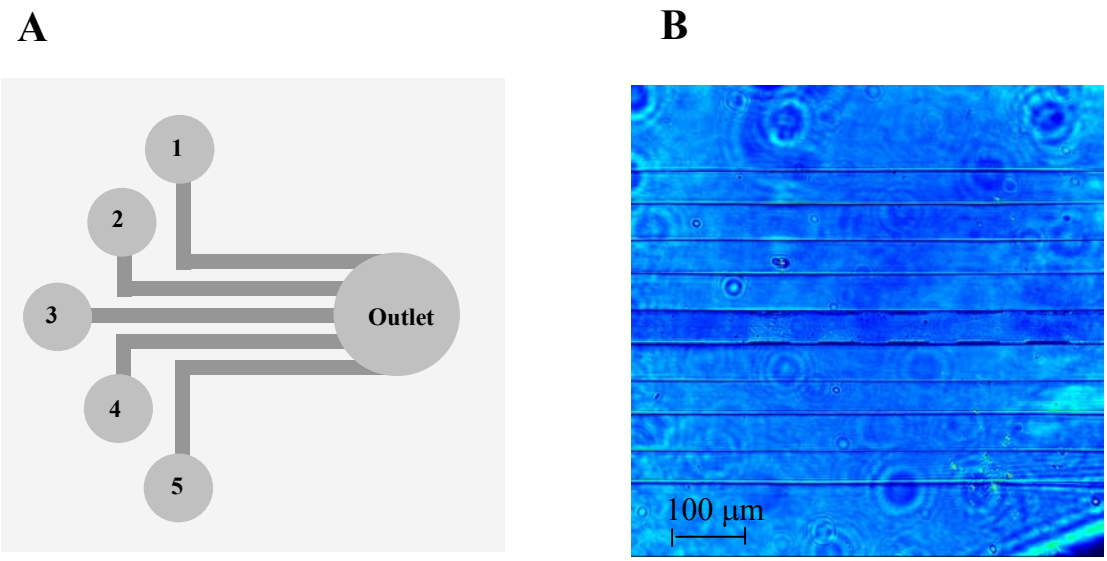

Fig. 4.3 (A) Design of the microfluidic network used to pattern capture probes, and (B) microscopy picture of PDMS channels placed on a glass slide.

MINIMIZING THE BACKGROUND BINDING

In chapter 3, we investigated methods for preventing the nonspecific binding of liposomes and targets to gold surfaces in a microfluidic chip. A mixed layer of mercaptohexane and blocking liposomes was found suitable for decreasing the

nonspecific binding to an acceptable level. However, microarray chips prepared with the same blocking layers exhibited very low hybridization. The experiments indicating this were two assays. The first assay was conducted with a control sample that did not contain target, and the second assay was conducted with a sample that contained synthetic target at a concentration of 400 fmol/μL in a sample volume of 12.5 μL. Figure 4.4 shows a picture of the microfluidic channels in which the positive sample had been analyzed. Although the sample contained a high concentration of target, the fluorescence in the channels was very low. This may have been caused by dissolution of components of the PDMS by mercaptohexane and the deposition of this component on the capture probe layer, thereby inhibiting hybridization. A slightly increased fluorescence appeared at places where no capture probes were immobilized, but where the PDMS was in contact with the gold in the first deposition step. This result suggests that the direct contact of cleaned gold with PDMS modified the gold so that the mercaptohexane could not assemble as a monolayer. Thiolated reagents assemble on gold only if it has been chemically cleaned prior to the deposition. A possible explanation could be that the hydrophilic –OH termination generated on the gold surface by cleaning it with a solution containing sulfuric acid and hydrogen peroxide is damaged when the PDMS is applied.

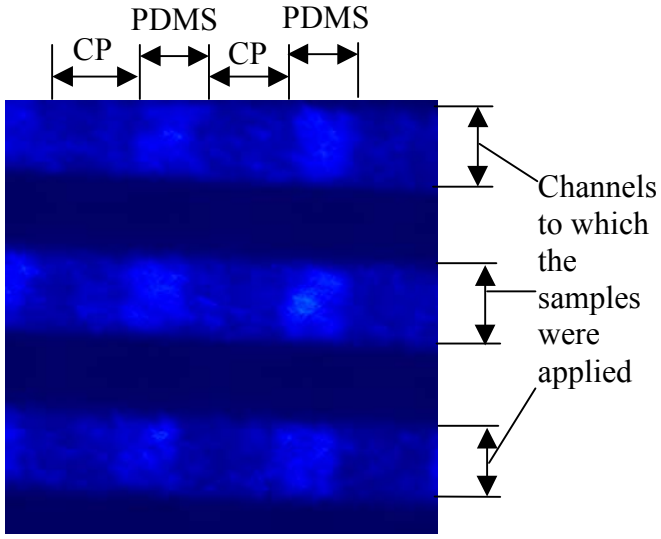

Fig. 4.4 Fluorescence after conducting assays in an array that had been blocked with mercaptohexane and blocking liposomes. The vertical channels were used to apply the capture probes (CP). The horizontal channels were used to apply the samples. The target concentration in the samples was 400 fmol/μL. Although the samples contain targets in high concentrations and should therefore generate high fluorescence, the fluorescence in the horizontal channels is low (dark blue coloration). The fluorescence is slightly increased at the places where the PDMS was applied in the first capture probe deposition step (lighter blue).

Chapter 3 showed that a BSA blocking layer decreased nonspecific binding in a microfluidic channel with a gold surface. We therefore tested BSA as an alternative blocking reagent in the microarray chip and conducted the same experiment as described above using an array that was prepared with the new blocking layer. Figure 4.5, which was taken from these experiments, shows that high fluorescence occurred at the places where capture probes were immobilized. The high fluorescence resulted from the specific hybridization of synthetic target, capture probes, and reporter probes. Low fluorescence was observed at places where no capture probe was immobilized and also in the array in which the negative control was analyzed. This proves that the nonspecific binding of target and liposomes was low. The result further assures us that, in fact, specific hybridization took place when the positive sample was detected. Additionally, in the array in which the positive sample was detected the fluorescence is confined to squares that measure 50 μm by 50 μm. In all squares of that size the fluorescence is approximately the same.

The same hybridization rate in each channel will enable us to obtain not only qualitative information but also quantitative information about the detected pathogens. Although it would be possible to calibrate each channel individually, the results of the detection will be easier to interpret if all channels follow the same hybridization conditions and therefore the same calibration curve.

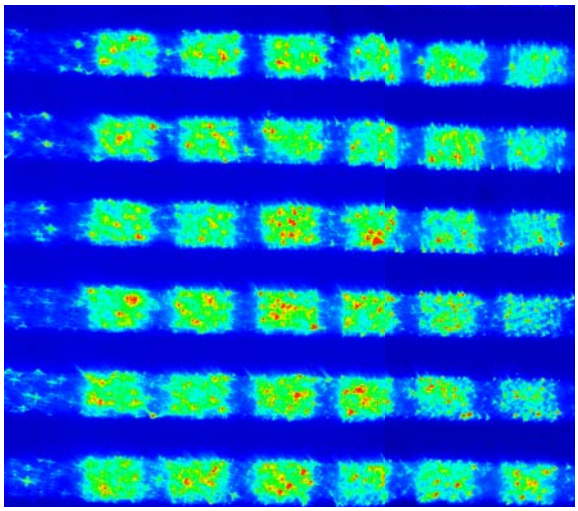

Fig. 4.5 Fluorescence in a microfluidic array after analyzing the same sample (400 fmol/μL) in each of the five channels. Low fluorescence is indicated by blue coloration, medium fluorescence by green, high fluorescence by yellow, and very high fluorescence by red.

ANALYZING MULTIPLE SAMPLES SIMULTANEOUSLY

To demonstrate the array's potential for simultaneous analysis of multiple samples we utilized the optimized array device to conduct assays with samples that contained different concentrations of synthetic target oligonucleotide. After finishing the assay, we measured the fluorescent signals in each square in the array (see fig. 4.6). The channels exhibited low fluorescence for samples with low target concentrations and increased fluorescence for samples with high target concentrations. Figure 4.7 shows the dose-response curve derived from fig. 4.6. The error bars represent the variation of fluorescence within each channel. The low variation confirms the uniformity of capture probe application and the uniformity in rate of hybridization.

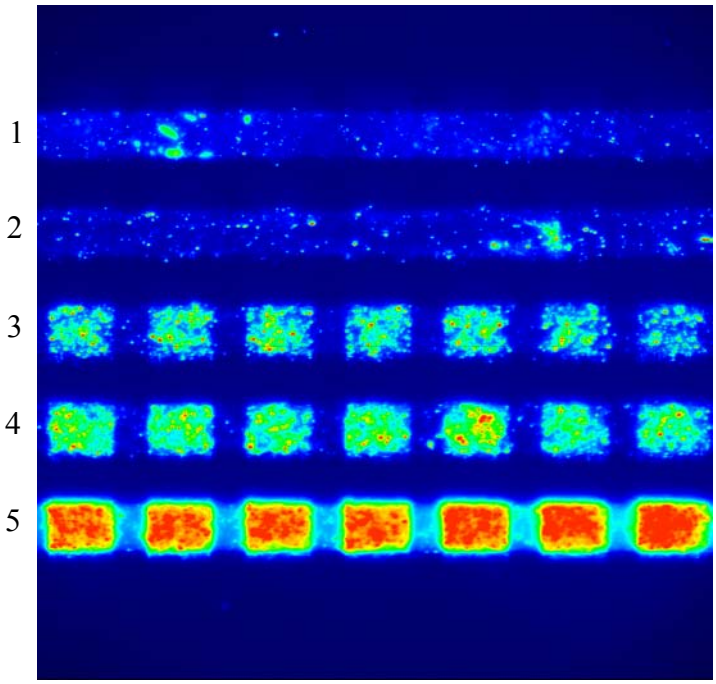

Fig. 4.6 Fluorescence in a microfluidic array in which samples with different target concentrations were analyzed: #1: control; #2: 5 fmol/μL; #3: 19 fmol/μL; #4: 78 fmol/μL; #5: 312 fmol/μL. Low fluorescence is indicated by blue coloration, medium fluorescence by green, high fluorescence by yellow, and very high fluorescence by red.

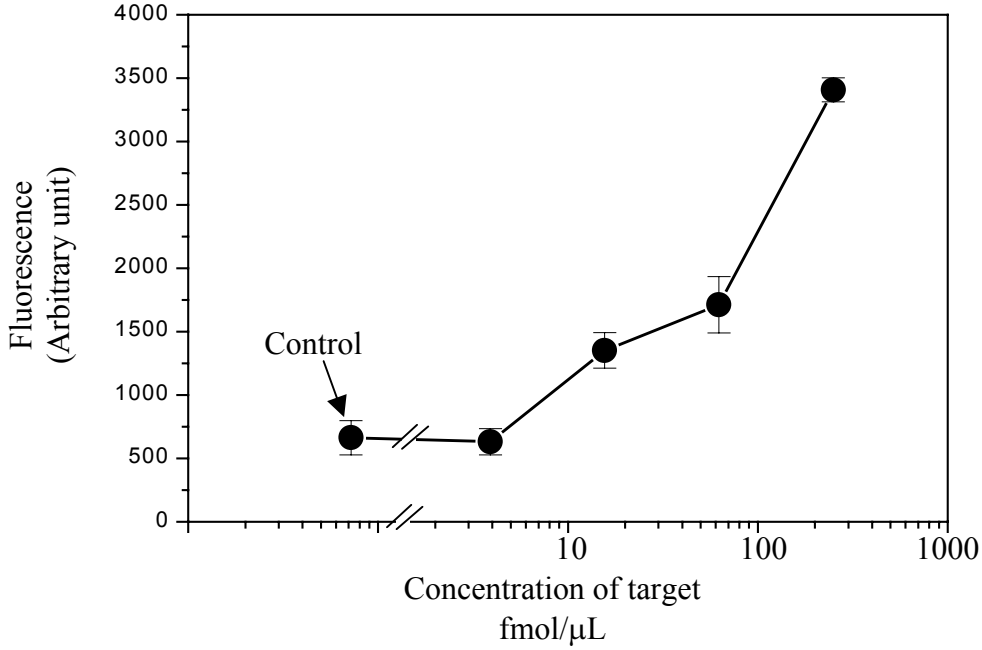

Fig. 4.7 Dose-response curve obtained by analyzing multiple samples containing different concentrations of target oligonucleotide in an array. The standard deviation represents the variation of the different sites in one channel.

CONCLUSIONS

The fabrication method we developed is a fast and easy way to produce prototype arrays for multiple sample analysis based on the sensing system developed in chapter 3. Besides multiple sample analysis, the array can also be utilized for detecting multiple analytes in a single sample. This requires that different capture probes be immobilized in each channel in the deposition step, and it also requires that liposomes be modified with the appropriate reporter probe tags. In the case of detecting *C. parvum* in water samples, it would be desirable to simultaneously detect organisms such as *Giardia duodenalis*.[18]

The most efficient way to utilize the array is to integrate it into a "lab-on-a-chip" device that amplifies targets from *C. parvum* and other organisms simultaneously in a single amplification step and then transfers the sample to the array for detection.

5

Electrochemical Detection of *Cryptosporidium parvum* Using Interdigitated Microelectrode Arrays in a Microfluidic Chip

ABSTRACT

A microfluidic chip with integrated interdigitated array electrodes (IDAs) for the detection of nucleic acids was developed. Electrochemical detection of a hybridization event is achieved by utilizing reporter probe-tagged liposomes that contain ferri- and ferrohexacyanide inside the cavity formed by the phospholipidic membrane. After sandwich-hybridization of the target with reporter probes and immobilized capture probes, the liposomes are lysed by adding the purified detergent octyl glucopyranoside (OG). The IDA electrodes are operated in a two-electrode configuration without a reference electrode. Monitoring the resulting current gives information about the presence or absence of the nucleic acid of interest. Factors that influence the detection are investigated.

INTRODUCTION

BACKGROUND

Electrochemical sensors offer benefits of technical simplicity, speed, sensitivity, and the convenience of recording data that are directly transduced from the sensor to electronic equipment. Therefore, there has been considerable interest among researchers to utilize electrochemical techniques in biosensors for diagnostic point-of-care devices and for environmental monitoring.[1]

For example, Perez et al. have developed a sensor for detecting *Escherichia coli* in water samples (from drinking-water supplies and recreational waters) by an enzymatic reaction combined with amperometric detection.[2] After capturing the microorganisms, investigators culture them in a substrate supplemented with 4-aminophenyl-ß-D galactopyranoside. The bacterial enzyme β-galactosidase hydrolyses this substrate and generates a product that can be detected amperometrically. Enzymatic reactions are also used in the diagnostic biosensor array developed by Sangodkar and co-workers.[3] This sensor consists of microelectrodes on which three different enzymes have been immobilized. The sensor detects glucose, urea, and triolein simultaneously in a single electrochemical measurement.

In addition to detection schemes that directly aim at detecting the product of an enzymatic reaction,[2-5] other sensors based on immunological recognition use enzymatic reactions merely to generate signals for the sensor.[6-8] These immunosensors often use enzymes, such as horseradish peroxidase, as labels on antibodies. They detect the actual analyte indirectly by means of the enzymatic reaction.[7, 8]

To enhance the performance of electrochemical biosensors, researchers have recently used electroactive polymers such as polyaniline (PANI).[3, 9, 10] The biological components of the sensor, such as enzymes or antibodies, are immobilized in the polymer matrix that is in direct contact with carbon-paste electrodes. Polyaniline itself undergoes redox cycling and can couple electrons directly from an enzyme-active site to the electrode surface and thereby decrease the limits imposed by diffusion processes. However, electroactive polymers have not been utilized so far for the electrochemical detection of nucleic acids.

Nucleic acids are often detected by the different electrochemical signal that single-stranded and hybridized nucleic acids generate when they interact with small marker molecules. Commonly used electroactive marker molecules include ethidium bromide,[11] tris(1,10-phenanthroline)cobalt(III) perchlorate [$Co(phen)_3^{3+}$],[12, 13] tris (2,2'-bipyridyl) cobalt(III) perchlorate [$Co(bpy)_3^{3+}$],[14] ferrocenyl naphthalene diimide,[15] Hoechst 33258,[16] and methylene blue.[17] Because these molecules intercalate with double-stranded DNA more strongly than with single-stranded DNA, they are concentrated on the electrode surface only when the target nucleic acid has hybridized to the capture probes that are immobilized on the electrode. By detecting the

concentration of the indicator molecules, investigators can determine the amount of hybridized target.

Other researchers label oligonucleotides with electroactive molecules such as aminoferrocene (AFC)[18] and anthraquinone (AQ).[19] These labels generate different voltammetric signals when associated with single and double-stranded DNA.

Finally, Aoki et al. used the electrostatic properties of DNA. The electrostatic properties of a layer of immobilized peptide nucleic acids changes when a target DNA hybridizes to that layer.[20] The bulk solution contains the redox marker $[Fe(CN)_6]^{4-/3-}$ whose redox reaction on the electrode is hindered by the double-stranded DNA because of electrostatic repulsion.

Electrochemical Detection Using Liposomes and Interdigitated Microelectrode Arrays

In this study we explore the possibility of using liposomes containing electroactive molecules (ferri- and ferrohexacyanide) as labels in nucleic acid hybridization assays. Using liposomes as carriers for the electrochemically active species in nucleic acid hybridization assays has advantages over using conventional methods. Since on each double-stranded molecule there are limited binding sites to which intercalators can bind, the generated signal is limited. On the other hand, liposomes can contain up to 10^6 molecules in their aqueous cavity.[22] After the liposome membrane is disrupted with a detergent, the molecules are available for electrochemical measurements. The second advantage is that no intercalator is needed for the detection. Because of their interaction with DNA, intercalators are considered to cause cancer. Therefore, the detection with ferri- and ferrohexacyanide is safer than other methods.

To generate electrochemical signals from a nucleic acid hybridization event we utilize interdigitated microelectrode arrays (IDAs) that we integrate into microfluidic chips. These electrodes, which are up to 5 mm in length and 4.5 mm in width, consist of an array of interdigitated platinum or gold filaments (also called fingers) very closely spaced (up to 1 μm). For analytical purposes, these electrodes offer advantages over normal electrodes. Due to the close proximity of the sets of cathode and anode fingers,

molecules may be alternately oxidized and reduced. If oxidation and reduction take place on very closely spaced filaments the resulting current is no longer limited by diffusion. Further, the current obtained from an array of microelectrode fingers is much larger than the current obtained from electrodes that consist of single microelectrode fingers. The sophisticated electronics usually needed to detect the very small currents from single fingers are not needed with electrodes that consist of an array of such fingers. This makes the IDA electrodes very useful for field-portable detection devices.

EXPERIMENTAL SECTION

OLIGOMERS

For information on the sequence of the used oligomers the reader is referred to chapter 3. Information on the modifications of capture probes and reporter probes that allow them to be immobilized on the chip and on the liposome membrane is also given in chapter 3.

PREPARATION OF REPORTER PROBE-TAGGED LIPOSOMES CONTAINING FERRI- AND FERROHEXACYANIDE

The liposome encapsulant, a solution containing 100 mM $K_4Fe(CN)_6$, 100 mM $K_3Fe(CN)_6$, and 0.1 mM sulforhodamine B, was prepared in 0.02 M HEPES (N-2-hydroxyethyl-piperazine-N'-2-ethanesulfonic acid) buffer (pH 7.5). The osmolality of the encapsulant was 625 mOsmol/kg. The liposomes were prepared using the reverse phase evaporation method as described in chapter 3. The liposomes were kept at 4 °C in the dark in a buffer with an osmolality of 730 mOsmol/kg.

PREPARATION OF INTERDIGITATED ELECTRODE ARRAYS

The interdigitated microelectrode arrays were fabricated on microscope-glass slides (Corning Inc., Corning, NY) using an image-reversal method (summarized in

fig. 5.1). All procedures were performed using the clean-room and the equipment of the Cornell Nanofabrication Facility (CNF). The glass slides were first cleaned in a solution containing 500 mL of H_2O, 100 mL of concentrated NH_4OH, and 100 mL of H_2O_2 (30%). After rinsing with water and drying with nitrogen, we vapor-primed the glass slides in a vacuum oven (LP-III, Yield Engineering Systems Inc., San Jose, CA) with hexamethyldisilazane (HMDS). This procedure coats the surface of glass slides with hydrocarbon-rich $Si(CH_3)_3$ groups that promote the adhesion of photoresist. Photoresist (S1813, Microchem, Newton, MA) was spun on the slides at a rotation rate of 3000 rpm (fig. 5.1A). To harden the photoresist, we then baked the slides for 30 min at 90 ºC. Using a 5x g-line stepper (GCA 6300 DSW Projection Mask Aligner; Ultratech Stepper, Wilmington, MA) and a chromium mask (generated by a GCA pattern generator PG3600, Ultratech Stepper, Wilmington, MA), we exposed the negative images of the electrode arrays to UV light (436 nm) for 1.25 s (fig. 5.1B). Since the field size of the chip was too big to expose the electrodes and gold field (later used for immobilization) at once, the gold fields were exposed separately for 4.4 s to UV light (405 nm) via a contact aligner (HTG System 3HR Contact/Proximity Aligner, Hybrid Technology Group, San Jose, CA) and a metal mask prepared for this purpose. To harden the exposed photoresist, the slides were baked in an NH_3 vapor-priming oven (Yield Engineering Systems Inc., San Jose, CA). The entire slides were then exposed to UV light (405 nm) for 1 min (fig. 5.1C). While the photoresist that was exposed to UV light in the first two exposure steps was hardened by the NH_3 vapor, the resist covering the features that were not exposed in the first two exposure steps are susceptible to dissolution after the third UV exposure. After the features were developed with a developing solution (MF 321; Microchem, Newton, MA) for 2 min, we washed away these features, so that only negative images of the electrode arrays remained on the slide (fig. 5.1D). Using a thermal evaporator (CVC 4500; CVC Products Inc., Frement, CA), we deposited a 15 Å layer of chromium on the slides. This layer served as the adhesion layer for the following gold layer (450 Å), also deposited by thermal evaporation (fig. 5.1E). Developing the slides in stripping solution (developer 1165; Microchem, Newton, MA) dissolved the photoresist and thereby the gold covering the negative images of the electrodes were lifted off, leaving behind the positive features coated with gold (fig. 5.1F).

When IDA electrode chips were reused, the gold on the immobilization field was removed by etching with a 100 mM potassium iodide solution saturated with

iodine (KI_3). We subsequently polished these fields with aluminum powder to remove the chromium layer**.** The immobilization fields were exposed to chromium and gold deposition via thermal evaporation using a metal mask that covered the area around the fields, including the electrodes.

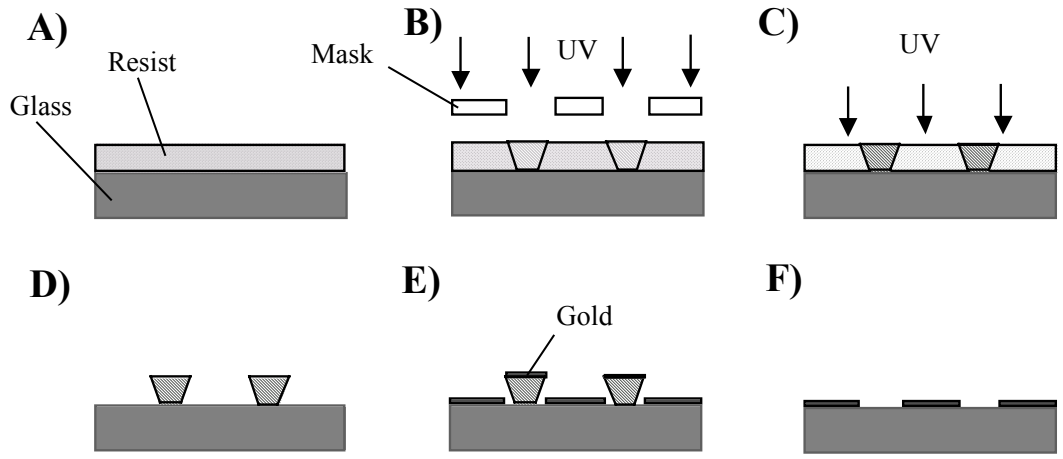

Fig. 5.1 Fabrication of interdigitated microelectrode arrays by image reversal: (A) The glass slide is covered with a 1.3 μm thick layer of photoresist; (B) The images of the electrodes are then covered with a mask and the area around the images are exposed to UV light. The exposed photoresist is hardened by baking with NH_3 (unexposed photoresist will not harden); (C) The entire glass slide is then exposed to UV light; (D) The areas in which the photoresist was not hardened are now susceptible to dissolution in a developing solution and are removed from the wafer, leaving behind the actual features of the electrode array. The remaining resist exhibits an undercut feature angled towards the glass; (E) After evaporating chromium and gold, the photoresist is dissolved with a second, stronger developing solution; (F) The features of the electrode arrays are now patterned on the glass slide.

PREPARATION OF THE MICROFLUIDIC CHIP

Capture probes (diluted in 1 mM potassium phosphate buffer, pH 7.0) were immobilized on the gold as described in chapter 3. After placing PDMS channels on the slides, we primed the channels with ethanol. The ethanol was slowly replaced by 0.5 M phosphate buffer. To block nonspecific adsorption in the channels, we filled them with blocking liposomes for 30 min and then washed them with 2x SSPE.

Assay Procedure

The assay was conducted as described in chapter 3. The last step of the assay is washing the channel with 2x SSPE containing a 50% volume fraction of formamide. This solution is then replaced by 2x SSPE. The electrochemical measurements were started as described below. The solution in the channel is changed to a 100 mM octyl glucopyranoside solution (OG) in 0.25 M phosphate buffer. As the OG solution flows through the channel, it destabilizes the liposome membranes and thereby releases the ferri- and ferrohexacyanide solution. This results in an electrical current, the height and area of which are subsequently analyzed using the Turbochrom software (Perkin Elmer Analytical Instruments Inc., Norwalk, CT).

Electrochemical Detection and Quantification

After finishing the assay, we conducted the electrochemical measurements while flowing 2x SSPE through the channel. We conducted chronoamperometric measurements as optimized by Roberts for detecting ferri- and ferrohexacyanide solutions.[21] We applied a potential step of 400 mV to the interdigitated array electrodes in a two-electrode configuration. The resulting current was measured using a potentiostat. Software (Turbochrom, PerkinElmer Analytical Instruments Inc., Norwalk, CT) and a PC computer were used to monitor the current in real time.

In experiments in which the response of the IDAs towards varying concentrations of ferri- and ferrohexacyanide was measured, 50 μL of ferri- and ferrohexacyanide solution were pipetted onto the electrodes for each experiment. A typical current-time curve obtained from such an experiment is shown in fig. 5.2C. The steady-state current reached after 60 s of measurement is used to compare various conditions.

For characterizing the electrochemical measurements inside the microfluidic channels and after conducting an assay, the solutions flowed through the channels with a flow velocity of 92.4 μm/s ± 5.4 μm/s. This corresponds to a flow rate of 1.5 nL/s ± 0.09 nL/s.

RESULTS AND DISCUSSION

DESIGN AND FABRICATION OF THE CHIP

The chip design used in this project is very similar to that used in the project described in chapter 3, thereby retaining its advantages. The chip was modified only to integrate the interdigitated electrode arrays into the channel (see design in fig. 5.2A and fig. 5.2B). The modified design deposits the features of the electrode arrays directly behind the gold field used for immobilizing the capture probes. Since the PDMS seals on glass, even when small metallic features extend to the outside of the channel, the contacts to the electrodes were easily accessible.

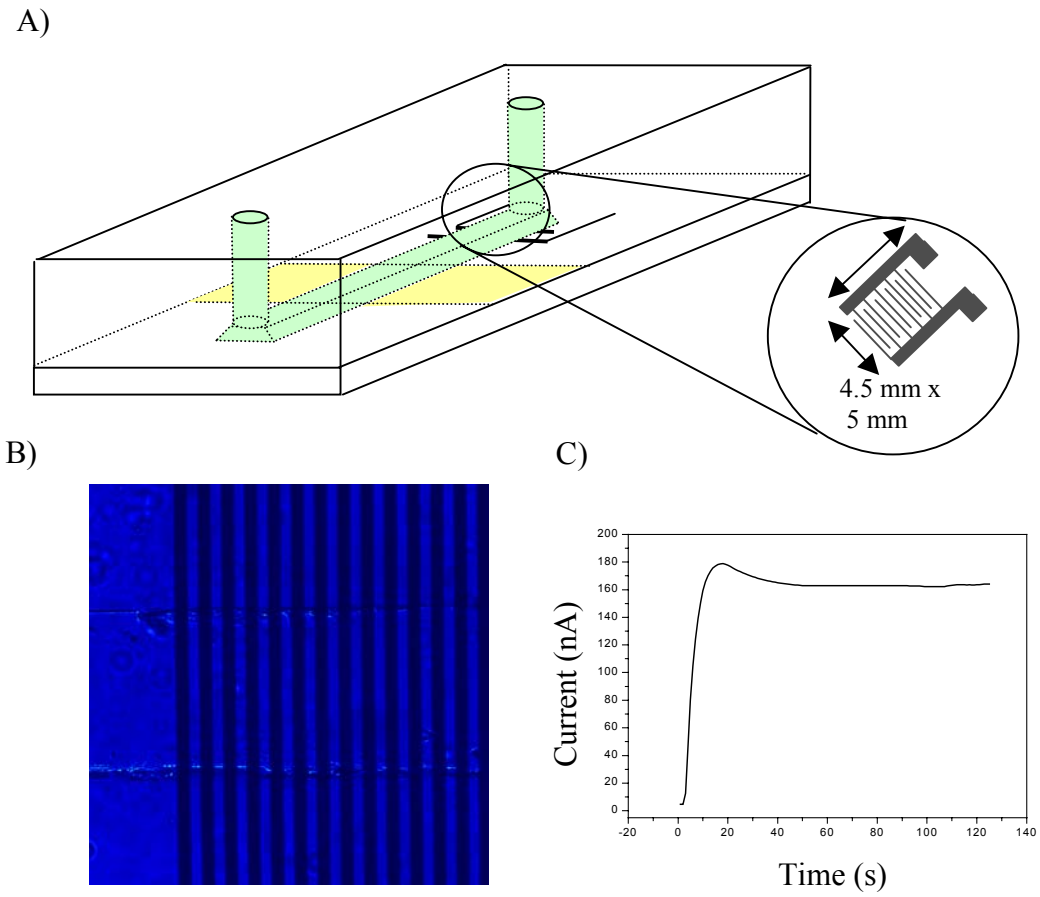

Fig. 5.2 Design of the microfluidic chip: (A) The channels are formed by PDMS and glass slides. The interdigitated microelectrode array is positioned directly behind the gold area used for immobilizing the capture probes; (B) Photomicrograph of a section of the microfluidic channel containing the electrode array; (C) Typical current-time plot yielded by chronoamperometric measurements of ferri- and ferrohexacyanide solutions (applied voltage step: 400 mV; concentration of ferri- and ferrohexacyanide: 6.1 μM).

During the immobilization step, great care was taken to immobilize capture probes on the gold field only and not directly on the electrode. This was done because immobilization of oligonucleotides may alter the properties of the electrodes. For the same reason, we used blocking liposomes instead of mercaptohexane to block nonspecific binding.

The IDA electrodes were fabricated using an image reversal method. The electrodes covered an area of 5 mm x 4.5 mm with a 1 μm spacing between the single fingers and a finger width of 2 μm. Because of the close proximity of the sets of fingers to each other, we fabricated the electrodes by initially patterning a negative image on the photoresist and then reversing this image by baking it with nitride. This created an overhang of photoresist at the edges of the electrode fingers, so that the gold deposited on the glass was not in contact with the gold that covered the photoresist, thereby making it easier to develop it and to strip away the gold from the top (see figure 5.1).

After the fabrication was completed, we examined the electrodes using a microscope. We also measured the resistance between the two sets of fingers. The resistance indicated any connections (short-circuits) between the electrodes. Electrodes whose finger-sets were completely separated from each other exhibited a resistance greater than 1MΩ. However, initially only 50% of the electrodes did not have a short circuit. The remaining electrodes had at least one connection between their finger-sets, resulting in a resistance of only 100-200 kΩ. These short-circuits probably resulted from a connection between the gold on the glass and the gold on top of the photoresist. This could happen when the angled resist edge created by the image-reversal method is partly damaged during the fabrication (fig. 5.3).

However, despite the fact that the quantity of usable electrodes was low initially, we increased that number by repairing the electrodes that were short-circuited. This was achieved by cutting the connecting metal using a focused gallium-ion beam (fig. 5.4A and fig. 5.4B). This procedure takes about 30 min and is therefore preferred to preparing new electrodes. All electrodes that were treated with the focussed ion beam exhibited very high resistances and did not lose their ability to perform electrochemical detections.

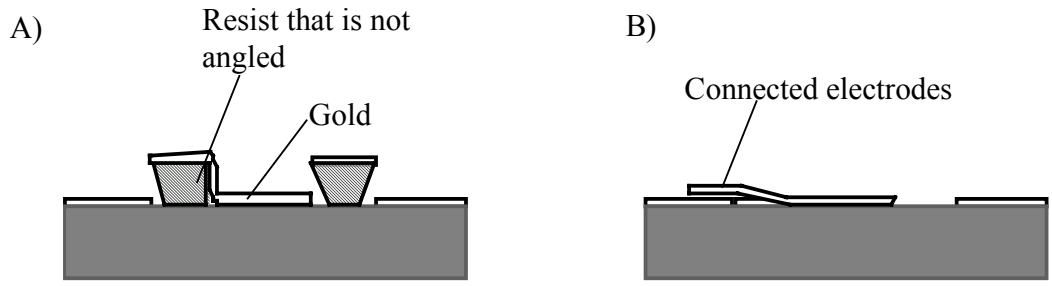

Fig. 5.3 A Possible complication during the fabrication of microelectrode arrays: (A) The angled photoresist edge created by the image reversal process is partly damaged. As a result, the gold on top of the photoresist is not completely separated from the gold deposited directly on the glass; (B) This causes the gold to remain on the glass slide and fall into a position where it comes in contact with the adjacent electrode, thereby short-circuiting the two finger-sets.

The design of the chip made it possible to reuse most of its components except the gold field used for immobilization. In the course of this project, it became clear, while the electrodes and PDMS channels did not exhibit memory effects from previous experiments, using a fresh gold surface that had not been in contact with thiolated reagent is more advantageous for immobilizing the capture probes. A new gold surface was prepared on the used chips by disassembling them and stripping off the used gold field with potassium iodide (KI_3) solution. The chromium adhesion layer was removed by polishing the surface with aluminum powder. The glass slides were then cleaned by soaking them in a solution containing hydrogen peroxide and sulfuric acid in a volume ratio of 3:7 (see experimental section), and, using a metal mask, a new gold field was deposited on the area above the electrode. The chip was then reassembled and used for the next experiment. It should be noted that, in chapter 3, it was shown that the immobilized capture probes were reusable for multiple detections after dehybridization. In the present study we did not reuse chips in the same way because we wanted to avoid erroneous results during the developmental stage of the project.

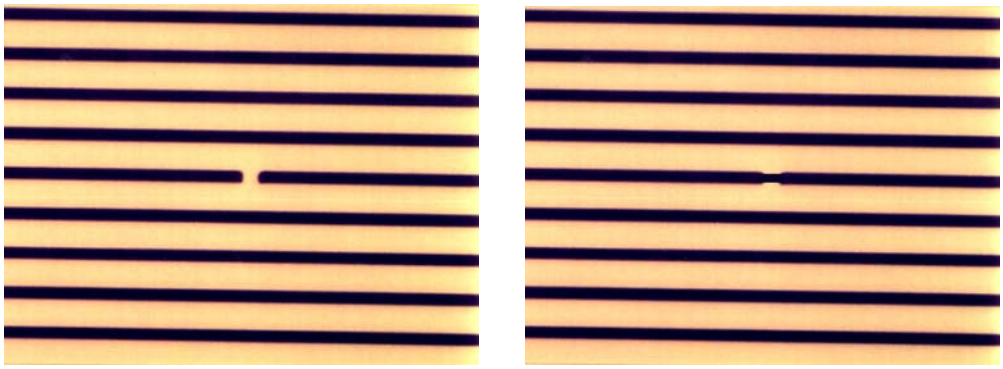

A) B)

Fig. 5.4 Electrodes that are short-circuited between their finger-sets: (A) Connected finger-sets; (B) Electrode after removal of the metal connection by a gallium-ion beam ablation.

CHARACTERIZATION OF LIPOSOMES

For this study, ferri- and ferrohexacyanide were incorporated into the liposome cavity. Since the molecules encapsulated do not come in contact with the electrodes, intact-liposome solutions show small currents when applied to an interdigitated microelectrode array. Measuring the current resulting from lysed liposomes (free ferri- and ferrohexacyanide in solution), we calculated an encapsulation efficiency of 2.8%, assuming that the concentration of encapsulated ferri- and ferrohexacyanide equaled the initial bulk concentration of 100 mM.

We used dynamic light scattering to measure the diameter of the prepared liposomes, finding it to be 267 nm with a standard deviation of 91 nm.

DETECTION OF FERRI- AND FERROHEXACYANIDE USING INTERDIGITATED ELECTRODE ARRAYS

The fabricated electrode arrays were first compared with commercially available electrode arrays. We found that the response of our electrodes was very similar to that obtained by commercial electrodes, thereby indicating their usefulness. Fig. 5.5 shows how the measured current was related to the concentration of the ferri- and ferrohexacyanide solution. The curves show that the fabricated electrodes with a finger-set spacing of 1 μm (total electrode area 4.5 x 5.0 mm) gave a slightly higher

response than the commercial electrode with a finger-set spacing of 20 μm (total electrode area 3.0 x 6.0 mm). We also fabricated electrodes covering an area of 4.5 x 5.0 mm with a finger-set spacing of 20 μm. They were slightly less sensitive towards ferri- and ferrohexacyanide solutions than the commercial electrodes (results not shown).

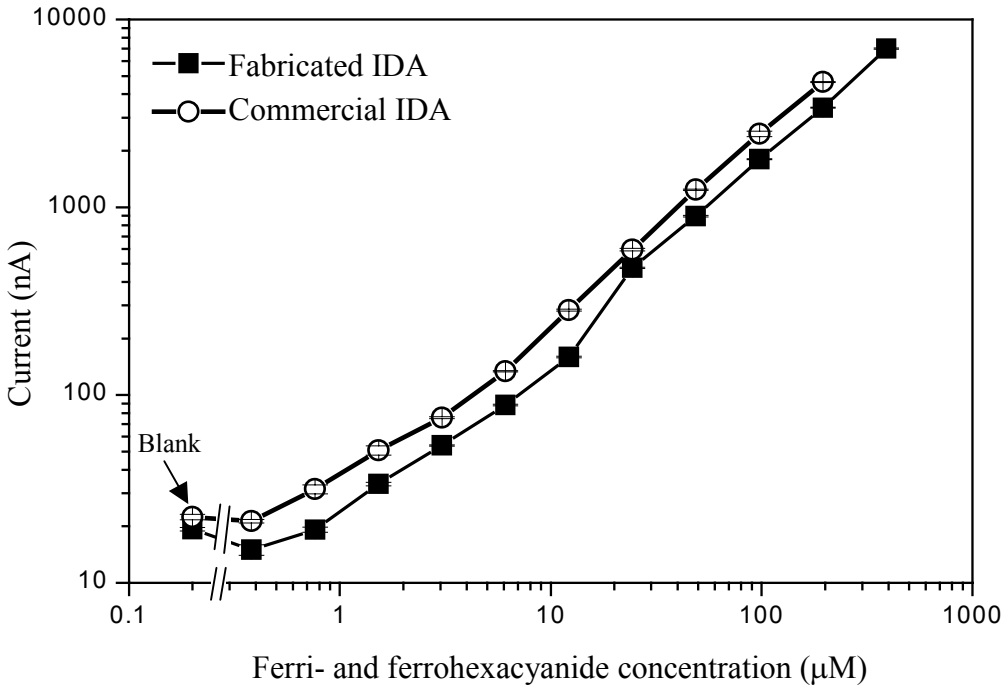

Fig. 5.5 Comparison of fabricated electrodes (fingerspacing 1 μm) and commercially available electrodes [fingerspacing 20 μm, length 3 mm (IME 2025.3); Abtech Inc., Richmond, VA]. We applied a potential of 400 mV across the two finger-sets of the electrode array. Varying concentrations of ferri- and ferrohexacyanide were applied to the electrode and the resulting current was measured.

The performance of the electrodes was monitored over time. Fig. 5.6 compares the response of an electrode after three months of usage to its response immediately after fabrication. The curves indicate that over time the generated current is slightly decreased. However, the measurements are still very reproducible, as indicated by the standard deviations derived from three experiments (represented as the error bars).

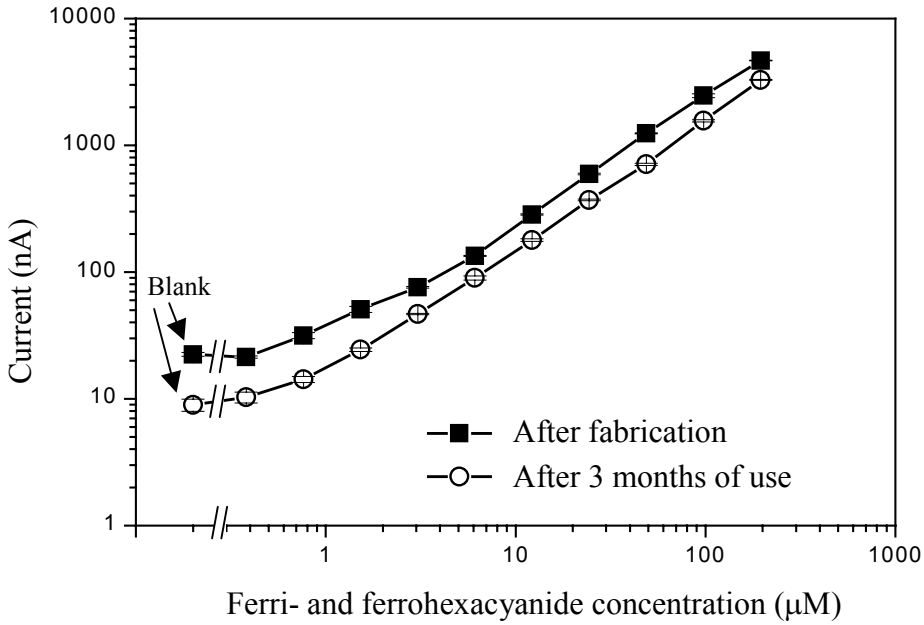

Fig. 5.6 Aging of electrode arrays. The measured current is plotted against the concentration of ferri- and ferrohexacyanide for the same electrode immediately after fabrication and after 3 months of use.

Next we investigated the response of the electrode when integrated into the chip. The PDMS channel on the chip was 50 μm deep and at the bottom 335.5 μm wide (the top width was 300 μm). Because the area which is exposed to the ferri- and ferrohexacyanide solution is much smaller when the solution flows over the electrode guided by the channel (exposed area: 6 mm x 335.5 μm), and the current is proportional to the electrode area exposed we expected a decrease in current when using the IDAs with the microchannels described. As Fig. 5.7 shows, the response decreases when only the channel area is exposed to solution in comparison with covering the entire electrode surface. At high ferri- and ferrohexacyanide concentrations the current is decreased by one magnitude. However, while the solution flows through the channel with a flow rate of 1.5 nL/s ± 0.09 nL/s the solution is not flowing when the entire electrode area is used. The flow occurring in the channel may have a positive effect on the measurement because the movement of ions is not only facilitated by diffusion.

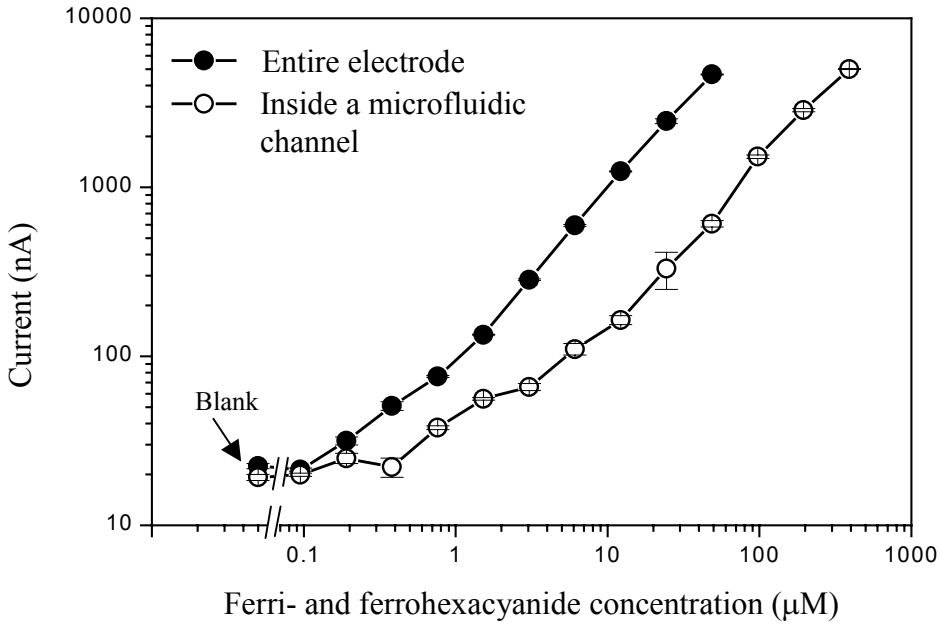

Fig. 5.7 Change in current depending on the covered area. At an applied potential of 400 mV the current was measured for ferri- and ferrohexacyanide solutions with different concentrations that covered the entire electrode surface (total electrode area 4.5 x 5.0 mm), or flowed through a microchannel with the dimensions of 335.5 μm x 50 μm. When using the microchannel, the area exposed to the ferri- and ferrohexacyanide solution is 335.5 μm x 5 mm.

INFLUENCE OF ASSAY REAGENTS ON THE DETECTION WITH INTERDIGITATED ELECTRODES

Because single-stranded target oligonucleotide may non-specifically adsorb onto the electrode surface during the hybridization assay, we investigated whether this adsorption would inhibit the electrochemical measurements. Experiments were conducted in which we incubated the electrode surface inside the microchannel with single-stranded target oligonucleotide (without conducting the entire assay), and then measured the response to varying concentrations of ferri- and ferrohexacyanide solution. The results are presented in fig. 5.8 The dose-response curves show that the adsorbed oligonucleotide did not lower the currents that were measured.

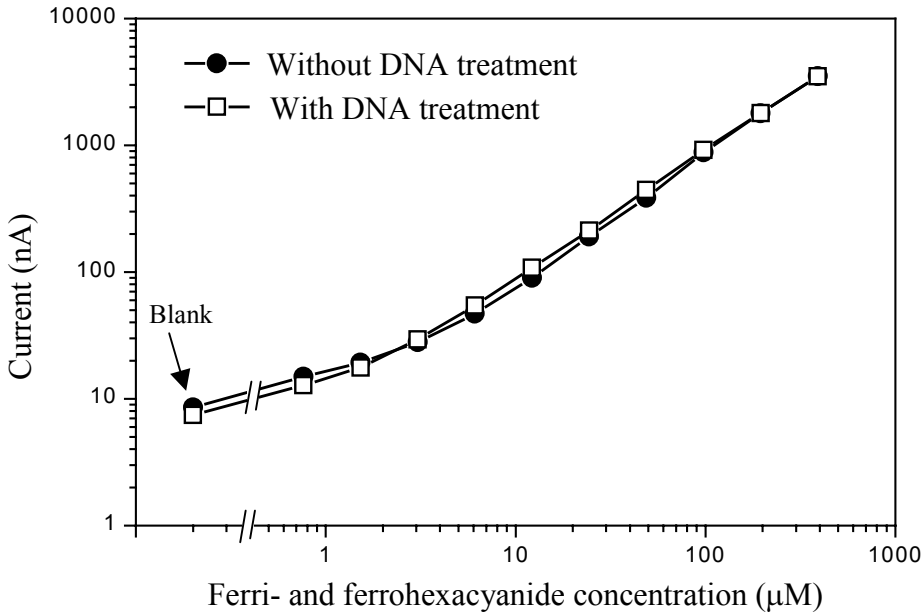

Fig. 5.8 Influence of single-stranded DNA adsorbed to the gold electrodes on the current. Microelectrode arrays were incubated with a solution containing 400 fmol of DNA per μL. This solution was exchanged against ferri- and ferrohexacyanide solutions and the current was measured at a constant potential of 400 mV.

We also investigated the influence of the detergent, octyl glucopyranoside (OG), on the responses of the electrodes. Purified OG was mixed with ferri- and ferrohexacyanide solutions so that the final concentration of OG was 50 mM and the concentration of ferri- and ferrohexacyanide varied from 0 to 195 μM. The current is slightly decreased for solutions containing ferri- and ferrohexacyanide at concentrations below 1 μM, and slightly increased above that concentration (fig. 5.9). Experiments that were conducted with varying OG concentrations suggest that OG at concentrations higher than 12.5 mM increases the current obtained and therefore adds a background current to the current resulting from the buffer solution not containing OG (see fig. 5.10). However, at ferri- and ferrohexacyanide concentrations below 1 μM this is not true (see fig. 5.9).

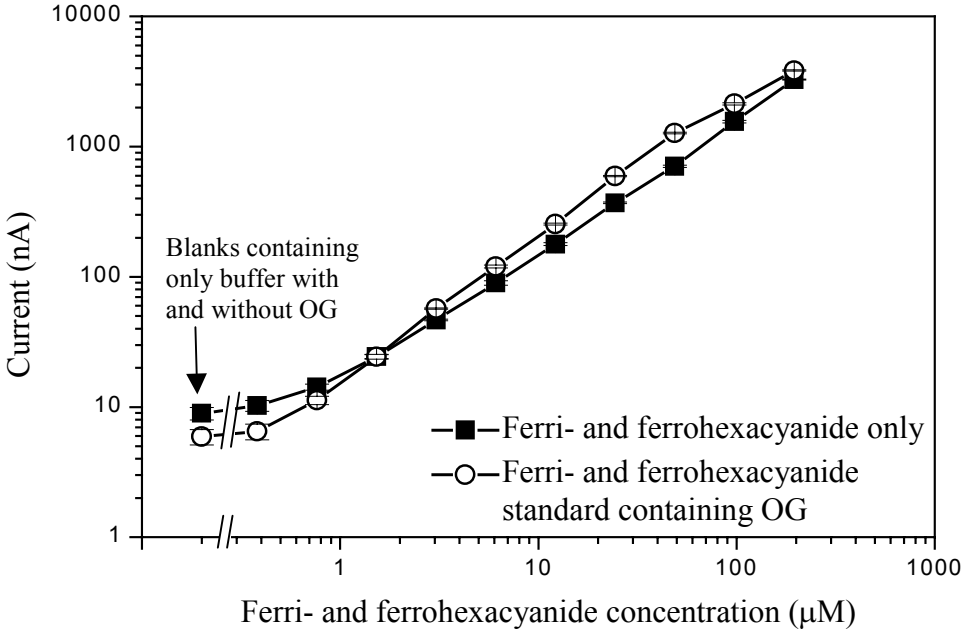

Fig. 5.9 Influence of OG on the current. The current-response is measured for ferri- and ferrohexacyanide solutions with and without 50 mM OG.

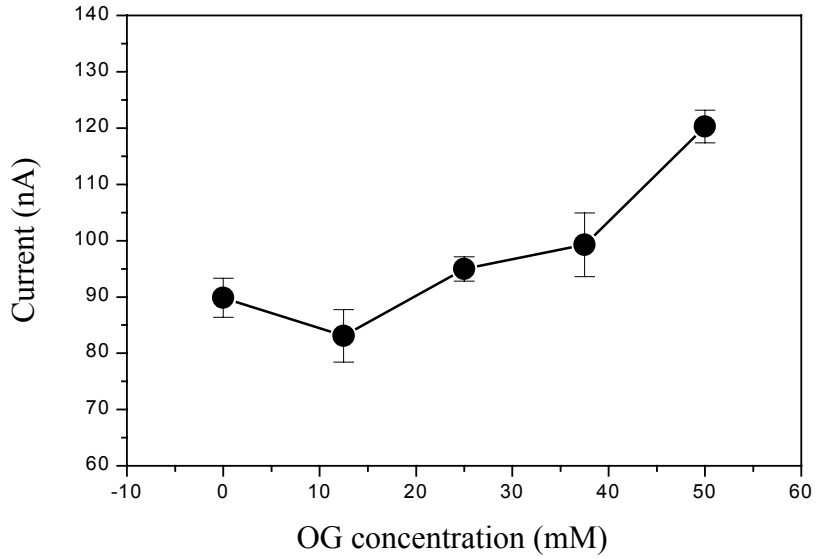

Fig. 5.10 Influence of the concentration of OG on the electrochemical measurement. Solutions containing 6.1 μM ferri- and ferrohexacyanide and varying concentrations of OG were applied to a microelectrode array. Applying a potential of 400 mV the resulting current is measured and plotted against the OG concentration in the solution.

To prevent any inhibition from the blocking reagents we used in the chip, blocking liposomes only were used for blocking. We assume that the blocking liposomes not only adsorb at the gold field at which the capture probe is immobilized, but also to the surface of the IDAs. After the assay is conducted the liposomes containing the ferri- and ferrohexacyanide solution are lysed by OG to facilitate the electrochemical measurement. During this process the blocking liposomes are also lysed and thereby removed from the electrode surface. The lipids from the liposome membranes are then free in solution. We conducted experiments to investigate whether these lipids influence the response of the IDAs. Fig. 5.11 shows that lipids in a 6.1 μM ferri- and ferrohexacyanide solution that also contains 50 mM OG decreased the measured current only slightly.

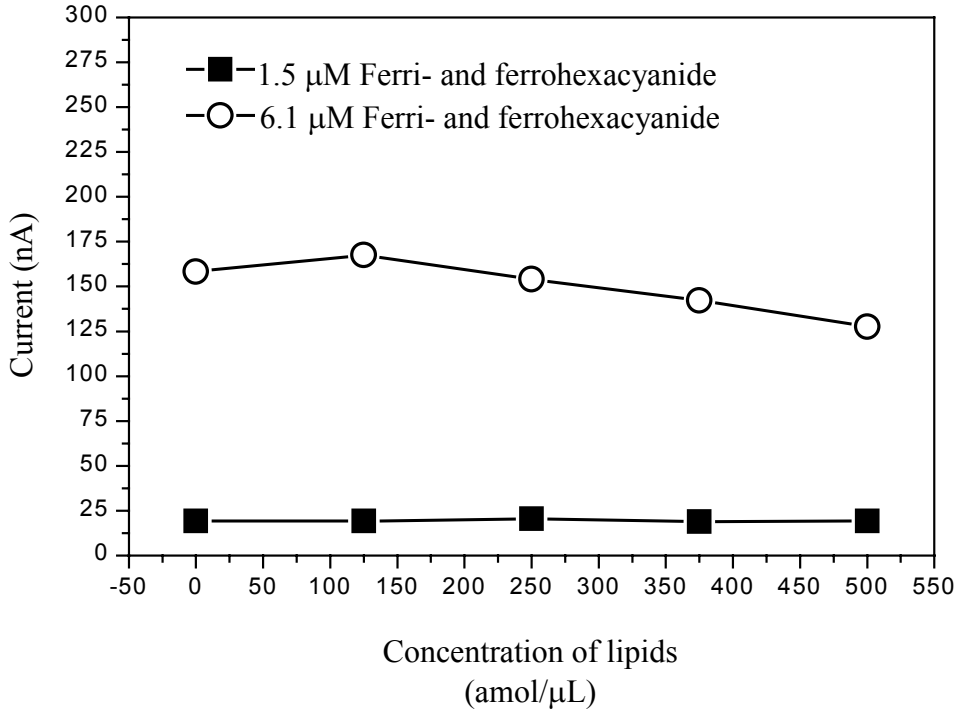

Fig. 5.11 Influence of liposome lipids on electrochemical measurements. Solutions containing 1.5 μM and 6.1 μM ferri- and ferrohexacyanide, 50 mM OG, and varying concentrations of liposomes were applied to the entire electrode area (The amounts of liposome solutions used were typical for conducting and assay and ranged from 5 to 20 μL per 80 μL of test solution, resulting in concentrations in the amol/μL range). The OG lyses the liposomes and sets the lipids free in solution. The resulting current (applied voltage is 400 mV) is plotted against the lipid concentration in the solution.

DOSE-RESPONSE CURVE

To evaluate the performance of the sensor, we conducted hybridization assays with samples that contained synthetic target at a concentration of 400 fmol/μL and with control samples that did not contain any target. Representative curves are shown in fig. 5.12. Because the detergent is flowing through the channel at a constant flow rate, the current reaches a peak when most of the electrode is covered with the solution from the liposomes. As soon as this solution passes over the electrode, the current decreases until it reaches the normal background value produced by the OG solution. The area and the peak height give information on how many liposomes were captured by the hybridization of capture probes, reporter probes, and targets. The curve obtained for the control sample containing no target exhibits a peak value of 64.2 nA and has an area of 1.3 mA/s. The peak value obtained for the sample containing the target is 216.2 nA with an area of 3.7 mA/s. This indicates that the sensor performs in the expected way.

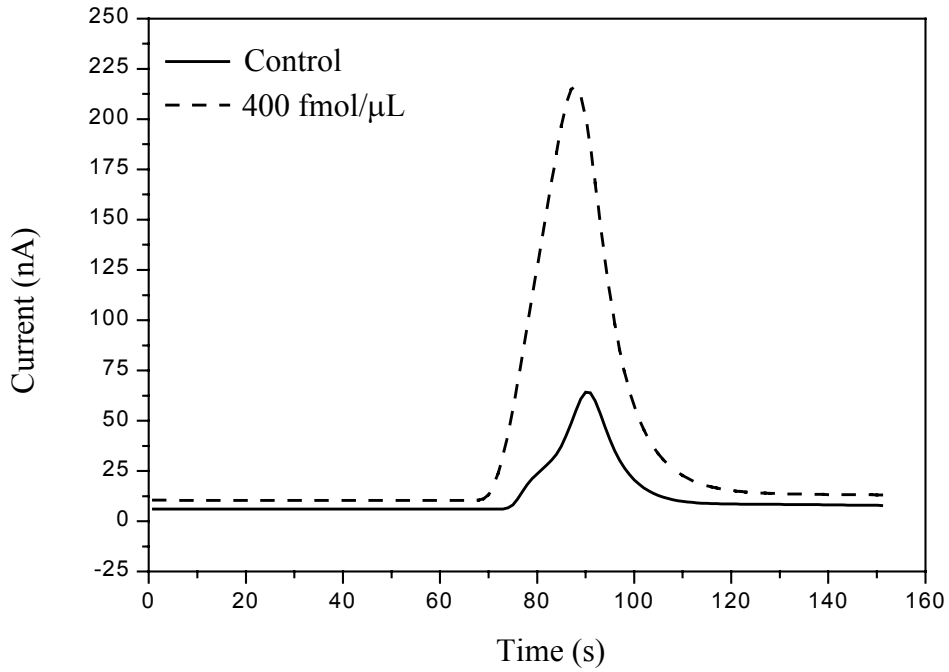

Figure 5.12: Dose-response obtained from microchannels in which assays were conducted with control samples and with solutions containing 400 fmol/μL of synthetic target.

However, the difference between the control sample and the sample containing the target is not as large as the difference that was measured in the sensor that utilized the detection of a fluorescent dye. Further, the repeatability of the experiments was not acceptable since the standard deviations of the peak heights were 50.7 nA for controls and 101 nA for positive samples. Because the experiments did not indicate that the assay components had major influences on the measurements, the large variation in the results may be attributed to variations in the prototype devices themselves. Optimizing the flow rate in these devices by using a syringe pump may help improve the reproducibility of the results. An additional approach to reducing variations in the measurements would be to redirect the fluid flow so that the IDA is unexposed to reagents as long as the actual assay is conducted. For the electrochemical measurement the flow could be directed so that the IDA is exposed to the solution.

CONCLUSIONS

We successfully fabricated IDA electrodes that performed highly sensitive electrochemical measurements of ferri- and ferrohexacyanide solutions comparable to those obtained with commercially available electrodes. We integrated the fabricated electrodes into microfluidic chips and performed nucleic acid detections by utilizing sandwich hybridization and liposomes as reporter-particles. Although the basic concept of the sensor was found to be applicable, more research needs to be done to optimize the sensor's performance. Investigating the influences of various detergents used for lysing the liposomes may improve our understanding of the processes involved. The sensitivity of the electrochemical detection may not be as high as that achieved for the test-strip or the microfluidic chip with detection of fluorescein, yet electrochemical detection may have advantages when applied to field-portable devices.

6

Oligonucleotide Detection by Surface Plasmon Resonance Spectroscopy

ABSTRACT

In this chapter we employ Surface Plasmon Resonance (SPR) spectroscopy to generate optical (nonfluorescent) signals from nucleic acid hybridization events. We demonstrate that these optical signals are enhanced when reporter probe-tagged liposomes are used in the assay. Liposomes generate SPR signals that are twice as great as the signals generated without these reporter particles.

To yield specific hybridization when utilizing liposomes for signal amplification, it is necessary to block the surface from nonspecific adsorption of liposomes. We used the SPR method to investigate the influences of two different blocking layers on the hybridization of capture probes, targets, and reporter probes.

INTRODUCTION

BACKGROUND

In the field of molecular biology it has become important to investigate molecular interactions on surfaces. These interactions include covalent binding of molecules to surfaces, nonspecific adsorption of molecules to surfaces, and the specific interaction of molecules with other molecules that are immobilized on the surface (for example, proteins that bind to immobilized antibodies, or DNA hybridization).

The investigation of such interactions is especially important when developing sensors that are based on specific molecular binding. The sensitivity of such sensors is often limited not by the biochemical reaction or the measurement method employed but by the nonspecific adsorption of the analyte or the reporter particle to the surface of the

sensor (for example, to the plastic walls of in a 96-well plate in enzyme-linked immunosorbent assays). Investigating the nonspecific adsorption of molecules such as the analyte itself leads to a better understanding of the interactions involved. Furthermore, it is important to take account of the interferences caused by molecules that are present in a sample in addition to the analyte (such as the various components of blood in a blood sample). The acquired knowledge can then be utilized to decrease the nonspecific binding. The preparation of the surface could be changed, for example, by using a blocking reagent to prevent the adsorption of molecules. This enhances the performance of the sensor with regard to both specificity and sensitivity.

Several methods are available for investigating molecular interactions that occur directly on surfaces. These are traditional methods such as labeling the molecules that interact with the surface;[1] or more recently employed methods such as ellipsometry,[2-5] or total internal reflection fluorescence spectroscopy.[6] A method that is useful for studying interactions directly on surfaces with submonolayer sensitivity is surface plasmon resonance (SPR) spectroscopy. SPR spectroscopy has been used to study antibody/antigen, protein/ligand, and protein/protein interactions on metal surfaces.[7-10] These studies have revealed information useful for immunodiagnostic devices. For devices that detect nucleic acids, SPR spectroscopy studies report findings about the properties of oligonucleotide layers immobilized on metal surfaces such as gold surfaces, and the ability of such oligonucleotides to hybridize with target molecules.[11-13]

SPR spectroscopy is an optical measurement method that utilizes an energy-coupling process that occurs on the interface between a metal and a dielectric when the interface is illuminated with p-polarized light (i. e., light with its electric field vector oriented parallel to the plane of incidence).[14-16] If the light hits the surface at a particular angle, the energy from the photons can be coupled into oscillating modes of electron density, thereby creating surface plasmon polaritons (electromagnetic evanescent waves that propagate away from the interface into the medium having the lower refractive index). The excitation of surface plasmon polaritons decreases the amount of light that is reflected from the surface. The angle at which surface plasmon polaritons are created (the surface plasmon angle) can be determined by measuring the reflected light at a range of angles at which the energy-coupling process is expected to take place. The refractive index of the medium immediately adjacent to the metal

surface influences the surface plasmon angle. Materials with different refractive indices shift the surface plasmon angle to different values.

Only the environment immediately adjacent to the surface affects the SPR measurements because this is the environment into which the evanescent wave penetrates. Therefore, SPR measurements will be sensitive to biomolecules that modify this environment. For example, the self-assembly of organic monolayers on gold has been investigated by SPR spectroscopy.[17,18] In another study it was found that organic monolayers resist or attract biomolecules such as proteins, depending on the atoms with which these monolayers terminate.[19] In these studies the angle shift gave information about the amount of molecules adsorbed to the monolayer.

SPR SPECTROSCOPY AND NUCLEIC ACID HYBRIDIZATION

SPR spectroscopy is an excellent method for quickly and accurately investigating DNA hybridizations in which oligonucleotides are immobilized on a gold surface. With this method, DNA hybridization can be monitored *in situ*. The rate of hybridization becomes immediately apparent when monitoring the SPR angle shift continuously throughout a hybridization experiment. Since SPR measurements are very sensitive, the nucleic acids involved do not need to be modified with any labels. Further, because SPR measurements focus on the surface only, no washing steps are required before hybridization can be detected. This enables researchers to conduct homogeneous hybridization assays.

Because of the advantages that SPR spectroscopy offers, we investigated whether it is an alternative method for signal generation in a microfluidic sensor based on the sensing scheme developed in chapter 3. This sensor is based on nucleic acid sandwich-hybridization involving capture probes immobilized on a gold surface. The usefulness of combining SPR spectroscopy with the sensor developed in chapter 3, and with the findings concerning the use of certain blocking reagents in the prototype array from chapter 4, lies in the potential for assembling a microfluidic sensor that uses SPR imaging to generate signals from multiple analytes in an array. Others have used SPR imaging to monitor hybridization events at spatially separated sites on a gold surface.[20, 21] Normal SPR spectroscopy (as used in this study) is not capable of measuring optical

signals at different sites; however, the findings of this study are applicable to SPR imaging.

Further, we investigated the usefulness of liposomes as amplifying particles for hybridization measurements by SPR. Liposomes are 200 to 400 nm in diameter, and therefore they should generate larger SPR angle shifts upon hybridizing with oligonucleotides on a gold surface than when oligonucleotides do not have a tag.

EXPERIMENTAL SECTION

OLIGOMERS

See chapter 3 for information on the sequence of reporter probe, capture probe, and target. Modifications of capture probe and reporter probe are also described in chapter 3.

PREPARATION OF REPORTER PROBE-TAGGED LIPOSOMES

Liposomes containing a 100 mM carboxyfluorescein solution were prepared and subsequently tagged with acetylthioacetate at the outside surface of their membranes. These groups were deprotected and coupled to reporter probes. The detailed protocol used for this preparation is described in chapter 3.

EXPERIMENTAL SETUP FOR SPR SPECTROSCOPY

The SPR spectroscopy experiment setup utilized in this study (see fig 6.1) follows the configuration by Kretschmann in which a thin gold film is in direct contact with a glass prism.[22] (The alternative Otto setup requires an air or electrolyte gap on the order of the wavelength of light between the prism and the gold.[23]) A gold-coated cylindrical lens with high refractive index (n = 1.723 or 1.762) was mounted on a rotating table (Aerotech Inc., Pittsburgh, PA) so that its gold-coated side faced the inside of the custom-made Teflon reaction chamber. The optical elements included a

polarized helium/neon (HeNe) laser (Newport, Irvine, CA; wavelength 632.8 nm), a cylindrical lens that spreads the reflected light beam and thereby reduces fluctuations, a fast-response silicon photodiode (Mellis Griot Inc., Rochester, NY), and a wide bandwidth current amplifier (Mellis Griot Inc., Rochester, NY). Custom-made software that controlled the collection of real-time experimental data was provided by Geoffrey Saupe and Michael Tarlov, National Institute of Standards and Technology (NIST).

DEPOSITING GOLD ON THE LENS

The glass prism was cleaned by soaking it for 30 min in 70% (volume fraction) concentrated sulfuric acid and 30% (volume fraction) hydrogen peroxide [30% (volume fraction) H_2O_2 in H_2O]. *See chapter 3 for safety instructions to be followed when working with this solution.* It was then rinsed with 18 MΩ deionized water and dried under a stream of nitrogen. Using a thermal evaporator, we deposited a 15 Å chromium layer and a 450 Å gold layer on the flat side of the prism. After the deposition, we cleaned the prism thoroughly with the cleaning solution described above and subsequently washed it with water. We then mounted the prism on the rotating optical stage as shown in fig 6.1.

PREPARING ORGANIC LAYERS ON THE GOLD SURFACE

To immobilize the capture probes we filled the chamber with a 1 mM solution of disulfide-modified capture probe (diluted in 1 mM potassium phosphate buffer, pH 7.0) and let the adsorption proceed for 60 min. The chamber was then washed with 18 MΩ water and subsequently filled with the blocking reagent (either a 1 mM mercaptohexanol solution diluted in ethanol, or a BSA solution containing a volume fraction of 2% BSA in 50 mM phosphate buffer). After 60 min of incubation at room temperature, the chamber was washed with water (18 MΩ) and then the hybridization assay was conducted.

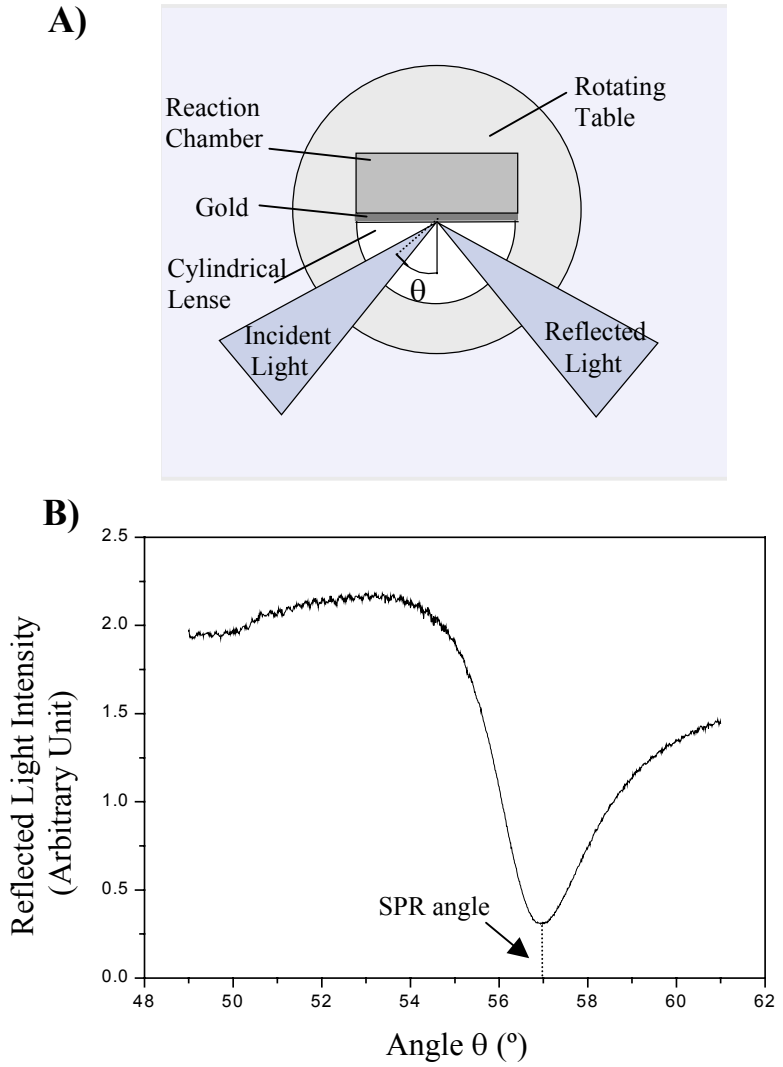

Fig. 6.1 (A) SPR experiment setup and (B) SPR curve measured with a gold surface and water as adjacent medium.

ASSAY PROTOCOL

We filled the Teflon reaction chamber with 1 mL of sample solution containing synthetic target oligonucleotide diluted in hybridization buffer. After the target was added, the concentrations of the components in the hybridization buffer were 0.6 M NaCl, 0.06 M NaH_2PO_4, 2 mM EDTA [2 times concentrated Standard Saline Phosphate buffer with EDTA (2x SSPE)] and a volume fraction of 40% formamide. The hybridization was allowed to proceed for 60 to 120 min. We then washed the chamber

with 2x SSPE buffer. Next, the reporter probe-tagged liposomes (diluted in hybridization buffer) were introduced into the reaction chamber. After addition of the liposomes, the concentrations of the components in this buffer were a volume fraction of 5% of liposome solution (as recovered from the Sepharose column), SSPE concentrated four times (4x), a volume fraction of 20% formamide, a volume fraction of 0.2% Ficoll (type 400), and 0.125 M sucrose. This buffer had been optimized for the use with liposomes in hybridization studies in chapter 2. The hybridization was allowed to proceed overnight.

DATA ANALYSIS

As Hanken et al. describe in their review about SPR spectroscopy studies, the reflectivity curves derived from SPR experiments can be modeled with theoretical Fresnel calculations.[24] From these models one can obtain the thickness of organic films assembled onto the gold surface. The Fresnel calculations are based on reflection and transmission of light from a one-dimensional multilayer dielectric stack that consists of multiple planar phases. A number of papers have derived reflectivity equations that consider three, four, or N phases.[25-29] To analyze the results in this study, we used a software that generates theoretical SPR curves, custom-made by Geoffrey Saupe (National Institute of Standards and Technology). The calculations using this software closely follow a 4-phase calculation derived from the N-phase calculations by Hansen and colleagues.[30] Using this software, we fitted the experimental data to theoretical SPR curves.

Although in theory it is possible to extract both the index of refraction and the thickness of the assembled organic layer from SPR-reflectivity curve shapes, experimental uncertainties make this difficult to realize.[27, 28] To yield both the index of refraction and the thickness of the layer from SPR experiments only, multiple wavelengths or different solvents must be used.[11, 28, 29] The SPR experiments described here calculate the mass loadings or thickness of the assembled organic layers on the basis of either estimated indices of refraction or indices of refraction that had been

determined by another analytical method in another study. As discussed by Hanken et al. the refractive indices for organic layers usually lie between 1.4 and 1.55, and a variation of +/- 0.05 due to estimation leads to an error of approximately +/- 7% (i.e., 0.1 nm for every 1.5 nm of film thickness).[24]

RESULTS AND DISCUSSION

IMMOBILIZATION OF CAPTURE PROBES AND DEPOSITION OF BLOCKING LAYERS ON A GOLD SURFACE

The design of the sensor developed in chapter 3 includes the immobilization of capture probes by means of thiolated C6-linkers on a gold surface. In chapters 3 and 4 it was observed that the sandwich-hybridization that takes place among the immobilized capture probes, the targets, and the reporter probe-tagged liposomes is specific only when nonspecific binding is blocked with blocking reagents such as mercaptohexane, blocking liposomes, or BSA. Since the practical application of the developed sensor will be an array, and since BSA proved to be the most suitable blocking reagent for the prototype array that we designed in chapter 4, we utilized the SPR measurements to observe and investigate the assembly of the capture probe layer and the BSA blocking layer. On the other hand, Levicky et al. reported that thiol-tethered, single-stranded oligonucleotides on gold hybridize more specifically with their complement when the oligonucleotide layer is modified with mercaptohexanol, thereby yielding a mixed monolayer.[31] Because in Levicky's study (as in this study) the oligonucleotides were bound to the gold by a thiolated C6-linker, the treatment with mercaptohexanol removed not only nonspecifically adsorbed oligonucleotides from the gold but also made the oligonucleotides stand erect, extending away from the surface. This made the oligonucleotides more easily accessible for hybridization with the target. However, mercaptohexanol did not prove to be useful for blocking nonspecific binding of reporter probe-tagged liposomes to capture probe-modified gold surfaces. Therefore, we utilize this study to investigate the effects that blocking with BSA has on the hybridization of

capture probes and targets; and we compare these effects to the effects mercaptohexanol has on this hybridization.

To observe the assembly of the capture probes on the gold surface, we first filled the Teflon reaction chamber with a 1 mM solution of capture probes diluted in a 1 mM phosphate buffer. The shift in SPR angle was constantly monitored using a computer and customized software. Fig 6.2 presents the shifts in the SPR angle over a period of 70 min in a typical experiment. The overall angle shift measured in capture probe assembly experiments was 0.182º ± 0.029º. If we use an estimated refractive index of 1.51 for single-stranded oligonucleotides,[11] this corresponds to a mass loading of capture probe of 15.07 μg/cm^2 ± 3.31 μg/cm^2 .

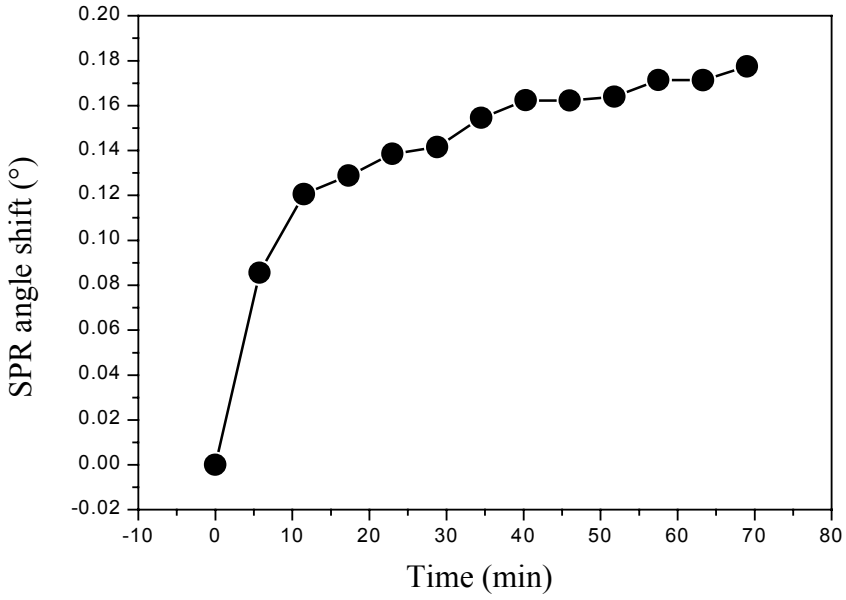

Fig. 6.2 SPR angle shifts obtained for the assembly of thiol-modified capture probes on a gold surface.

The assembly of layers of mercaptohexanol and BSA as blocking layers on oligonucleotide-modified gold surfaces was investigated next. Fig 6.3 shows the shift in SPR angle over a period of 53 min for each of the blocking reagents that were self-assembling on the gold surface (representative graphs are shown). When mercaptohexanol was applied, no net increase in SPR angle was observed (θ = 0.0018° ± 0.0037°). Instead, in several experiments the angle increased slightly at first

(+ 0.01°), but eventually decreased to the original value. This result agrees well with the results of Levicky and colleagues.[32] The explanation is that marcaptohexanol actually removes nonspecifically adsorbed oligonucleotides, thereby merely replacing material already adsorbed. This would not lead to a net increase, because molecules were merely exchanged.

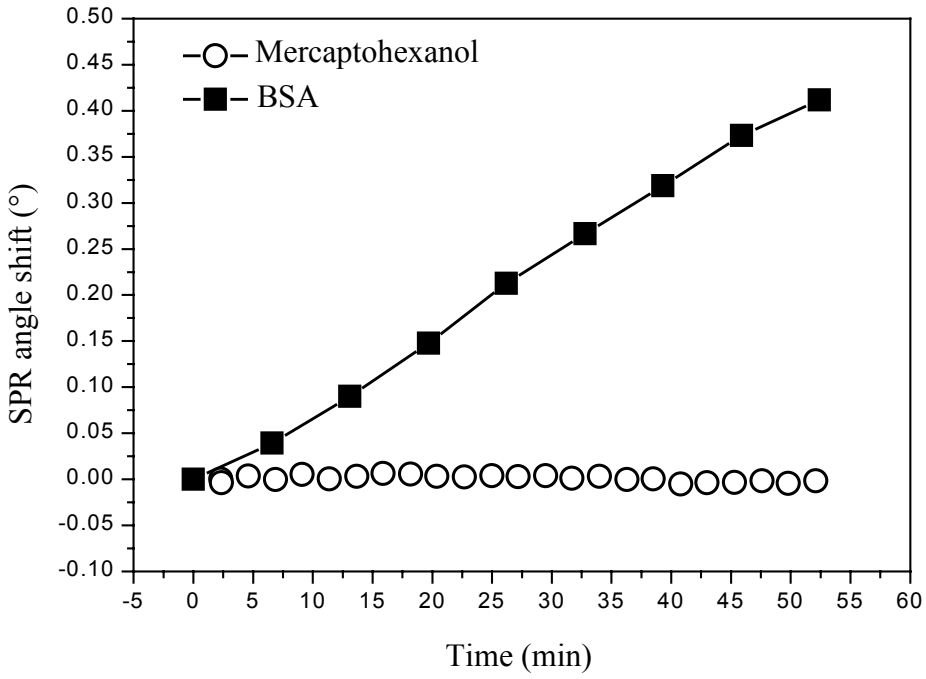

Fig.6.3 SPR angle shifts obtained for the self-assembly of mercaptohexanol and BSA on a capture probe-modified gold surface.

On the other hand, the adsorption of BSA causes the SPR angle to shift about 0.43° after 53 min. This result can be attributed in part to the size of BSA molecules (molecular weight: 66,000 Da), which are comparatively large. Further, BSA is not adsorbed to the gold by thiol–gold interactions, but by electrostatic interaction. This means that no oligonucleotide is displaced from the surface when BSA is deposited.

HYBRIDIZING TARGETS TO MIXED LAYERS OF CAPTURE PROBES AND BLOCKING MOLECULES

We investigated the influence of mercaptohexanol and BSA on the hybridization of the capture probes and the target. We conducted experiments in which samples containing synthetic target oligonucleotide at a concentration of 400 fmol/μL were added to surfaces prepared with capture probes and each of the two blocking reagents. While no change in SPR angle was observed for the control samples that contained no target, the positive samples caused a shift of 0.117° ± 0.029° on a capture probe/mercaptohexanol layer, and a shift of only 0.04° ± 0.014° on the capture probe/BSA layer. This corresponds to 13.36 μg/cm^2 ± 3.31 μg/cm^2 of target on the capture probe/mercaptohexanol layer and 4.03 μg/cm^2 ± 1.60 μg/cm^2 of target on the capture probe/BSA layer. Fig 6.4 shows the angle shifts yielded over a period of 225 min. While the curve is relatively smooth for the mercaptohexanol layer, it exhibits spikes for the BSA layer. This may have been because the target was unable to access

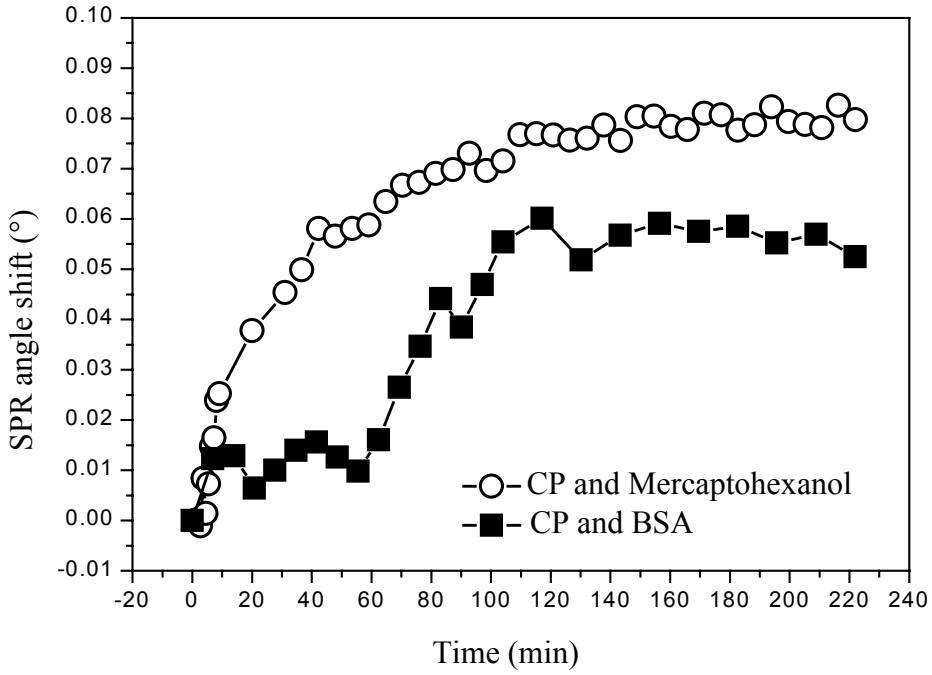

Fig. 6.4 SPR angle shifts measured for the hybridization of synthetic target to mixed monolayers of capture probes (CP) and mercaptohexanol, and of capture probes and BSA.

the capture probes as easily when BSA is blocking the nonspecific binding. This may also be the reason for the lower amount of target that hybridized to the capture probe/BSA-modified surface. In experiments conducted with control samples no angle shift was observed for surfaces that were prepared with either of the two blocking reagents.

SANDWICH HYBRIDIZATION WITH REPORTER PROBE-TAGGED LIPOSOMES

To test whether reporter probe-tagged liposomes can be detected in SPR measurements when they hybridize to capture probes and targets in a sandwich-type manner, we conducted experiments in which liposomes were added to layers prepared with capture probes, blocking layers, and target. Fig 6.5 shows the angle shifts yielded over a period of 375 min. The results show that liposomes adsorb to mixed layers of capture probe and mercaptohexanol in the presence, and also in the absence, of the target oligonucleotide. This indicates that the binding of liposomes to these layers is caused not only by specific hybridization with the target but also by nonspecific adsorption. This result is in agreement with the results found in chapter 3. On the other hand, when liposomes were added to layers of capture probes and BSA, they increased the angle shift only when the target oligonucleotide was present. This indicates that specific hybridization took place.

If we compare the angle shifts caused by hybridization of liposomes to surface containing capture probe, mercaptohexanol, target, and capture probe, BSA, target, it becomes apparent that the angle shift on the surface containing BSA is less than half as great as the angle shift on the other surface. Further, as already seen in the hybridization with target, the hybridization curve on the BSA-containing surface exhibits spikes. Both of these findings can be explained in terms of the mechanism by which BSA blocks the surface and its large size. The target oligonucleotides are not as easily accessible, and also some rearrangements of molecules during the hybridization may take place.

The size of the liposomes used in the SPR experiments was measured by dynamic light scattering and were found to be 349 nm, with a standard deviation of 120. However, the calculated thickness for liposome layers measured in the SPR

experiments were always under 100 nm. We explain this discrepancy by considering that the formed layer is not a complete monolayer. Unlike the microfluidic chip in which a constant flow of liposome solution provides liposomes close to the surface, the assay here is a static assay in which the hybridization is limited by diffusion. This causes a slower hybridization rate, which results in an incomplete layer. Further, the sensitivity of SPR measurements becomes limited the farther away the molecules are from the gold surface (see fig. 6.6). This contributes to the underestimation of the liposome layer according to SPR experiments.

Nevertheless, the angle shift resulting from the hybridization with the liposomes is more than twice as great as that resulting from the hybridization of target to the capture probes alone. This confirms the usefulness of liposomes in amplifying angle shifts measured with SPR spectroscopy.

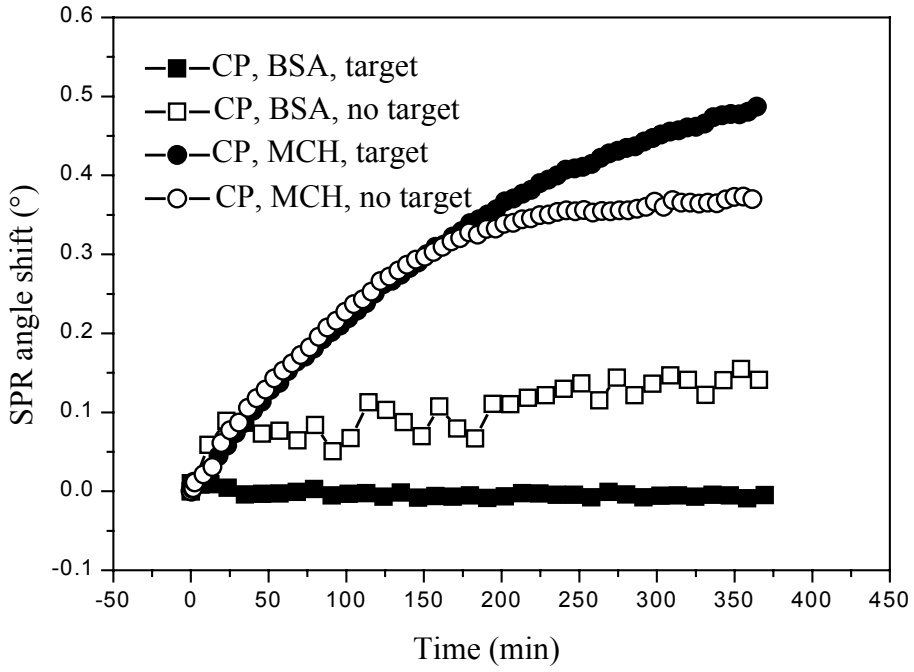

Fig. 6.5 Comparison of SPR angle shifts caused by liposomes hybridizing to surfaces with capture probes (CP), blocking reagents (Bovine Serum Albumin = BSA; Mercaptohexanol = MCH), and targets, or surfaces with capture probes, blocking reagents, and no target.

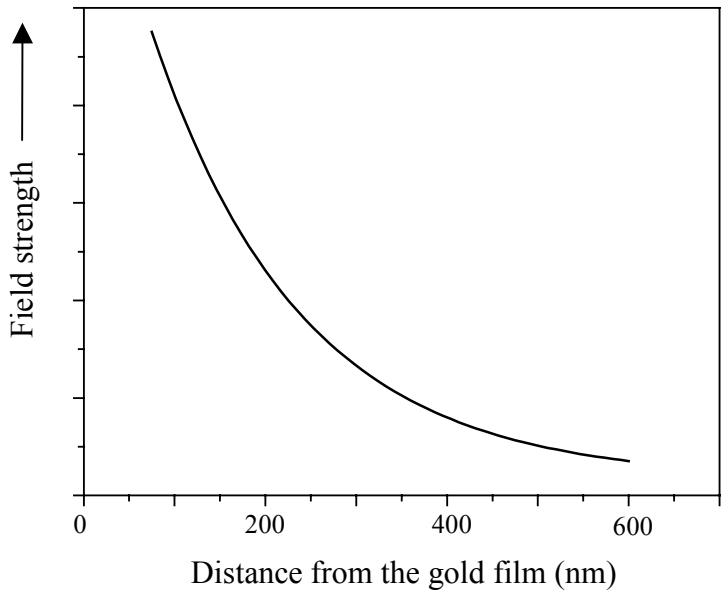

Fig. 6.6 The evanescent wave decays exponentially with increasing distance from the gold/buffer interface (theoretical plot).

CONCLUSIONS

In summary, we have shown that mercaptohexanol and BSA are both capable of blocking nonspecific binding of target oligonucleotide to gold surfaces that had been modified with thiolated capture probes. From the experiments, we conclude further that specific hybridization of the target to the capture probe takes place when the surface is blocked with mercaptohexanol or BSA. However, the hybridization is more efficient when mercaptohexanol is used.

Additionally, to the best knowledge of the author, reporter probe-tagged liposomes were for the first time successfully employed to enhance the shift in SPR angle when conducting oligonucleotide sandwich-hybridization assays on gold surfaces. While BSA was capable of blocking nonspecific adsorption of liposomes in these experiments, mercaptohexanol was not. The hybridization among the capture probe, the target, and the reporter probe on the liposome membrane is affected by the steric hindrance of the BSA. However, BSA was shown to be a suitable blocking

reagent in the prototype array developed in chapter 4. If we draw together the results from chapter 4 with the results from this study, we should now be able to fabricate a prototype array and employ SPR imaging as our means of measurement. When we then provide this experimental setup with a microfluidic flow cell similar to the one described in chapter 3, we are prepared to develop a nucleic acid sensor capable of high throughput analysis.

REFERENCES

CHAPTER 1: INTRODUCTION

1) Stryer, L., In Biochemistry, 1988, 3rd edition, New York: W. H. Freeman
2) Wallace, R. B.; Shaffer, J.; Murphy, R. F.; Bonner, J.; Hirose, T.; Itakura, K. *Nucl. Acids Res.* **1979**, *6*, 3543-3557.
3) Buvoli, M.; Biamonti, G.; Morandi, C. *Nucl. Acids Res.* **1987**, *15*, 9091.
4) Mullis, K. B.; Faloona, F. *Meth Enzymol.* **1987**, *155*, 335-350.
5) Saiki, R. K.; Scharf, S.; Faloona, F.; Mullis, K. B.; Horn, G. T.; Erlich, H. A.; Arnheim, N. *Science* **1985**, *230*, 1350-1354.
6) White, T. J.; Madej, R.; Persing, D. H. *Adv. Clin. Chem.* **1992**, *29*, 161-196.
7) Van Belkum, A. *Clin. Microbiol. Rev.* **1994**, *7*, 174-184.
8) Pfeffer, M.; Wiedmann, M.; Batt, C. A. *Vet. Res. Comm.* **1995**, *19*, 375-407.
9) Auerbach, A. D.; Allen, R. G. *Cancer Genetics and Cytogenetics* **1991**, *51*, 1-12.
10) Bieche, I.; Lidereau, R. *Genes Chromosomes & Cancer* **1995**, *14*, 227-251.
11) Theofilopoulos, A. N. *Immunology Today* **1995**, *16*, 150-159.
12) Van Elsas, J. D.; Duarte, G. F.; Rosado, A. S.; Smalla, K. *J. of Microbiol. Methods* **1998**, *32*, 133-154.
13) Atlas, R. M.; Sayler, G.; Burlage, R. S.; Bej, A. K. *Biotechniques* **1992**, *12*, 706.
14) Widmer, G.; Orbacz, E. A.; Tzipori, S. Appl. *Environ. Microbiol.* **1999**, *65*, 1584-1588.
15) Southern, E. M.*J. Mol. Biol.* **1975**, *98*, 503-517.
16) Thomas, P. S. *Proc. Natl. Acad. Sci. USA* **1980**, *77*, 5201-5205.
17) Leary, J. J.; Brigati, D. J.; Ward, D. C. *Proc. Natl. Acad. Sci. USA* **1983**, *80,* 4045-4049.
18) Harvey, B. M., Wheeler, C. B. In Methods in Molecular Biology, Vol. 28: Protocols for Nucleic Acid Analysis by Nonradioactive Probes; Isaac, P. G., Ed.; Humana Press Inc.: Totowa, NJ, 1994, pp 135-140.
19) In Methods in Molecular Biology, Vol. 28: Protocols for Nucleic Acid Analysis by Nonradioactive Probes; Isaac, P. G., Ed.; Humana Press Inc.: Totowa, NJ, 1994.
20) Kafatos, F. C.; Jones, C. W.; Efstratiadis, A. *Nucl. Acids Res.* **1979**, *7*, 1541-1552.

21) Saiki, R. K.; Walsh, P. S.; Levenson, C. H.; Erlich, H. A. *Proc. Natl. Acad. Sci. USA* **1989**, *86*, 6230-6234.

22) Matthews, J. A.; Kricka, L. J. *Anal. Biochem.* **1988**, *169*, 1-25.

23) Manak, M. M. 1993, In: DNA Probes, Stockton Press, New York, pp. 199-253.

24) Davies, E.; Hodge, R.; Isaac, P. G. In Methods in Molecular Biology, Vol. 28: Protocols for Nucleic Acid Analysis by Nonradioactive Probes; Isaac, P. G., Ed.; Humana Press Inc.: Totowa, NJ, 1994, pp 121-126.

25) Karp, A. In Methods in Molecular Biology, Vol. 28: Protocols for Nucleic Acid Analysis by Nonradioactive Probes; Isaac, P. G., Ed.; Humana Press Inc.: Totowa, NJ, 1994, pp 161-166.

26) Liu, S.; Ye, J.; He, P.; Fang, Y. *Anal. Chim. Acta* **1996**, *335*, 239-243.

27) Wang, J.; Cai, X.; Rivas, G.; Shiraishi, H. *Anal. Chim. Acta* **1996**, *326*, 141-147.

28) Wang, J.; Rivas, G.; Cai, X.; Dontha, N.; Shraishi, H.; Luo, D.; Valera, F. S. *Anal. Chim. Acta* **1997**, *337*, 41-48.

29) Millan, K. M.; Mikkelsen, S. R. *Anal. Chem.* **1993**, *65*, 2317-2323.

30) Yamashita, K.; Takagi, M.; Kondo, H.; Takenaka, S. *Chemistry Letters* **2000**, *9*, 1038-1039.

31) Fan, C. H.; Li, G. X.; Gu, Q. R.; Zhu, J. Q.; Zhu, D. X. *Analytical Letters* **2000**, *33*, 1479-1490.

32) Erdem, A.; Kernman, K.; Meric, B.; Akarca, U. S.; Ozsoz, M. *Anal. Chim. Acta* **2000**, *422*, 139-149.

33) Van Amerongen, A.; Van Loon, D.; Berendsen, L. B. J. M.; Wichers, J. H. *Clin. Chim. Acta* **1994**, *229*, 67-75.

34) Snowden, K.; Hommel, M. *J. immunol. Methods* **1991**, *140*, 57-65.

35) Leuvering, J. H. W.; Thal, P. J. H. M.; Van der Waart, M.; Schuurs, A. H. W. M. *J. of Immunoassay* **1980**, *1*, 77-91.

36) Leuvering, J. H. W.; Thal, P. J. H. M.; Van der Waart, M.; Schuurs, A. H. W. M. *J. Immunonol. Mthods* **1980**, *45*, 183-184.

37) Keele, D. K.; Remple, J.; Bean, J.; Webster, J. *J. Clin. Endocrinol. Metab.* **1962**, *22*, 287-299.

38) Kung, V. T.; Maxim, P. E.; Veltri, R. W.; Martin, F. J. *Biochim. Biophys. Acta* **1985**, *839*, 105-109.

39) Siebert, S. T. A.; Reeves, S. G.; Durst, R. A. *Anal. Chim. Acta* **1993**, *282*, 297-305.

40) O'Connel, J. P.; Campbell, R. L.; Fleming, B. M.; Mercolino, T. J.; Johnson, M. D.; McLaurin, D. A. *Clin. Chem.* **1985**, *31*, 1424-1426.

41) Bangham, A. D.; Standish, M. M.; Weissman, G. *J. Mol. Biol.* **1965**, *13*, 238-252.

42) Lasic, D. D. *Tibtech* **1998**, *16*, 307-321.

43) Monroe, D. *J. Liposome Res.* **1990**, *1*, 339-377.

44) Locascio-Brown, L.; Plant, A. L.; Horvath, V.; Durst, R. A. *Anal. Chem.* **1990**, *62*, 2587-2593.

45) Wu, E.-S.; Jacobson, K.; Papahadjopoulos, D. *Biochemistry* **1977**, *16*, 3936-3941.

46) Fahey, P. F.; Koppel, D. E.; Barak, L. S.; Wolf, D. E.; Elson, E. L.; Webb, W. W. *Science* **1977**, *21*, 305-306.

47) Laukkanen, M.-L.; Orellana, A.; Keinaenen, K. *J. Immunol. Methods* **1995**, *185*, 95-102.

48) Plant, A. L.; Brizgys, M. V.; Locascio-Brown, L.; Durst, R. A. *Anal. Biochem.* **1989**, *176*, 420-426.

49) Lee, M.; Durst, R. A.; Wong, R. B. *Anal. Chim. Acta***1997,** *354*, 23-28.

50) Crashaw, G. J.; Mehren, K. G., Cryptosporidiosis in zoo and wild animals., Proc. 29th Int. Symp Dis Zoo Anim, Cardiff, 1987, 353-362.

51) Current, W. L., The biology of Cryptosporidium. In: Parasitic Infections, edited by Leech, J. H., Sande, M. A., Root, R. K.; Churchill Livingstone, New York & London, 1988, 109-132

52) Current, W. L. *Am. Soc. Microbiol. News* **1988**, *54*, 605-611.

53) Current, W. L.; Garcia, L. S. *Clin. Microbiol. Rev.* **1991**, *4*, 325-358.

54) Cook, G. C. *Q. J. Med*. **1987**, *65*, 967-983.

55) Badenoch, J. (Chairman of the group of experts); Cryptosporidium in water supplies: Report of the group of experts, 1990, London: HMS; p. 16.

56) Smith, H. V.; Rose, J. B. *Parasitology Today* **1998**, *14*, 14-22.

57) Badenoch, J. (Chairman of the group of experts); Cryptosporidium in water supplies: Report of the group of experts, 1990, ondon: HMS; p. 37-45.

58) Lisle, J. T.; Rose, J. B. *J. Water SRT—Aqua* **1995**, *44*, 103-117.

59) Badenoch, J. (Chairman of the group of experts); Cryptosporidium in water supplies: Report of the group of experts, 1990, London: HMS; p. 3-6.

60) Smith, H. V.; Robertson, L. J.; Ongerth, J. E. *J. Water SRT—Aqua* **1995**, *44*, 258-274.

61) Gergory, J.; Ives, K. J.; Scutt, J. E.; Makanjuola, D. B., Removal of Cryptosporidium oocysts by water treatment methods in laboratory scale. Final Report to the Deprtment of the Environment, London, 1991.

62) Badenoch, J. (Chairman of the group of experts); Cryptosporidium in water supplies: Report of the group of experts, 1990, London: HMS; p. 26-36.

63) Campbell, I.; Tzipori, A. S.; Hutchinson, G.; Angus, K. W. *Vet. Rec*. **1982**, *111*, 414-415.

64) Korich, D. G.; Mead, J. R.; Madore, M. S.; Sinclair, M. A.; Sterling, C. R. *Appl. Environ. Microbiol.* **1990**, *56*, 1423-1428.

65) Fricker, C. R.; Crabb, J. H. *Advances in Parasitology* **1998**, *40*, 241-278.

66) Moore, A. G.; Vesey, G.; Champion, A.; Scandizzo, P.; Deere, D.; Veal, D.; Williams, K. L. *Int. J. Parasit.* **1998**, *28 (8)*, 1205-1212.

67) Graczyk, T. K.; Cranfield, M. R.; Fayer, R. *The American Journal of Tropical Medicine and Hygiene* **1996**, *54*, 274-279.

68) Slifko, T. R.; Friedman, D.; Rose, J. B.; Jakubowski, W. *Appl. Environ. Microbiol.* **1997**, *63 (9)*, 3669-3675.

69) Slifko, T. R.; Friedman, D. E.; Rose, J. B.; Upton, S. J.; Jakubowski, W. *Water Science and Technology* **1997**, *35 (11-12)*, 363-368.

70) Wagner-Wiening, Ch.; Kimmig, P. *Appl. Environ. Microbiol.* **1995**, *61 (12)*, 4514-4516.

71) Stinear, T.; Matusan, A.; Hines, K.; Sandery, M. *Appl. Environ. Microbiol.* **1996**, *62 (9)*, 3385-3390.

72) Kaucner, Ch.; Stinear, T. *Appl. Environ. Microbiol.* **1998**, *64 (5)*, 1743-1749.

73) Widmer, G.; Orbacz, E. A.; Tzipori, S. *Appl. Environ. Microbiol.* **1999**, *65 (4)*, 1584-1588.

74) Vesey, G.; Ashbolt, N.; Fricker, E. J.; Deere, D.; Williams, K. L.; Veal, D. A.; Dorsch, M. *J. Appl. Microbiol.* **1998**, *85 (3)*, 429-440.

75) Johnson, D. W.; Pieniazek, N. J.; Griffin, D. W.; Misener, L.; Rose, J. B. *Appl. Environ. Microbiol.* **1995**, *61 (11)*, 3849-3855.

76) Baeumner, A.J.; Humiston, M.; Montagna, R.A.; Durst, R. A. *Anal. Chem.* (in press)

77) Kievits, T.; van Gemen, B.; van Strijp, D.; Schukkink, R.; Dircks, M.; Adriaanse, L.; Sooknanan, R.; Lens, P. J. *Virol. Methods* **1991**, *35*, 273-286.

78) van Gemen, B.; van Beuningen, R.; Nabbe, A.; van Strijp, D.; Jurriaans, P.; Lens, P.; Kievits, T. *J. Virol. Methods* **1994**, *49*, 157-168.
79) Malek, L.; Sooknanan, R.; Compton, J. *Methods in Molecular Biology* **1994**, *28*, 253-260.
80) Heim, A.; Grumbach, I. A.; Zeuke, S.; Top, B. *Nucleic Acid Research* **1998**, *26*, 2250-2251.

CHAPTER 2:

1) Baeumner, A.J.; Humiston, M.; Montagna, R.A.; Durst, R. A. *Anal. Chem.* (in press).
2) Bej, A. K.; Mahbubani, M. H.; Atlas, R. M. *Crit. Rev. Biochem. Molec. Biol.* **1991**, *26*, 301-334.
3) Birkenmeyer, L. G.; Mushahwar, I. K. *J. Virolog. Meth.* **1991**, *35*, 117-126.
4) Walker, G. T.; Little, M. C.; Nadeau, J. G.; Shank, D. D. *Proc. Nat. Acad. Sci. USA* **1992**, *89*, 392-396.
5) Kievits, T.; van Gemen, B.; van Strijp, D.; Schukkink, R.; Dircks, M.; Adriaanse, L.; Sooknanan, R.; Lens, P. J. *Virol. Methods* **1991**, *35*, 273-286.
6) van Gemen, B.; van Beuningen, R.; Nabbe, A.; van Strijp, D.; Jurriaans, P.; Lens, P.; Kievits, T. *J. Virol. Methods* **1994**, *49*, 157-168.
7) Malek, L.; Sooknanan, R.; Compton, J. *Methods in Molecular Biology* **1994**, *28*, 253-260.
8) Heim, A.; Grumbach, I. A.; Zeuke, S.; Top, B. *Nucleic Acid Research* **1998**, *26*, 2250-2251.
9) Siebert S. T. A., Reeves S. G, Durst R. A. *Anal. Chim. Acta* **1993**, *282*, 297-305.
10) Keller, G. H., Molecular Hybridization Technology, In: DNA Probes, Keller, G. H.; Manak, M. M. (edit.); Stockton Press: New York NY, 1993; pp. 8-9.
11) Wolf, S. F.; Haines, L.; Fisch, J.; Kremsky, N.; Dougherty, J. P.; Jacobs, K. *Nucleic Acids Research* **1987**, *15*, 2911-2926.
12) Reinhartz, A.; Alajem, S.; Samson, A.; Herzberg, M. *Gene* **1993**, *136*, 221-226.
13) Lee, M.; Durst, R. A.; Wong, R. B. *Anal. Chim. Acta* **1997**, *354*, 23-28.

14) Laidler, K. J.; Meiser, J. H., Physical Chemistry; Benjamin/Cummings Publishing: Reading MA, 1982; pp. 826.
15) Rule S. R.; Montagna R. A.; Durst R. A. *Clin. Chem.* **1996**, *42 (8)*, 1206-1209.
16) Sulaiman, I. M.; Morgan, U. M.; Thompson, R. C. A.; Lal, A. A.; Xiao, L. *Appl. Environ. Microbiol.* **2000**, *66*, 2385-2391.

CHAPTER 3:

1) Service, R. F. *Science* **1998***, 282*, 399-401.
2) Ruzicka, J.; Hansen, E. H. "Flow Injection Analysis", Wiley, NY, 1988.
3) Siebert, T. A.; Reeves, S. G.; Durst, R. A. *Anal. Chim Acta* **1993**, *282*, 297-305.
4) Roberts, M. A.; Durst, R. A. *Anal. Chem.* **1995**, *67*, 482-491.
5) Pollema, C. H.; Ruzicka, J.; Christian, G. D.; Larnmark, A. *Anal. Chem.* **1992**, *64*, 1356-1361.
6) Bauer, C. G.; Eremenko, A. V.; Kuhn, A.; Kurzinger, K.; Makower, A.; Scheller, F. W. *Anal. Chem.* **1998**, *70*, 4624-4630.
7) Branebjerg, J., Fabius, B., Gravesen, P. "Application of Miniature Analyzers from Microfluidic Components to μTAS", van den Berg, A., Bergveld, P. (eds.), Proceedings of Micro Total Analysis Systems Conference, Twente, Netherlands, Nov. 21-22, 1994, pp.141-151.
8) Miyake, R., Lammerink, T. S. J., Elwenspoek, M., Fluitman, J. H. J., "Micro Mixer with Fast Diffusion", Proceedings of the IEEE 1993, Micro Electro Mechanical Systems Workshop (MEMS '93), Ft. Lauderdale, FL, Feb. 2-7, 1993, pp.248-253.
9) Smith, L., Hoek, B., "A Silicon Self-Aligned Non-Reverse Valve", Proceedings of Transducers '91, the 1991 International Conference on Solid State Sensors and Actuators, San Francisco, CA, June, 24-27, 1991, pp.1049-1051.
10) Evans, J., Liepmann, D., Pisano, A. P., "Planar Laminar Mixer", Proceedings of the IEEE 10th Annual Workshop of Micro Electro Mechanical Systems (MEMS '97), Nagoya, Japan, Jan. 26-30, 1997, pp. 96-101.
11) Kovacs, G. T. A., "Micromachined Transducers Sourcebook" 1998, McGraw-Hill Companies Inc., New York, NY
12) Fuhr, G.; Schnelle, T.; Wagner, B. *J. Micromech. Microeng.* **1994**, *4*, 217-226.

13) Manz, A; Graber, N.; Widmer, H. M. *Sens. Actuators B* **1990**, *1*, 244-248.

14) Harrison, D. J.; Manz, A.; Fan, Z. H.; Ludi, H.; Widmer, H. M. *Anal. Chem.* **1992**, *64*, 1926-1932.

15) Jacobson, S. C.; Hergenroder, R.; Koutny, L. B.; Ramsey, J. M. *Anal. Chem.* **1994,** *66*, 1114-1118.

16) Ehrlich, D. J.; Matsudaira, P. *Trends Biotech* **1999**, *17*, 315-319.

17) Kopp, M. U.; de Mello, A. J.; Manz, A. *Science* **1999**, *280*, 1046.

18) Shoffner, M. A.; Cheng, J.; Hvichia, G. E.; Kricka, L. J.; Wilding, P. *Nucleic Acids Res.* **1996,** *24*, 375-379.

19) Cheng, J.; Shoffner, M. A.; Hvichia, G. E.; Kricka, L. J.; Wilding, P. *Nucleic Acids Res.* **1996**, *24,* 380-385.

20) Cheng, J.; Waters, L. C.; Fortina, P.; Hvichia, G. E.; Jacobson, S. C.; Ramsey, J. M.; Kricka, L. J.; Wilding, P. *Anal. Biochem.* **1998,** *257*, 101-106.

21) Cheng, J; Shoffner, M. A.; Mitchelson, K. R.; Kricka, L. J.; Wilding, P. *J. Chrom. A* **1996,** *732,* 151-158.

22) Guo, Z.; Guilfoyle, R. A.; Thiel, A. J.; Wang, R.; Smith, L. M. *Nucleic Acids Res.* **1994,** *22,* 5456-5465.

23) Proudnikov, D.; Kirillov, E.; Chumakov, K.; Donlon, J.; Rezapkin, G.; Mirzabekov, A. *Biologicals* **2000**, *28*, 57-66.

24) Wilding, P.; Kricka, L. J.; Cheng, J.; Hvichia, G. E.; Shoffner, M. A.; Fortina, P. *Anal. Biochem.* **1998,** *257*, 95-100.

25) Esch, M. B.; Locascio, L. A.; Tarlov, M. J.; Durst, R. A. 2001, *Anal. Chem.*, in press.

26) Baeumner, A.; Siebert, S. T.; Durst, R. A. *in preparation.*

27) Siebert, S. T. A.; Reeves, S. G.; Durst, R. A. *Anal. Chim. Acta* **1993**, *282*, 297-305.

28) Esch, M. B.; Baeumner, A.; Durst, R. A. *2001, Anal. Chem.* in press

29) Herne, T. M.; Tarlov, M. J. *J. Am. Chem. Soc.* **1997**, *119*, 8916-8920.

30) Levicky, R.; Herne, T. M.; Tarlov, M. J.; Satija, S. K. *J. Am. Chem. Soc.* **1998**, *120,* 9787-9792.

31) Law, B.; Malone, M. D.; Biddlecombe, R. A. In Immunoassay, A practical Guide; Law, B., Ed.; Taylor & Francis Inc.: Bristol, PA, 1996; p 143.

32) Vanderah, D. J.; Meuse, C. W.; Silin, V.; Plant, A. L. *Langmuir* **1998**, *14*, 6916-6923.

33) Harder, P.; Grunze, M.; Dahit, R. *J. Phys. Chem. B* **1998**, *102,* 426-436.
34) Rodbard, D. *Anal. Biochem.***1978,** *90*, 1-12.
35) Biddlecomb, R. A.; Law, B. In Immunoassay, A Practical Guide; Law, B., Ed.; Taylor & Francis Inc.: Bristol, PA, 1996; p 178.
36) Plant, A. L.; Gray, M.; Locascio-Brown, L.; Yap, W. T. In Liposome Technology: Liposome Preparation and Related Techniques (2nd edition, volume 1); Gregoriadis, G., Ed.; CRC Press Inc.: Boca Raton, FL, 1993; p 439-453.
37) Rule, G. S.; Montagna, R. A.; Durst, R. A. *Clin. Chem.* **1996**, *42*, 1206-1209.
38) Sulaiman, I. M.; Morgan, U. M.; Thompson, R. C. A.; Lal, A. A; Xiao, L. *Appl. Environ. Microbiol.* **2000**, *66,* 2385-2391.
39) Smith, H. V.; Rose, J. B. *Parasitology Today* **1998**, *14,* 14-22.
40) Cook, G. C. *Q. J. Med*. **1987,** *65*, 967-983
41) Wagner-Wiening, Ch.; Kimmig, P. *Appl. Environ. Microbiol.* **1995***, 61 (12),* 4514-4516.
42) Johnson, D. W.; Pieniazek, N. J.; Griffin, D. W.; Misener, L.; Rose, J. B. *Appl. Environ. Microbiol*. **1995**, *61(11)*, 3849-3855.

CHAPTER 4:

1) Lysov, Yu. P.; Florentiev, V. L.; Khorlyn, A. A.; Khrapko, K. R.; Shick, V. V.; Mirzabekov, A. D. *Dokl. Akad. Nauk SSSR* **1988**, *303*, 1508-1511.
2) Bains, W.; Smith, G. C. *J. Theor. Biol.* **1988**, *135*, 303-307.
3) Drmanac, R.; Labat, I.; Brukner, I.; Crkvenjakov, R. *Genomics* **1989**, *4*, 114-128.
4) Pease, A. C.; Solas, D.; Sullivan, E. J.; Cronin, M. T.; Holmes C. P.; Fodor, S. P. A. *Proc. Natl. acad. Sci. USA* **1994**, *91*, 5022-5026.
5) Lemieux, B.; Aharoni, A.; Schena, M. *Molecular Breeding* **1998**, *4*, 277-289.
6) Chee, M.; Yang, R.; Hubbel, E.; Berno, A.; Huang, X. C.; Stern, D.; Winkler, J.; Lockhart, D. J.; Morris, M. S.; Fodor, S. P. A. *Science* **1996**, 610-614.
7) Cronin, M. T.; Fucini, R. V.; Kim, S. M.; Masino, R. S.; Wespi, R. M.; Miyada, C. G., *Human Mutation* **1996**, *7*, 244-255.
8) Drmanac, S.; Kita, D.; Labat, I.; Hauser, B.; Schmidt, C.; Burczak, J. D.; Drmanac, R. *Nature Biotech.* **1998**, *16*, 54-58.

9) Hacia, J. G.; Brody, L. C.; Chee, M. S.; Fodor, S. P. A.; Collins, F. S. *Nature Genet.* **199**, *14*, 441-447.
10) Fodor, S. P. A.; Read, J. L.; Pirrung, M. C.; Stryer, L.; Tsai Lu, A.; Solas, D. *Science* **1991**, *251*, 767-773.
11) Blanchard, A., Synthetic DNA arrays. In Genetic Engeneering, Principles and Methods, Plenum Press 1998.
12) Augenlicht, L.: United States Patent 4,981,783 (1991).
13) Drmanac, R. T.; Crkvenjakov, R. B.: United States Patent 5, 202, 231.
14) Khrapko, K. R.; Khorlin, A. A.; Ivanov, I. B.; Chernov, B. K.; Lysov, Y. P.; Vasilenko, S. K.; Florent'ev, V. L.; Mirzabekov, A. D. *Mol Biol* **1991**, *25*, 581-591.
15) Schena, M.; Shalon, D.; Davis, R. W.; Brown, P. O. *Science* **1995**, *270*, 467-470.
16) Bernard, A.; Michel, B.; Delamarche, E. *Anal. Chem.* **2001**, *73*, 8-12.
17) Kovacs, G. T. A., "Micromachined Transducers Sourcebook" 1998, McGraw-Hill Companies Inc., New York, NY, p. 791.
18) Smith, H. V.; Hayes, C. R. *Water Sci. Tech.* **1997**, *35*, 369-376.

CHAPTER 5:

1) Ivnitski, D.; Abdel-Hamid, I.; Atanasov, P.; Wilkins, E.; Stricker, S. *Electroanalysis* **2000**, *12*, 317-325.
2) Perez, F.; Tryland, I.; Mascini, M.; Fiksdal, L. *Anal. Chim. Acta* **2001**, *427*, 149-154.
3) Sangodkar, H.; Sukeerthi, S.; Srinivasa, R. S.; Lal, R., Contractor, A. Q. *Anal. Chem.* **1996**, *68*, 779-783.
4) Hintsche, R.; Paeschke, M.; Wollenberger, U.; Schnakenberg, U.; Wagner, B.; Lisec, T. *Biosensors and Bioelectronics* **1994**, *9*, 697-705.
5) Wollenberger, U.; Paeschke, M.; Hintsche, R. *Analyst* **1994**, *119*, 1245-1249.
6) Lim, T. K.; Nakamura, N.; Ikehata, M.; Matsunaga, T. *Electrochemistry* **2000**, *68*, 872-874.
7) Laschi, S.; Franek, M.; Mascini, M. *Electroanalysis* **2000**, *12*, 1293-1298.
8) Van Es, R. M.; Setford, S. J.; Blankwater, Y. J.; Meijer, D. *Anal. Chim. Acta* **2001**, *429*, 37-47.

9) Killard, A. J.; Zhang, S.; Zhao, H.; John, R.; Iwuoha, E. I.; Smyth, M. R. *Anal. Chim. Acta* **1999**, *400*, 109-119.
10) Killard, A. J.; Micheli, L.; Grennan, K.; Franek, M.; Kolar, V.; Moscone, D.; Palchetti, I.; Smyth, M. R. *Anal. Chim. Acta.* **2001**, *427*, 173-180.
11) Liu, S.; Ye, J.; He, P.; Fang, Y. *Anal. Chim. Acta* **1996**, *335*, 239-243.
12) Wang, J.; Cai, X.; Rivas, G.; Shiraishi, H. *Anal. Chim. Acta* **1996**, *326*, 141-147.
13) Wang, J.; Rivas, G.; Cai, X.; Dontha, N.; Shraishi, H.; Luo, D.; Valera, F. S. *Anal. Chim. Acta* **1997**, *337*, 41-48.
14) Millan, K. M.; Mikkelsen, S. R. *Anal. Chem.* **1993**, *65*, 2317-2323.
15) Yamashita, K.; Takagi, M.; Kondo, H.; Takenaka, S. *Chemistry Letters* **2000**, *9*, 1038-1039.
16) Fan, C. H.; Li, G. X.; Gu, Q. R.; Zhu, J. Q.; Zhu, D. X. *Analytical Letters* **2000**, *33*, 1479-1490.
17) Erdem, A.; Kernman, K.; Meric, B.; Akarca, U. S.; Ozsoz, M. *Anal. Chim. Acta* **2000**, *422*, 139-149.
18) Xu, C.; Cai, H.; He, P. G.; Fang, Y. Z. *Analyst* **2001**, *126*, 62-65.
19) Kertesz, V.; Whittemore, N. A.; Inamati, G. B.; Manoharan, M.; Cook, P. D.; Baker, D. C.; Chambers, J. Q. *Electroanalysis* **2000**, *12*, 889-894.
20) Aoki, H.; Buhlmann, P.; Umezawa, Y. *Electroanalysis* **2000**, *12*, 1272-1276.
21) Roberts, M. A., 1996, Ph. D. Dissertation at Cornell University: The Development, Characterization, and Use of Liposomes for Rapid Analysis of Environmental Toxicants.
22) Locascio-Brown, L.; Plant, A. L.; Horvath, V.; Durst, R. A. *Anal. Chem.* **1990**, *62*, 2587-2593.

CHAPTER 6:

1) Nimeri, G.; Lassen, B.; Golander, C. G.; Nilsson, U.; Elwig, H. *J. Biomater. Sci. Polymer Edn.* **1994**, *6*, 573.
2) Jonson, U.; Malmquvist, M.; Ronnberg, I. *J. Colloid Interface Sci.***1985**, *10*3, 360.
3) Martensson, J.; Arwin, H. *Langmuir* **1995**, *11*, 963.

4) Malmsten, M. *J. Colloid Interface Sci.* **1994**, *166*, 333.
5) Malmsten, M. *J. Colloid Interface Sci.* **1995**, *172*, 106.
6) Hlady, V.; Andrade, J. D. *Colloids and Surfaces* **1988**, *32*, 359.
7) Bringham-Burke, M.; Edwards, J. R.; O'Shannessy, D. J. *Anal. Biochem.* **1992**, *205*, 125-131.
8) VanCott, T. C.; Loomis, L. D.; Redfield, R. R.; Birx, D. L. *J. Immunol. Methods* **1992**, *146*, 163-176.
9) Cunningham, B. C.; Wells, J. A. *J. Mol. Biol.* **1993**, *234*, 554-463.
10) Marengere, L. E. M.; Songyang, Z.; Gish, G. D.; Schaller, M. D.; Parsons, J. T.; Stern, M. J.; Cantley, L. C.; Pawson, T. *Nature* **1994**, *369*, 502-505.
11) Peterlinz, K. A.; Georgiadis, R. M.; Herne, T. M.; Tarlov, M. J. *J. Am. Chem. Soc.* **1997**, *119*, 3401-3402.
12) Piscevic, D.; Lawall, R.; Veith, M.; Okahata, Y.; Knoll, W. *Appl. Surf. Sci.* **1995**, *90*, 425-436.
13) Persson, B.; Stenhang, K.; Nilsson, P.; Larsson, A.; Uhlen, M.; Nygren, P.-A. *Anal. Biochem.* **1997**, *246*, 34-44.
14) Burstein, E.; Chen, W. P.; Chen, Y. J.; Hartstein, A. *J. Vac. Sci. Technol.* **1974**, *11*, 1004-1019.
15) Raether, H., in Physics of Thin Films, Vol. 9, Academic, New York, 1977, p.145.
16) Agranovich, V. M.; Mills, D. L., in Surface Polaritons: Electromagnetic Waves at Surfaces and Interfaces, North Holland, Amsterdam, 1982.
17) Ulman, A., An Introduction to Ultrathin Organic Films, Academic, New York, 1991.
18) Peterlinz, K. A., Georgiadis, R. *Langmuir* **1996**, *12*, 4731-4740.
19) Silin, V.; Weetall, H.; Vanderah, D. J. *J. Colloid Interface Sci.* **1997**, *185*, 94-103.
20) Thiel, A. J.; Frutos, A. G.; Jordan, C. E.; Corn, R. M.; Smith, L. M. *Anal. Chem.* **1997**, *69*, 4948-4956.
21) Hickel, W.; Knoll, W. *J. Appl. Phys.* **1990**, *67*, 3572-3575.
22) Kretschmann, E.; Raether, H. *Z. Naturforsch. Teil A* **1968**, *23*, 2135.
23) Otto, A. *Z. Phys.* **1968**, *216*, 398.
24) Hanken, D. G.; Jordan, C. E.; Frey, B. L.; Corn, R. M. *Electroanal. Chem.* **1998**, *20*, 141-225.
25) Peterlinz, K. A.; Georgiadis, R. *Langmuir* **1996**, *12*, 4731.

26) Hatta, A.; Suzuki, S.; Suetaka, W. *Appl. Surf. Sci.* **1989**, *40*, 9.

27) Schildkraut, J. S. *Appl. Opt.* **1988**, *27*, 3329.

28) De Bruijn, H. E.; Altengurg, B. S. F.; Kooyman, R. P. H.; Greve, J. *Optics Commun.* **1993**, *82*, 425.

29) De Bruijn, H. E.; Minor, M.; Kooyman, R. P. H.; Greve, J. *Optics Commun.* **1993**, *95*, 183.

30) Hansen, W. *J. Opt. Soc. Am.* **1968**, *58*, 380-390.

31) Levicky, R.; Herne, T. M.; Tarlov, M. J.; Satija, S. K. *J. Am. Chem. Soc.* **1998**, *120*, 9787-9792.